Exploring Flexibility in Natural Gas Reforming Processes

A Case Study on the Potential of Flexible Blue Hydrogen to Balance the Intermittent Supply of Green Hydrogen

Diederick Verbree

Delft University of Technology

TU Delft

Exploring Flexibility in Natural Gas Reforming Processes

A Case Study on the Potential of Flexible Blue Hydrogen to Balance the Intermittent Supply of Green Hydrogen

by

Diederick Verbree

Student Name	Student Number
Diederick Verbree	4921348

Supervisor:	Prof. Dr. Ir. W. de Jong	TU Delft
	Dr. Ir. L. Zubeir	TNO
	Dr. Ir. J. Boon	TNO
Committee:	Prof. Dr. Ir. W. de Jong	
	Prof. Dr. Ir. K. Hooman	
	Dr. Ir. M. Ramdin	
Project Duration:	March, 2024 - December, 2024	
Faculty:	Faculty of Mechanical Engineering, Delft	

TU Delft

TNO innovation for life

Preface

I am proud to present my master thesis about the potential of flexible natural gas reforming processes. Making the industry more sustainable is one of the biggest challenges of this century. I wanted to choose a topic where I could apply the knowledge gained throughout my master program and contribute to accelerate the transition toward a more sustainable future.

This thesis could not have been completed without the wonderful help of several people. First and foremost, I would like to express my gratitude to Professor Dr. Ir. Wiebren de Jong for his guidance and support. I enjoyed all our scientific discussion we had along the way.

I am especially thankful to my daily supervisor at TNO, Dr. Ir. Lawien Zubeir. During this thesis, I learned so much from him, from mastering process simulations in Aspen to improving my scientific writing. He was always there to answer my questions and most importantly made it a wonderful time a TNO. The innovative work done at this company is truly inspiring, accelerating the development of new technologies the world urgently needs.

I would also like to thank Jurriaan Boon for leading the Adaptable Industry project and for giving me the opportunity to contribute to this work at TNO. Additionally, I am grateful to Mark Roelands, Robert de Kler, Marija Saric and Rene Peters for sharing their expertise and knowledge during the course of this project.

Finally, I am grateful to my family, friends and all the other people who have encouraged me along this journey.

I hope this thesis will contribute towards a better understanding on how flexible natural gas reforming can support the energy transition and how the chemical industry can adapt to the growing challenge of intermittency.

Diederick Verbree
Delft, December 2024

Abstract

Driven by the need to reduce the destructive and irreversible effects of global warming caused by greenhouse gas emissions, the world is transitioning away from fossil fuels towards renewable alternatives. This transition brings the growing challenge of intermittency, as the availability of renewable energy from wind and solar fluctuates. This creates a big challenge for the chemical industry, which still relies on a continuous supply of energy and materials. Therefore, the chemical industry must adapt by using flexible processes capable of handling these fluctuations.

One application of flexible chemical processes is blue hydrogen production. Hydrogen is essential for decarbonizing hard-to-abate sectors such as heavy transport, steel, and chemical industries. While green hydrogen, produced from renewable electricity, offers a zero-emission solution, its supply is typically variable due to the intermittency of renewables. Flexible blue hydrogen production, made from natural gas with carbon capture and storage, can provide a reliable back-up supply, ensuring a stable supply of hydrogen for industrial processes with steady demand. By integrating flexibility into blue hydrogen production, the chemical industry can enhance system stability and support the transition to a sustainable hydrogen economy.

The aim of this research is to evaluate the potential of flexible natural gas reforming with carbon capture and storage to stabilize the intermittent supply of green hydrogen, ensuring a stable supply of hydrogen for downstream processes. This is done through a case study where blue hydrogen production compensates for fluctuations in green hydrogen generated from offshore wind energy, with limited hydrogen storage capacity. Using a hypothetical large scale ammonia synthesis plant in the port of Rotterdam as the downstream process. This research identifies process uncertainties, uses strategies to enhance flexibility, and quantifies their effects on process efficiency, costs and emissions.

To evaluate the potential of flexible blue hydrogen production, three case studies were simulated using Aspen Plus V12. The first case modeled a blue hydrogen plant operating continuously at maximum capacity (22.9 tons/h). This was used to clearly define the process steps needed for blue hydrogen production, serving as a benchmark for comparing continuous and flexible operations. In the second case study, an uncertainty is introduced to which the plant needs to adapt to. This uncertainty is modeled using hourly data from the Hollandse Kust Noord offshore wind farm, which supplies electricity to electrolysers with limited hydrogen storage capacity. The fluctuating green hydrogen output (0-11.3 tons/h) and steady hydrogen demand for ammonia synthesis (22.9 tons/h) determined the hourly blue hydrogen production. Multiple steady-state simulations were made in Aspen to model the plant at varying throughputs. In the last case, increased wind power output required the blue hydrogen plant to adapt with higher volume flexibility. An operating envelope of the blue hydrogen plant was developed to find the bottlenecks, and design strategies were applied to increase volume flexibility.

Results show that flexible blue hydrogen, using autothermal reforming with a gas heated pre-reformer, can effectively stabilize fluctuating green hydrogen production. The plants volume flexibility can be increased through design strategies such as selecting inherently flexible equipment, storage for intermediate production and using techniques like inert gas for load regulation. But there is a trade-off between flexibility and cost. The plant produces hydrogen at the lowest cost when operating continuously at maximum capacity, with a levelised cost of hydrogen (LCOH) at 3.19 €/kg. Increasing the volume flexibility of the blue hydrogen plant too much resulted in a LCOH of at least 4.02 €/kg, making alternatives like hydrogen storage a cheaper option for balancing out the intermittent supply of green hydrogen. However, when operating flexibly within its base volume flexibility the LCOH is cost effective compared to some alternatives as it increases only slightly to 3.47-3.57 €/kg. Mainly due to underused CAPEX, but also because of transient state losses and reduced efficiency at lower capacities.

This research shows the potential of flexibility in natural gas reforming processes and how it can play a key role in future energy systems. While there is still much to learn, integrating flexibility into the chemical industry enables it to adapt to the ever growing intermittently available feedstock and energy.

Contents

List of Figures

List of Tables

Nomenclature

Abbreviations

Abbreviation	Definition
AEL	Alkaline Electrolysis
ASU	Air Separation Unit
ATR	Autothermal Reforming
BAT	Best Available Technology
BOD	Basis of Design
CAPEX	Capital Expenditures
CCS	Carbon Capture and Storage
CEPCI	Chemical Plant Cost Indexes
CI	Carbon Intensity
CPO	Catalytic Partial Oxidation
ESA	Electric Swing Adsorption
FCI	Fixed Capital Investment
FCOP	Fixed Cost of Production
GHG	Greenhouse Gas
GHSV	Gas Hourly Space Velocity
GHR	Gas Heated Reformer
HDS	Hydrodesulfurization
HEN	Heat Exchanger Network
HHV	Higher Heating Value
IEA	International Energy Agency
IRENA	International Renewable Energy Agency
ISBL	Inside Battery Limits
KPI	Key Performance Indicator
LCA	Life Cycle Assessment
LCHS	Levelised Cost of Hydrogen Storage
LCOH	Levelised Cost of Hydrogen
LIN	Liquefied Nitrogen
LNG	Liquefied Natural Gas
LOX	Liquefied Oxygen
LHV	Lower Heating Value
MINLP	Mixed-Integer Nonlinear Programming
NLP	Nonlinear Programming
NPV	Net Present Value
OSBL	Outside Battery Limits
OPEX	Operating Expenditures
PEM	Proton Exchange Membrane Electrolysis
POX	Partial Oxidation
PSA	Pressure Swing Adsorption
PSRK	Predictive Redlich-Kwong-Soave
SMR	Steam Methane Reforming
SOEC	Solid Oxide Electrolysis
SST	Sea Surface Temperature
STP	Standard temperature and pressure
TEA	Techno-Economic Assessment

Abbreviation	Definition
TNO	Nederlandse Organisatie voor Toegepast Natuurwetenschappelijk Onderzoek
TRL	Technology Readiness Level
TSA	Temperature Swing Adsorption
TTF	Title Transfer Facility
VLE	Vapor-Liquid Equilibrium
VSA	Vacuum Swing Adsorption
WGSR	Water Gas Shift Reaction

Symbols

Symbol	Definition	Unit
A_t	Total annual cost	[Euro/year]
C	Cost of equipment	[Euro]
C_i	CO_2 equivalent emission rate	[CO_2-eq/h]
C_{max}	Maximal capacity	[t/year]
C_{min}	Minimal capacity	[t/year]
CI	Carbon Intensity	[kg CO_2-eq/ kg$_{H_2}$]
E	Energy	[kWh]
F_t	Fixed operating cost	[Euro/year]
G	Gibbs free energy	[J]
H	Enthalpy	[J]
H_i	Hydrogen production rate	[kg/h]
I_O	Initial investment	[Euro]
K	Number of ramping events per operating year	[-]
$LCOH$	Levelised Cost of Hydrogen	[Euro/kg]
LHV	Lower Heating Value	[kJ/kg]
M_t	Total mass hydrogen	[kg]
m	Mass	[kg]
m_{CO_2-eq}	Mass of CO_2 equivalent	[kgCO_2-eq]
n	Life time of equipment	[Years]
n_s	Scaling factor	[-]
O_i	Operating cost for a given throughput state	[Euro/h]
P_{down}	Percentage decrease in throughput	[%]
P_{up}	Percentage increase in throughput	[%]
r	Real discount rate	[-]
R	Actual discount rate	[-]
S	Size or capacity of equipment	[kg/s]
S_{down}	Ramp-down speed	[%/h]
S_{up}	Ramp-up speed	[%/h]
T	Temperature	[K]
$T_{transient}$	Transient time	[h]
t	Time	[h]
$\Delta\ H_{actual}$	Actual required energy per kg	[kWh/kg]
$\Delta\ H_{min}$	Minimum required energy per kg	[kWh/kg]
VF	Volume flexibility	[-]
η	Efficiency	[-]

1

Introduction

The 2015 Paris Agreement set an ambition to limit global warming to well below 2 degrees above pre-industrial levels [136]. In addition, the EU aims to be climate-neutral by 2050 which means an economy with net-zero greenhouse gas emission [36]. These reductions in greenhouse gas emissions aim to decrease the destructive and irreversible effect of global warming.

Renewable energy sources will play a critical role in the clean energy transition away from fossil fuels. It is expected that in 2028 the renewable energy sources will account for over 42% of global electricity generation, with the share of wind and solar PV doubling to 25% [53]. However, despite this promising trajectory, the inherent intermittency of these renewable sources poses a significant challenge to the stability and reliability of the energy supply.

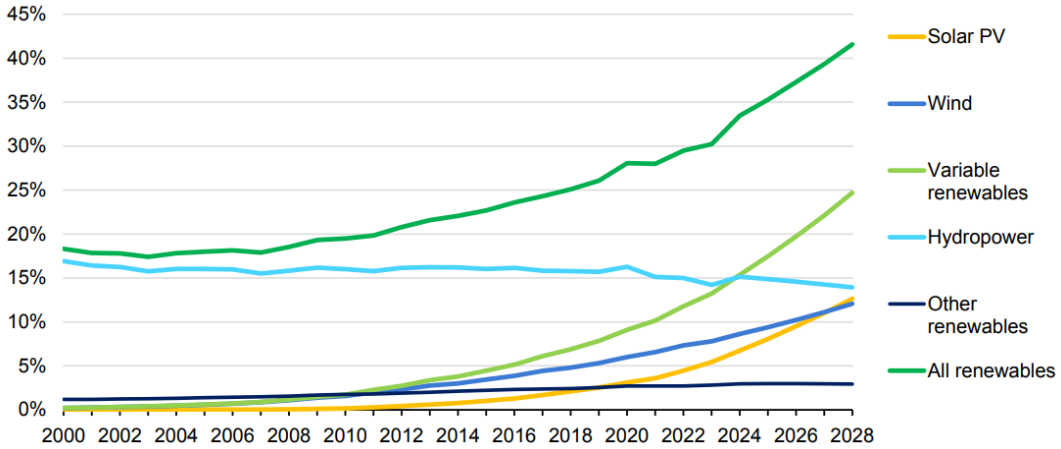

Figure 1.1: Share of global renewable electricity generation by technology [54].

1.1. The need for flexible chemical processes

The circular and carbon neutral industry is required to work with these ever growing intermittently available feedstock and energy. The timescales of intermittency vary widely, from hours to months and years [28]. The current chemical industry relies on fossil inputs that are relatively constant in availability, price and quality [80]. Therefore, the 'intermittency issue' is likely to significantly impact the economy and efficiency of chemical industries.

Old thinking in terms of individual unit operations and site optimization has led to reasonably efficient yet inflexible process systems. Currently, expected issues with intermittency are outsourced relative to the core processes. Relying on energy storage, anticipating a constant supply of feedstock, pointing

to other industries for solving the intermittency issue. However, inherently flexible chemical processes show great potential, as they can enhance the reliability of the energy system and potentially reduce costs for the industry by adapting to these fluctuations in feedstock and energy [15].

Despite the promising potential of flexible chemical processes, the feasibility of implementing flexible operations in the chemical industry remains uncertain. The most important factor is that the revenue model for flexibility is still unknown. It is uncertain if the benefits of flexible operations will outweigh the additional costs necessary to invest in more flexible processes [15]. In addition, there is a lack of knowledge on how to design and enhance flexibility in chemical processes, particularly beyond electrolysis-based sectors. Flexibility is not yet an academically mature concept, hindering the development of flexible process design [69].

While various frameworks have been proposed to quantify process flexibility, a standardized methodology is still lacking [89]. There is a significant overlap in terminology and concepts found regarding flexibility in chemical processes. This is making it difficult to understand and compare flexibility potential and constraints across alternative processes designs.

Addressing these knowledge gaps is essential for adapting the chemical process industry to a green future. A better understanding of flexible process design, quantification methods, and economic viability is necessary to facilitate the transition towards more sustainable and resilient chemical processes.

1.2. Flexible blue hydrogen

One of the applications where flexible chemical processes could be beneficial in the future is for blue hydrogen production in the Netherlands. Hydrogen is a versatile energy carrier, which can help tackle various critical energy challenges. It can decarbonize hard-to-abate sectors like long-haul heavy transport, chemicals, and iron and steel production, where it has been difficult to reduce emissions using other approaches like direct electrification [39].

Currently, over 95% of global hydrogen production relies on fossil fuels without carbon capture and storage, resulting in direct CO_2 emissions of more than 900 Mt CO_2 [60]. The Netherlands is no exception, with most of its hydrogen produced through Steam Methane Reforming (SMR). This so called grey hydrogen is produced from natural gas while emitting CO_2 into the atmosphere.

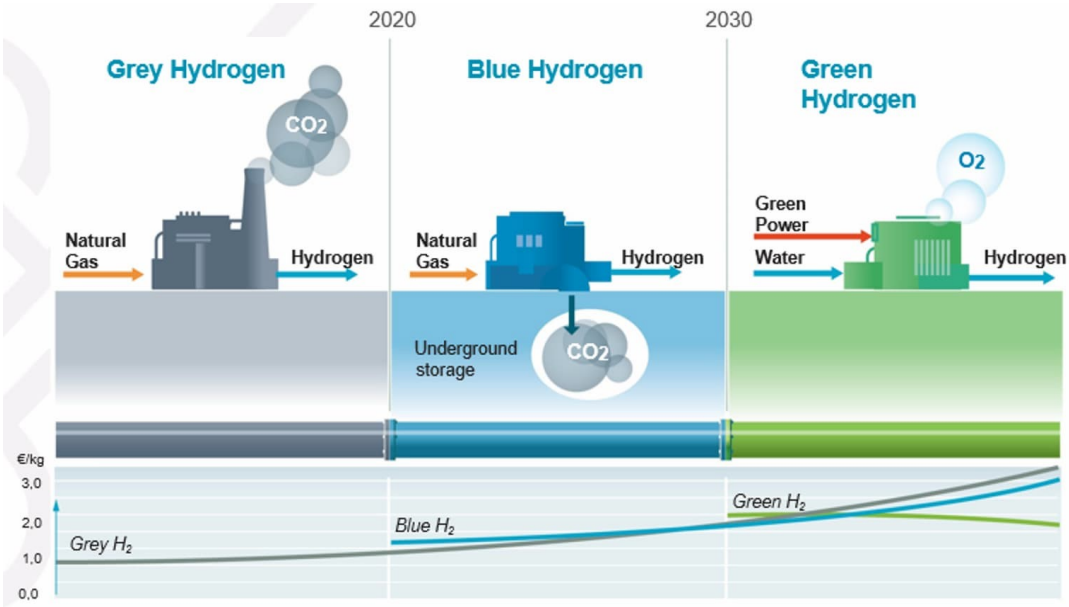

Figure 1.2: Transition of hydrogen production from grey to green. (Note: The hydrogen prices provided are for illustrative purposes only and do not represent actual production costs)

To reduce these emissions, alternative methods of hydrogen production are being developed in the Netherlands, along with the creation of a hydrogen grid to facilitate the transition to a decarbonized

energy system. In the future, a greater share of hydrogen will be produced using renewable electricity from sources like offshore wind farms through a process called electrolysis. This method avoids the use of fossil fuels or emits greenhouse gases, making production of green hydrogen truly emissions-free.

However, despite the promise of green hydrogen, it is currently 2-3 times more expensive than blue hydrogen [119]. Blue hydrogen is a low-carbon solution where hydrogen is produced from natural gas with carbon capture and storage to reduce greenhouse gas emissions. Consequently, a combination of blue and green hydrogen is expected to be supplied to the hydrogen grid of the Netherlands in the future.

So, with an expected increase in the supply of hydrogen from variable sources after 2030, the hydrogen grid in the Netherlands will need more stabilizing options [106]. This is because industrial processes that use hydrogen typically require a stable baseload supply to maintain efficient operations.

Ensuring a constant hydrogen supply with intermittent green hydrogen can be achieved in three ways. The first options is to build large-scale storage. For long-term storage, old salt caverns can be used while a potential hydrogen grid can accommodate short-term fluctuations trough line packing. However, each storage options has it limitations, ranging from discharge time to capacity size.

The second option is to import hydrogen either as liquefied hydrogen or as ammonia. This method is highly flexible and can support variations in hydrogen supply. However, future import costs of hydrogen remain uncertain.

The last option is to produce alternative hydrogen sources like blue hydrogen more flexibly. A study shows that blue hydrogen will play an important back-up role to the hydrogen system in the Netherlands [106]. The report states that in all future scenarios, all stability providing options are needed only with different importance.

The extent to which blue hydrogen production can operate flexibly and the consequences of such flexible operations are currently unknown. For this reason, a case study is made which aims to demonstrate the potential flexible blue hydrogen production. Addressing these question will be crucial for optimizing the hydrogen system ensuring a stable, efficient and sustainable energy future.

1.3. Research Question

To demonstrate the potential of flexible chemical processes in blue hydrogen production, a case study on flexible natural gas reforming with carbon capture and storage is conducted. The hydrogen produced is used for a typical end user, such as ammonia production, which requires a continuous hydrogen supply. The research question is proposed as follows:

"What is the potential of flexible natural gas reforming with carbon capture and storage for balancing the intermittent supply of green hydrogen to ensure continuous ammonia production in the harbour of Rotterdam?"

In order to find the potential a few sub-questions need to be answered:

- What will the overall process design of blue hydrogen in combination with electrolysis be for large scale NH_3 production?
- What are the expected uncertainties for which the process plant needs to adapt?
- What is the possible volume flexibility of the process and how can it be increased?
- Which key performance indicators can be used to evaluate the effect of flexible operations?
- How will the economy of the process be impacted by the need for flexibility? What will be the impact of 'underused CAPEX' on the overall process?

1.4. Objective & Scope

This study is done for TNO under the work package flexible industry. Their are two main objectives for this case study that have been set out.

The first objective is to give a clear framework for comparing and assessing the potential of flexibility in the chemical industry. This is done with a case study of a chemical process of converting natural gas into hydrogen with carbon capture and storage. With this case-study new methods to enhance flexibility will be simulated and compared to the base case. This will show to possible revenue model of designing a more flexible process that can handle more uncertainty.

The second objective, of the case study, is to find the potential of blue hydrogen to support green hydrogen production ensuring hydrogen supply for processes with a static hydrogen demand. By exploring the technical, economic, and environmental considerations of this approach, the research will provide an insight into the feasibility and viability of this solution as part of a strategy to ensure a reliable and sustainable hydrogen supply for the energy transition.

The scope of the project can be seen in Figure 1.3. Here a brief overview is given of case study where the intermittent supply of renewables from a wind farm produces a variable supply of green hydrogen. This will be compensated by using flexible blue hydrogen production using imported Liquefied Natural Gas (LNG). This hydrogen is then used for the production of ammonia which requires an extra Air Separation Unit (ASU) for the supply of nitrogen. The production of ammonia is assumed to always run continuous and there is limited storage for hydrogen.

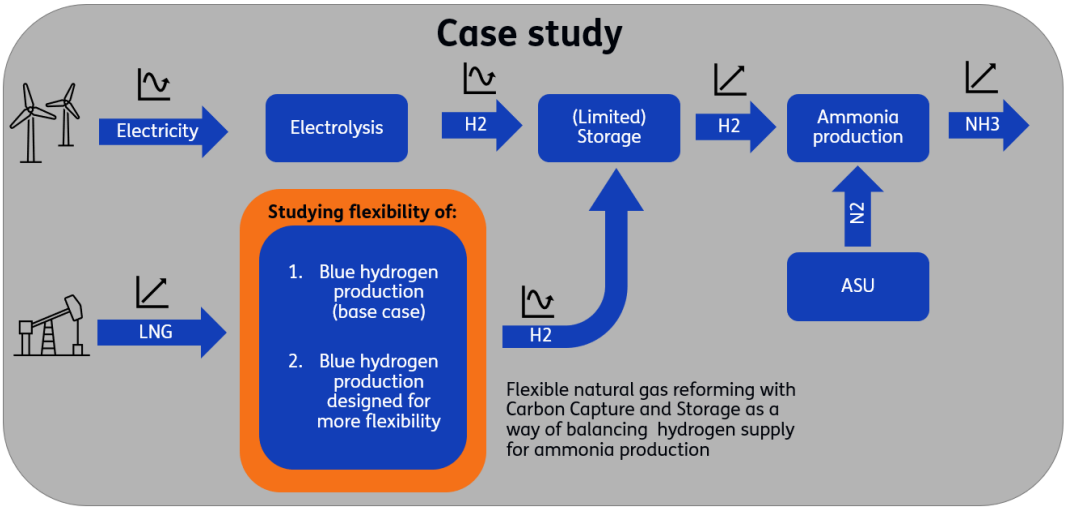

Figure 1.3: Schematic overview of the case study

1.5. Approach

To answer the research question, an approach is implemented based on the conceptual framework by Luo et al. [89]. This framework, used to evaluate the potential of flexible blue hydrogen production, consists of four steps: Define uncertainties, Define flexibility, Apply design strategies for flexibility and Evaluate flexibility. However, an addition is made to this framework. First the case study is clearly defined using a Basis of Design (BOD). Then, the steps proposed by Luo et al. are followed to evaluate the flexibility.

Figure 1.4: Framework for comparing and assessing flexibility

The following steps will be taken:

1. **Define case study/ Basis of Design:** Define the case for which flexibility will be assessed and compared. Achievements and desired targets are specific to each case.
2. **Define uncertainties:** Identify the uncertainties to which the design needs to respond. Search the potential sources of the uncertainties for the process plant and find the boundaries of this uncertainty. In addition, look at the expected frequency of changes in operating parameters, over a given time horizon.
3. **Define flexibility:** Once the uncertainties are identified, the necessary flexibility requirements must be defined. There are many types of flexibility that can help a process plant handle uncertainties, so it is crucial to determine the appropriate type of flexibility that needs to be increased.
4. **Apply design strategies for flexibility:** Identify and select strategies to increase the desired flexibility of the process plant.
5. **Evaluate flexibility:** Evaluate the effect of increased flexibility on the process plant by using the relevant key performance indicators.

1.6. Organization of this document

The report will begin with an in-depth literature study in Chapter 2 to gather the necessary knowledge for answering the research question.

Chapter 2.1 will explore the theoretical foundations of flexible chemical processes, divided into four parts: the uncertainties faced in the chemical industry, the different types of flexibility found in literature, various design strategies for increasing flexibility and methods for evaluating flexibility.

Chapter 2.2 will delve into the production of blue hydrogen, detailing the working principles and the different techniques available for each step of the process. Following this, Chapter 2.3 will briefly explain the production of green hydrogen.

Chapter 2.4 will focus on the challenges and opportunities associated with hydrogen storage, transportation, and networks. This analysis will provide the information to better compare flexible blue hydrogen production with alternative solutions.

The final chapter of the literature study, Chapter 2.5, will explain the process of ammonia production. This is done because ammonia is used as the end-user in the case study, making it important to understand how this process works.

Chapter 3 will present the basis of design, integrating the knowledge gained form the literature study. This chapter will include the selection of unit operations based on the literature study, along with design considerations and assumptions made for the case study.

Once the basis of design is completed, the Aspen simulation can be developed. The different choices made for simulating the different processes in Aspen are explained in Chapter 4.

Chapter 5 shows how the techno-economic assessment is made. It explains all the assumptions about how the plants initial cost is determined and which operating costs are included in calculating the total operating costs.

Chapter 6 will present and discuss the results from the different simulations. The first simulation will show data from continuous operations, followed by an adjusted model for variable operations. Then, the design of the plant will be adjusted to include more flexibility. Comparing these results using relevant KPI's will demonstrate the viability of flexible blue hydrogen production.

In Chapter 7, the conclusion will be made over the potential of flexible blue hydrogen production using the results from the previous chapter.

In Chapter 8, suggestions for future research will be made to address unexplored areas.

2

Literature Study

The goal of the literature study is to gather the knowledge on flexible chemical process in order to find the potential of flexible blue hydrogen production for balancing the intermittent hydrogen supply to ensure continuous ammonia production in the harbour of Rotterdam.

This literature study is done by retrieving information from various sources including books such as ”Introduction to Energy Analysis,” ”Hydrogen and Syngas Production and Purification Technologies,” and ”Advances in Synthesis Gas - Methods, Technologies, and Application.” Scientific data bases like Google Scholar and WorldCat provide essential research papers, while patent studies are used to study novel approaches. Reports from organizations such as IEA and IRENA are used for relevant data about the current and future energy system. Additionally, talking to industry experts from TNO provide valuable insights into the future of flexible chemical processes and hydrogen production in the Netherlands.

2.1. Flexible chemical processes

Flexible processes design is needed to cope with uncertainties and changes in the chemical industry [120]. This industry remains highly dynamic due to the acceleration of technological innovation, a global commitment to transition to sustainable energy and unpredictable geopolitical conflicts.

2.1.1. Uncertainties in the chemical industry

From literature different types of uncertainties are relevant to cope with in the future for chemical processes. These can be categorized in:

1. Feedstock and energy supply uncertainty [89]
    - Fluctuations in the quantitative supply and quality of raw materials
    - Supply of energy changes due to a growing share of renewable energy sources, coupling the chemical industry to the future power industry
    - Shift from fossil fuel based feedstock to renewables
2. Market and economic uncertainty
    - Volatility in demand for chemical products due to economic cycles, market trends or shift in consumer preferences
    - Volatility in the pricing for chemical products
    - Globalization creates new opportunities but also drives the need for individualized and specialized products to outperform competitors [16]
    - Changing global trade patterns for chemical products. The likely probability that energy intensive goods will become cheaper in countries with cheap renewable [2]
    - Carbon market and interest rates [27]

3. Policy uncertainty
    - Increasing pressure to decarbonize and improve environmental sustainability of chemical processes
    - More regulations and policies around emissions, waste and resource use
4. Technological uncertainties
    - Technological obsolescence or technological disruption. A new process such as electrolysis can become cheaper making current chemical processes obsolete
    - The need for developing new low-carbon technologies
5. Supply chain uncertainties
    - Increased competition for critical materials and resources
    - Supplier reliability
    - Geopolitical conflicts
6. Operational uncertainties
    - Faster deterioration of process plant components
    - Internal process uncertainty: transfer coefficients, reaction constants, efficiencies or physical properties [45]

2.1.2. Types of flexibility's

Their are many types of flexibility that can be incorporated for a chemical plant to deal with uncertainties. For instance, a plant can be designed to use different types of biomass in order to handle supply chain uncertainties. Or a process plant can be made to produce different types of products based on changing customer demand. However, a problem is that in literature different words for flexibility are being used to describe similar concepts. Therefore, the main types of flexibility are summarized in Figure 2.1.

Flexibility types	Definitions	Design recommendations
Feedstock	= ability to handle changes in quantities and/or qualities of inflow materials	- implement different production schemes to produce different product types - blend different types of feedstock - use equipment that can deal with variations in feed quality - install buffer units to regulate fluctuations in feed quality
Product	= ability to change the qualities of outflow materials	- select synthetic pathways that inherently produce multiple products - implement different production schemes
Capacity	= ability to vary throughput	- use equipment that can deal with variations in throughput - optimize equipment size (oversize) - install buffer units (intermediate products) - install parallel units or process line - robust scheduling
Scheduling	= ability to adjust resources allocation for different production cycles	- oversize equipment - install parallel same units or process lines
Production	= ability to switch to exercise another production scheme	- use equipment that handles varying input qualities and produces different output qualities - use equipment that can be switched on/off
Energy	= ability to adjust energy demand based on available energy supply	- storage - energy conversion technologies - energy efficiency (decrease energy demand) - rescheduling (load shifting) - change energy source

Figure 2.1: Flexibility types, definitions and design recommendations (adjusted from [89]).

In the case study, flexible blue hydrogen production should be able to vary its throughput to compensate for fluctuations in green hydrogen production caused by the variable nature of renewable energy sources. However, in literature there are several terms used for a chemical plants ability to vary its throughput [89]. The main term, capacity flexibility, can be subdivided into volume flexibility and expansion flexibility. Other terms used on literature for a plants ability to adjust the throughput are product flexibility and load flexibility.

Flexibility types for changing throughput and there definition are:

- Capacity flexibility = the ability of a plant to change its production output [123]
- Volume flexibility = the capability of adapting the production output to market changes by dynamically adjusting the production rate within the capacity range of a plant [123] [50].
- Expansion flexibility = the ability to increase the overall production capacity of a chemical plant by adding new equipment [123].
- Product flexibility = the ability of a system to produce different products at different throughput's [31].
- Load flexibility = the ability of processes to handle a range of dynamically fluctuating feed flow rates without violating safety and product specification constraints [37].

Based on the definitions above, the terms volume flexibility and load flexibility can best be used to look at the ability of the process plant in the case study to vary the throughput. Volume flexibility looks more at the whole process plant and load flexibility can better be used to a single unit operation. This is because load flexibility looks at four aspects: the load range, the start-up and shutdown times, the gradient and the limitations of load changes [37].

2.1.3. Design strategies for flexibility

Their are many different design recommendations found in literature to enhance a type of flexibility. These depend on which type of flexibility needs to be increased. Sometimes increasing one type of flexibility will lead to an increase of another type of flexibility. For instance, increase the operational flexibility can lead to an increase in the volume flexibility of the process plant.

Because of the project boundaries from TNO the literature study of design strategies for flexibility will mainly focus on increasing volume flexibility and the load flexibility, applied on natural gas reforming processes.

Inert gas as a method for load regulation on a reactor

One patented method from literature tries to increase the volume flexibility of the reactor for ammonia production to follow short-term fluctuations of the hydrogen feed [112]. Currently, the minimum flow rate to keep the reactor safe is usually at least 50% of the nominal flow rate.

The reactor can not operate at a low feed flow rate because there would be to much catalyst for the make-up gas, resulting in a dangerous increase of operating temperature due to the exothermic reaction. This overheating can be prevented by reducing the pressure of the synthesis loop by operating at partial load. However, the reactor vessel will suffer from fatigue stresses due to frequent pressurization and depressurization. In addition, the efficiency will much less compared to full capacity due to the higher specific energy consumption.

The idea of the patent is to operate the reactor at the nominal synthesis pressure, even at partial load, while compensating for the lower gas feed by increasing the concentration of argon and other inerts in the synthesis loop. Inerts will dilute the reagent and product gas in the reactor, thus protecting the reactor from overheating and preventing fatigue stresses on the vessel.

The advantage of using this technique is that it enables a reactor to run at partial load while keeping a good efficiency and preventing overheating of the reactor. This enables the ammonia plant to follow a time-varying feed source on a short-term basis of an hour or day.

The patent states that using this loop of inert gas can be implemented in reactors like autothermal reformer (ATR), partial oxidation (POX) and small-scale reformers in which the same problems occur when running below their nominal capacity. Using this technique can help to operate the reactor below its designed nominal capacity, thereby increasing the volume flexibility.

Parallel units

Another way of increasing the volume flexibility of a process plant is to add the same units or even entire process lines parallel so that some equipment can switch on/off or run on part-load to adjust the overall production level [89].

An example given in literature is for the use of compressor units in parallel. The operating envelope of the compressors in parallel allow for a large deviation in flow rates as seen in Figure 2.2 [151].

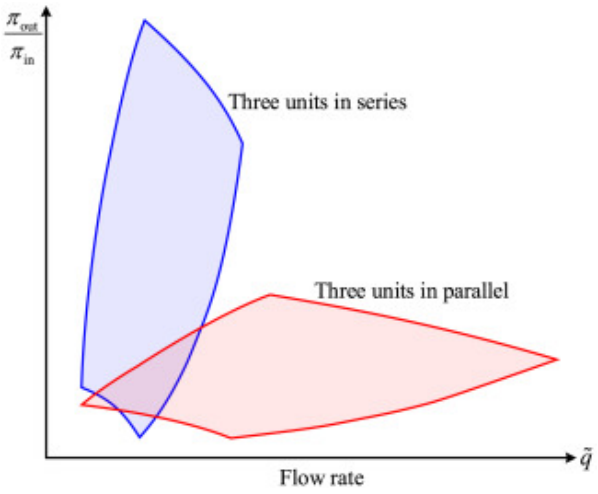

Figure 2.2: Operating envelopes of compressor station for different configurations [151].

This technique of using parallel units to increase volume flexibility can also be applied to absorption and distillation columns [115]. The limiting factors of these columns are induced by microscopic fluid dynamic phenomena like flooding, entrainment, weeping or dewetting. So to increase the volume flexibility of absorption and distillation columns the columns can be placed in parallel or the internal design of the column can be adjusted.

Oversizing

The volume flexibility of a plant can be increased by oversizing of the unit operation [123]. An example is given by oversizing chlor-alkali electrolysis cells which allows for operating at higher production rates than the nominal capacity when electricity prices are low [117]. This enables increased chlorine and sodium hydroxide production during cheap electricity periods. The optimal degree of oversizing is determined in this paper by solving an optimization problem that considers the trade-off between the capital costs of oversizing an the operational savings from demand side management. Clearly, higher oversizing allows for greater flexibility but at a higher investment cost.

Another example where oversizing is used for flexible production is in a power-to-methanol plant [19]. The case study found that the economic benefits of additional flexibility exceed the cost. This clearly demonstrates that process flexibility offers a viable route for future sustainable chemical production powered by renewables.

Storage for intermediate production

Storage tanks act as buffers, allowing plants to maintain continuous downstream operation despite fluctuations in production rates. This enables plants to operate at optimal levels regardless of demand fluctuations. For example, in chlor-alkali electrolysis, a chlorine storage tank acts as a product buffer that guarantees a constant supply to downstream processes even when the electrolysis rate varies [117]. So in order to increase flexibility of a whole process it can be usefull to look at the storability of the intermediate products [15]. This storage allows some units to run at high utilization while others draw from storage, providing flexibility in operations. However, implementing buffers requires additional investment, space, and possible safety risks that need to be taken into account [15].

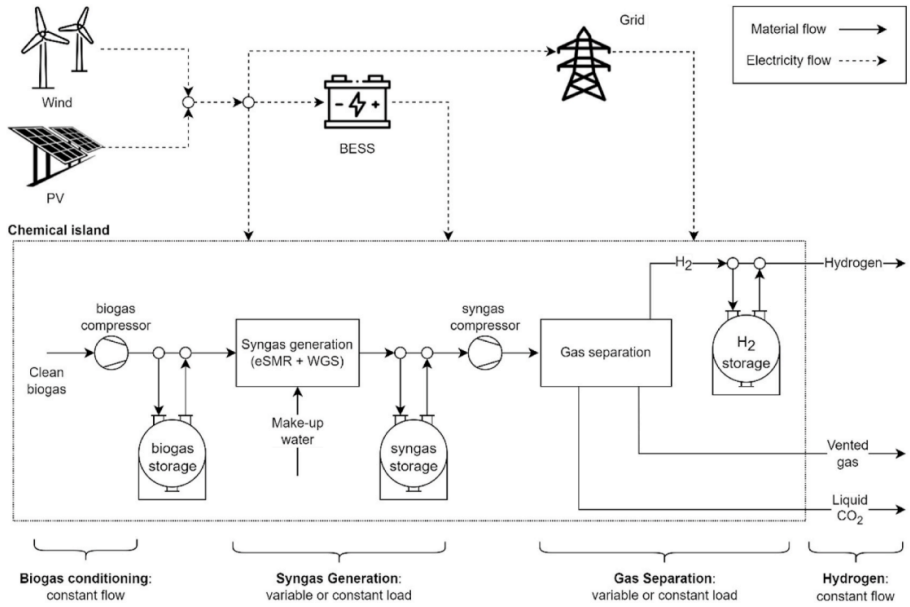

Figure 2.3: Block diagram of the biogas to hydrogen process with storage systems for intermediate production [100].

Another example of using storage to decouple throughput in a process plant can be seen in a biogas-to-hydrogen plant using electrified biogas reforming [100]. It uses electrified biogas reforming that can adapt to the intermittent nature of renewable sources. The syngas storage unit allows each section to operate at different loads by storing intermediate products, similar to how chlorine storage buffers chlor-alkali electrolysis. This increased load flexibility allows the electrified steam methane reformer (eSMR) to operate more efficiently by adjusting production rates independently.

Select inherent flexible equipment

Choosing the right flexible unit operation is important for increasing the volume and load flexibility of a chemical plant. For hydrogen production, water electrolysis offers inherent flexibility compared to traditional reforming methods. Some electrolysers can quickly ramp up or down their production rates, allowing them to respond fast to fluctuations in renewable electricity supply from renewable sources.

In contrast, the high-temperature and high-pressure reactors used in the process of natural gas reforming shows lower operational flexibility. These reactors require careful control of temperature, pressure and feed rates to maintain stable and efficient operation. Exothermic reactors like POX face challenges with heat removal during load changes, which can lead to equipment damage. Endothermic reactors such as SMR require an external heat sources which needs to adjust to the change in feed flow, limiting their ramp rates due to thermal inertia of the system.

Another constraint is the presence of a catalyst which also impacts the flexibility. Catalytic processes are more sensitive to changes in operating condition because these can lead to deactivation or loss in performance if the catalyst is exposed to sub-optimal temperatures, pressures or feed flows. So non-catalytic processes can offer larger flexibility at the cost of being less efficient. By strategically selecting unit operations that have inherent flexibility, chemical plants can better handle throughput fluctuations and improve their adaptability to dynamic market conditions.

2.1.4. Evaluation of flexibility

There is a lack of available metrics for evaluating specific types of flexibility [89]. However, this chapter shows the different ways of evaluating the potential of flexible blue hydrogen production. Different metrics will be explained in order to evaluate the viability of flexible chemical processes, considering effects on efficiency, costs and emissions.

Flexibility test & index

The analysis of the flexibility of chemical processes is closely related to the solution of optimization problems under uncertainty [150]. Grossmann et al. developed an optimization model to quantify process flexibility by solving the flexibility test problem and flexibility index problem.

Although the flexibility index offers a clear measurable insight into the flexibility of a chemical plant, its practical application on a large scale proves challenging due to the complexity of the calculations. While existing examples, often limited to scenarios like heat exchangers networks or basic pump and pipe system, show promise, extending this method to an entire process plant would be to complex and time-consuming for answering the simpler research sub-questions. A brief explanation about the working principle of the flexibility test and index can be found in the Appendix A.1.

Volume flexibility

Volume flexibility is determined by the lowest and highest production output that can be achieved with a given plant setup [123]. So, in order to evaluate the volume flexibility an investigation of the operating window of each unit operation is needed.

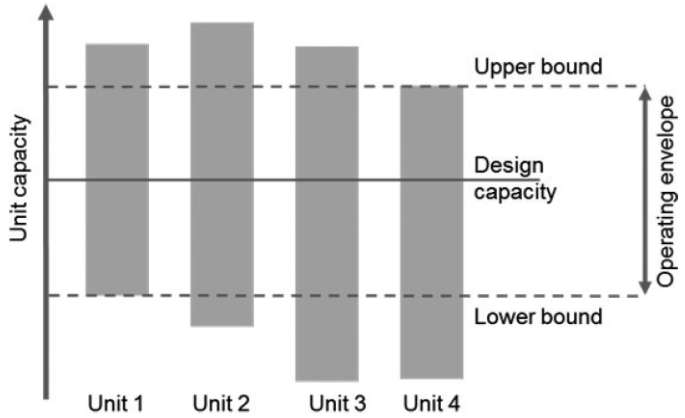

Figure 2.4: Schematic diagram for the determination of an operating envelope [123].

To calculate the volume flexibility:

$$\textit{Volume Flexibility} = \frac{C_{max} - C_{min}}{C_{max}} \tag{2.1}$$

In this method, the volume flexibility is described by the difference between the upper and the lower bound of the operating envelope ($C_{max} - C_{min}$) divided by the upper bound. Systems with very high volume flexibility have a value near 1 and systems with a fixed output are closer to 0 on this scale.

Turndown ratio

Calculating the turndown ratio of a chemical process involves determining the maximum and minimum flow rates or capacities at which the process can operate stably and efficiently.

The turn-down ratio is calculated as:

$$\textit{Turndown Ratio} = \frac{\textit{Maximum Flow Rate or Capacity}}{\textit{Minimum Flow Rate or Capacity}} \tag{2.2}$$

The overall process turndown ratio is limited by the equipment with the lowest individual turndown ratio. For example, if a reactor has a turndown ratio of 6:1 and a column has a turndown ratio of 3:1, the process turndown ratio is limited to 3:1. So the process turndown ratio is calculated by dividing the maximum process capacity by the minimum capacity determined by the most limiting equipment.

Ramp-up/down rates and transient time

Ramp-up and ramp-down rates describe the speed at which a chemical process can increase or decrease its output. It measures the rate of change in production capacity per unit of time. These rates are essential for evaluating a plants flexibility and ability to adapt to fluctuations in demand or feedstock changes. Faster ramp-up and ramp-down rates enable processes to adjust efficiently to sudden shifts, which is essential in industries like renewable energy where supply and demand can be volatile.

Comparing blue hydrogen production technologies, ATR offers ramping speeds of 1.5% per minute, allowing it to respond fast to rapid demand changes [67]. In contrast, SMR can ramp-up or ramp-down only 5% per hour, making it unsuitable for following frequent hourly demand variations [102].

For plants operating in dynamic markets where frequent output adjustment are expected, significant time spent in transient states can affect both efficiency and product quality [18]. In transient state, the plant is not operating at the its optimal conditions. Several process variables are affected during ramping up or down such as temperature and pressure fluctuations throughout the system, changes in residence time and also compositions variations. Plants with higher ramping speeds spend less time in this non-optimal transient state, thereby maximizing operation time under optimal conditions so improving overall performance.

Process efficiency

The performance of a SMR system is usually assessed based on its plant efficiency [126]. This efficiency is determined using the first-law energy balance, which involves dividing the total heat content of the hydrogen produced by the total energy input into the system.

The equation for process plant efficiency can be written as:

$$\eta_{\textit{Plant Efficiency}} = \frac{\dot{m}_{H_2} \times LHV_{H_2}}{\dot{m}_{feul} \times LHV_{fuel} + \textit{Power consumption}} \tag{2.3}$$

To calculate the loss of process efficiency due to flexible operations, the first step is to determine the efficiency of the process plant under steady-state conditions. This serves as a baseline for comparison. Next, evaluate the efficiency of the plant under flexible operation. Flexible operations will likely result in reduced hydrogen production while requiring more fuel and power for the process. Comparing the efficiencies under these two operating conditions will reveal the efficiency losses associated with flexible operations.

Levelised cost of hydrogen

One key performance indicator (KPI) for comparing hydrogen production methods is the Levelised Cost of Hydrogen (LCOH). The LCOH represents the total costs incurred over the plants lifetime for construction and operation divided by the total amount of hydrogen produced. The LCOH can be calculated using slightly different approaches such as the annuity method, the Net Present Value (NPV) method, or a more complex custom methods [76] [65]. This report uses the NPV method, as it accounts for the time value of money and is for that reason considered more accurate compared to simpler approaches like the annuity method. The NPV method achieves this by equating the discounted revenues from selling the hydrogen produced to the sum of all discount costs:

$$LCOH = \frac{\sum_{t=1}^{n} \frac{I_O + A_t}{(1+r)^t}}{\sum_{t=1}^{n} \frac{M_t}{(1+r)^t}} \tag{2.4}$$

Here, I_O is the initial investment, A_t the annual operational cost composed of the fixed and variable cost, M_t the total hydrogen produced each year and n is the plants lifetime. The real discount rate (r) can be approximated by actual discount rate (R) minus the rate of inflation (i):

$$r \approx R - i \tag{2.5}$$

A counter intuitive aspect of using the NPV method is that, besides the discounting of the expenses for the investment and the expenditures during hydrogen production, also the hydrogen production is

discounted. From a physical standpoint this may seem incomprehensible, but it is a result of financial mathematical transformation. Essentially, the hydrogen produced corresponds to the revenue generated from the sale of this hydrogen. Therefore, the further in the future this revenue is received, the lower its present value due to discounting [76].

The NPV method of calculating the LCOH can reveal the effect of underutilized CAPEX during flexible operations on hydrogen production costs. Comparing this additional cost with the levelised costs of storage and transportation will determine whether flexible operations are economically viable.

Carbon intensity

The last KPI for flexible blue hydrogen production is to look at the CO_2 intensity of the process. What will be the effect of flexible production on the emissions of the plant? Flexible blue hydrogen can be used to guarantee hydrogen supply even when green hydrogen production is low. The main reason that fossil fuels are replaced with renewable alternatives is to lower GHG emissions. So, if flexible blue hydrogen leads to significantly higher emissions it will surpass its purpose of reducing emissions.

The carbon intensity (CI) of the process is calculated by:

$$CI = \frac{m_{co_2-eq}}{m_{H_2}} \tag{2.6}$$

The carbon intensity measures the amount of CO_2-equivalent (CO_2-eq) emissions generated per kg of hydrogen produced. CO_2 equivalent is a metric that combines the global warming potential of various greenhouse gases (GHG) into a single number. This is important because other GHGs like methane have different warming effects compared to CO_2. By converting all GHG emissions into a CO_2-eq basis, it allows for simpler comparison between different production methods.

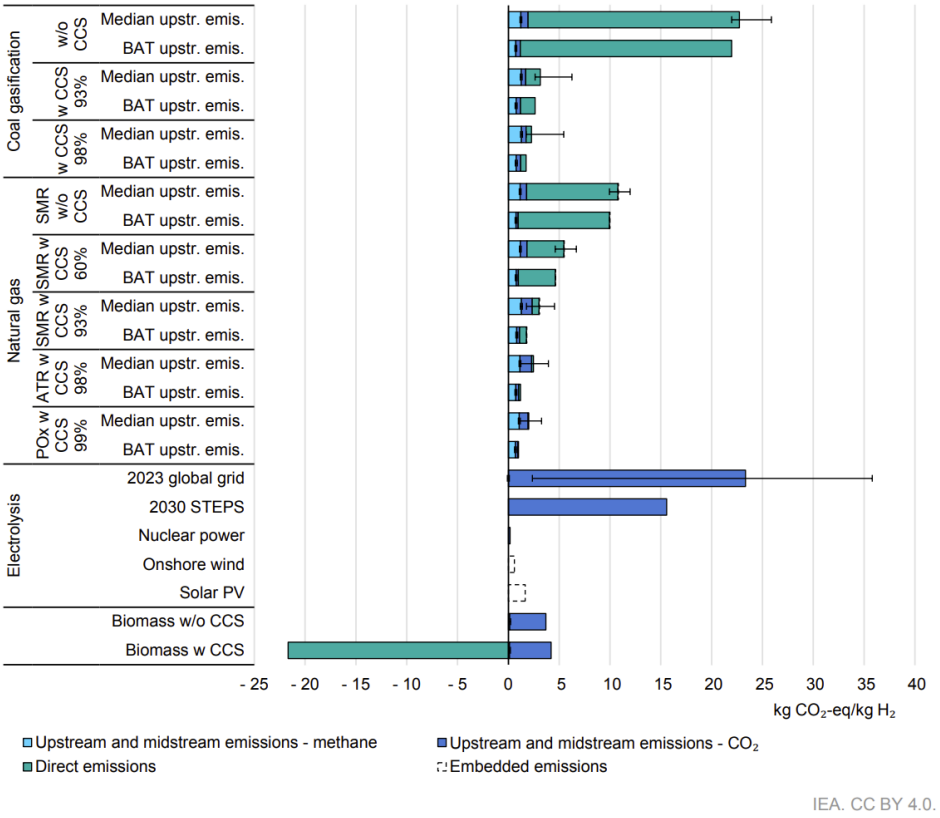

Figure 2.5: Carbon intensity of different hydrogen production methods [59]. Note BAT = best available technology, BAT upstream emis = Best available technology today to address upstream and midstream emissions.

A life-cycle assessment (LCA) would give a more complete overview on how flexibility in chemical processes impacts overall emissions across the entire process chain. Such an assessment would include various stages like raw material extraction, production, transportation, utilization and waste management, all of which would differ significantly in a system integrating flexible blue hydrogen. However, this LCA is outside the scope and therefore recommended as future study on how flexible chemical processes influence emissions.

2.2. Blue hydrogen production

Blue hydrogen production is done with a process that converts natural gas into hydrogen with the use of carbon capture and storage. Currently 62% of all the hydrogen produced is based on this process, of converting natural gas in hydrogen, without the carbon capture and storage [61]. For that reason it is called grey hydrogen. The general process steps of blue hydrogen are given in figure 2.6.

Figure 2.6: Simplified process flow diagram of blue hydrogen production.

For each of the steps different techniques are available. Which technique is used depends on parameters regarding efficiency, flexibility, maturity, cost, etc. This will be further explained in each subsection.

2.2.1. Feed pretreatment

The first steps of blue hydrogen production consist of the removal of impurities and conversion of higher hydrocarbons into methane before entering the main reformer.

Desulfurization

Desulfurization is the process of removing sulfur compounds from natural gas to protect downstream processes. The amount of sulfur in natural gas varies from a few parts per million volume (ppmv) to several hundred ppmv [130]. This sulfur can originate from naturally occurring compounds or from added substances, such as sulfur-containing odorants used in commercial fuel gas to aid in leak detection. Sulfur compounds, such as hydrogen sulfide (H_2S), carbonyl sulfide (OCS), methylmercaptan (CH_3SH), and diethylsulfide ($(C_2H_5)_2S$), can adhere to the active surfaces of catalysts used in natural gas reforming processes, thereby poisoning the catalyst and reducing both the efficiency and yield of the operation.

To address this issue, there are several methods for the desulfurization of natural gas. The three main techniques are dry desulfurization, wet desulfurization and catalytic adsorption [130]. For large-scale hydrogen production from natural gas, currently, catalytic adsorption is the preferred method of sulfur removal. This so called hydrodesulfurization (HDS) is a process in which the natural gas is mixed with a small quantity of added hydrogen and passed over a catalyst bed. The typical HDS catalysts is either Co-Mo/Al_2O_3 or Ni-Mo/Al_2O_3. The organic sulfer is reduced to hydrogen sulfide (H_2S) and hydrocarbons by reaction of the following kind:

$$CH_3SH\ (g) + H_2\ (g) \longrightarrow CH_4\ (g) + H_2S\ (g)$$

$$(C_2H_5)_2S\ (g) + 2H_2\ (g) \longrightarrow 2C_2H_6\ (g) + H_2S\ (g)$$

The H_2S produced can be removed by adsorption on a bed of ZnO sorent at a operating temperature of 300-400 °C. This happens with the following reaction:

$$ZnO\ (s) + H_2S\ (g) \longrightarrow ZnS\ (s) + H_2O\ (g)$$

Zinc sulfide (ZnS) can be regenerated by heating it in the presence of air and/or steam, converting it back to zinc oxide (ZnO) and releasing sulfuer dioxide (SO2) in the process. The regenerated ZnO sorbent can then be reused for futher desulfurization cycles.

Pre-reformer

The main task of the pre-reformer is to convert all higher hydrocarbon feedstock into methane. Hydrogen plants supplying hydrogen to refineries are often handling a broad range of feedstock, ranging from refinery off-gas to naphta. Liquified Natural Gas (LNG) imported from different countries also differs in composition. The addition of the pre-reformer therefore increases the feedstock flexibility of the process plant.

Adiabatic pre-reformer

An adiabatic pre-reformer operating range is typically from 400-550 °C [22]. The reactions that take place in the pre-reformer are:

$$\mathrm{C_nH_m}\ (g) + \mathrm{nH_2O}\ (g) \longleftrightarrow \mathrm{nCO}\ (g) + (n + 0.5m)\mathrm{H_2}\ (g)\ (1) \qquad (\Delta H_{298K} = +1108kJ/mol, n = 7)$$

$$\mathrm{CH_4}\ (g) + \mathrm{H_2O}\ (g) \longleftrightarrow \mathrm{CO}\ (g) + 3\mathrm{H_2}\ (g)\ (2) \qquad (\Delta H_{298K} = +206kJ/mol)$$

$$\mathrm{CO}\ (g) + \mathrm{H_2O}\ (g) \longleftrightarrow \mathrm{CO_2}\ (g) + \mathrm{H_2}\ (g)\ (3) \qquad (\Delta H_{298K} = -41.1kJ/mol)$$

Essentially, the pre-reforming reaction consist of steam reforming of these larger hydrocarbons(1), steam methane reforming (2) and the water gas shift reaction (3). For all hydrocarbons with a carbon chain length great than one (n>1), the steam reforming reaction (1) is typically regarded as irreversible [23]. Under the conditions that sufficient catalyst activity exist then all higher hydrocarbons are entirely transformed.

The steam-to-carbon ratio (S/C) of the adiabatic pre-reformer depend on the feedstock, operating temperature and the desired product of the process plant [22]. The typical operating conditions for natural gas into a syngas mixture of CO/H_2 is an inlet temperature of 350-550 °C and a steam-to-carbon ratio between 0.3-2.0.

There are many advantages of using a pre-reformer in hydrogen production plants. It allows for enhanced plant performance because the reactor can operate at lower overall steam-to-carbon ratio, reducing the fuel consumption [137]. Adding a unit operation often leads to an increase in CAPEX. However, the main reformer reactor size is reduced because of the pre-reformer leading to lower total CAPEX.

Gas Heated pre-Reformer

A Gas Heated Reformer (GHR) operates by utilizing the heat from the process gas outlet of the main reactor to drive the endothermic reforming reactions necessary for converting heavier hydrocarbons into methane. Essentially, the GHR serves as a large heat exchanger, pre-heating the incoming gas stream before it enters the main reactor, while also housing catalyst-filled tubes that facilitate the reforming process of the higher hydrocarbons.

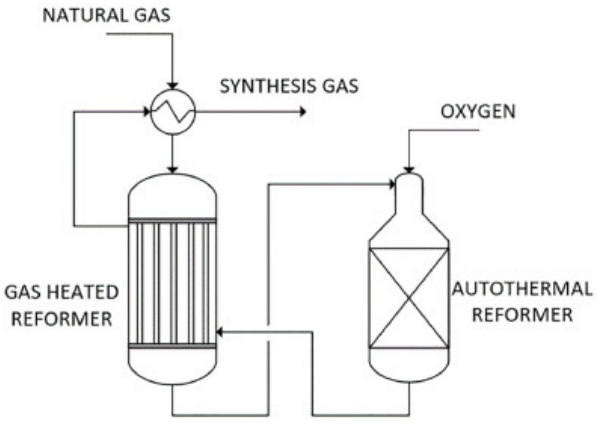

Figure 2.7: Serial placement of gas heated reformer and Autothermal Reformer.

A common configuration involves combining a GHR with an Autothermal Reformer (ATR) due to the exothermic nature of the combustion reaction inside the reformer. This combination is highly effective,

as the heat generated by the ATR reaction, which operates at around 1200 C, can be harnessed by the GHR. Consequently, the GHR operates at elevated temperatures around 800-950 C, ensuring efficient heat transfer and optimized reforming reaction [105].

Although there is limited literature on the exact operating conditions of the GHR, it is known that lower temperatures lead to better conversion of higher hydrocarbons. A steam-to-carbon ratio of around 0.25-0.5 is sufficient to convert almost all higher hydrocarbons [30]. However, when syngas from an ATR is cooled on the shell side of a GHR, metal dusting becomes a significant issue. To mitigate this, higher steam-to-carbon ratios are recommended for safe operation [140].

2.2.2. Reactor

The three most common and mature processes of reforming on industrial scale are steam methane reforming (SMR), autothermal reforming (ATR) and partial oxidation (POX). The reactions in their reactor differ slightly but have a large impact on the overall process design and operations of the plant. The principles and operational characteristics of each process are explained to find the best reactor suited for volume flexibility needed in the case study.

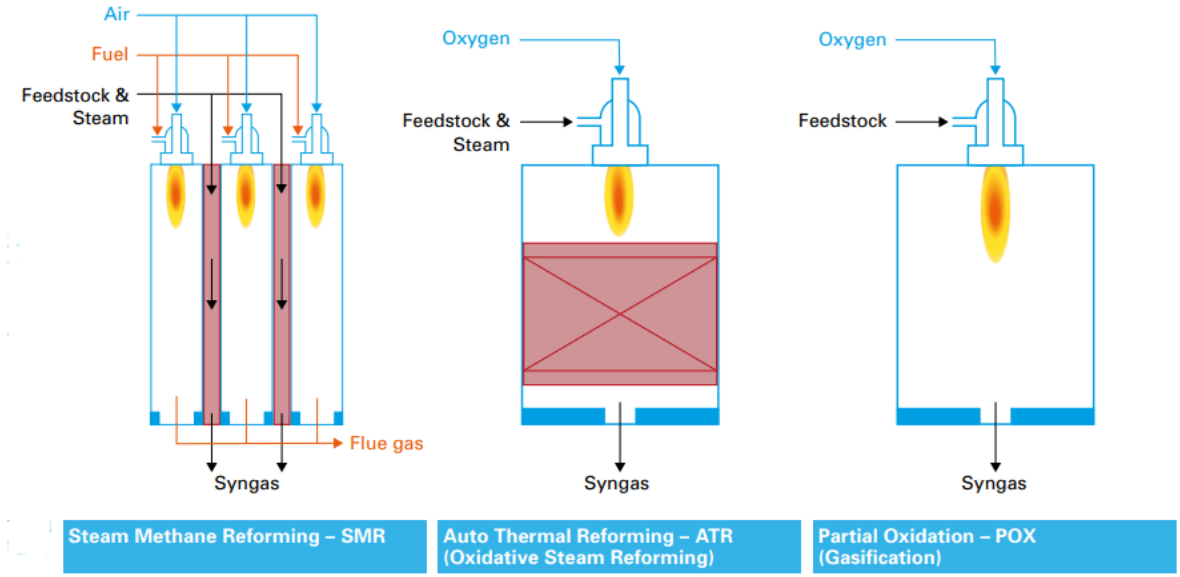

Figure 2.8: Three most common reactors for natural gas conversion

Steam methane Reforming (SMR)

Steam methane reforming (SMR) is the most widely used technology for natural gas-based hydrogen production [58]. This process accounts for around 50% of the global hydrogen supply [12]. In this process steam and methane react to form syngas containing mostly hydrogen and carbon monoxide.

The steam reforming reaction can be written as:

$$\mathrm{CH_4\ (g) + H_2O\ (g) \longleftrightarrow CO\ (g) + 3H_2\ (g)} \qquad (\Delta H_{298K} = +206 kJ/mol)$$

The methane and steam react over a high-temperature catalyst. The reaction is typically achieved over a nickel-based catalyst operating at high temperatures of 600-900 °C and pressures around 5-25 bar [127], with a steam-to-carbon ratio (S/C) of around 2.5-4.0 [43]. Depending on the operating conditions of the reformer, there may also be significantly amounts of CH_4, H_2O and CO_2 present in the syngas leaving the reactor.

In order to operate energy efficiently a low S/C ratio is preferred. Modern SMR-plants are designed to handle higher temperatures to shift the equilibrium toward a higher hydrogen yield. The energy efficiency of a SMR plant is typically around 80-85 % and is able to produce the most hydrogen per carbon compared to POX and ATR. The hydrogen to carbon monoxide (H_2/CO) molar ratio is typically between 3.5 and 5.5 in the reformed product.

One of the disadvantages of using steam methane reforming for blue hydrogen production is its complex CO_2 capture process. The steam reforming reaction is highly endothermic and for that reason needs continuous supply of heat to maintain the reactor operating temperature. Typically, this heat is supplied through burners outside the reactor tubes. This creates two separated streams of carbon dioxide. Around 60% of the CO_2 is produced in a concentrated stream which can be captured relatively easily using physical absorption. However, the remaining 40% of CO_2 is diluted in the flue gas from the burners which is more difficult and expensive to capture. With only pre-combustion capture the process can achieve around 60% CO_2 capture rate. Adding post-combustion capture of the burners the process can reach 90% capture rates but at significantly higher cost [26].

Another disadvantage of SMR is its limited volume flexibility. A conventional steam reformer using a burner cannot operate properly when throughput decreases too much below the design capacity [63]. It is estimated that the lower bound is equal to 80% of the nominal capacity, which strongly limits the integration of green hydrogen with blue hydrogen in a decentralised scenario where large scale hydrogen storage is not always possible [63].

A novel alternative to using burners is to use an electrically heated SMR. A higher heat flux is possible for electrically heated SMR. This allows for compact reactors that are two order of magnitude smaller than conventional fired reformers, while maintaining the same production capacity [144]. This smaller reactor has a faster thermal response to disruptions which allows for faster startup time within the minute time scale rather than days [143]. This load flexibility leads to the possibility of intermittent operation following the fluctuations of renewable energy sources. Despite these promising results, electrically heated SMR is not feasible in the case study because the available electricity is used for water electrolysis. When electricity production is low, blue hydrogen is needed, so this process should not rely heavily on electricity.

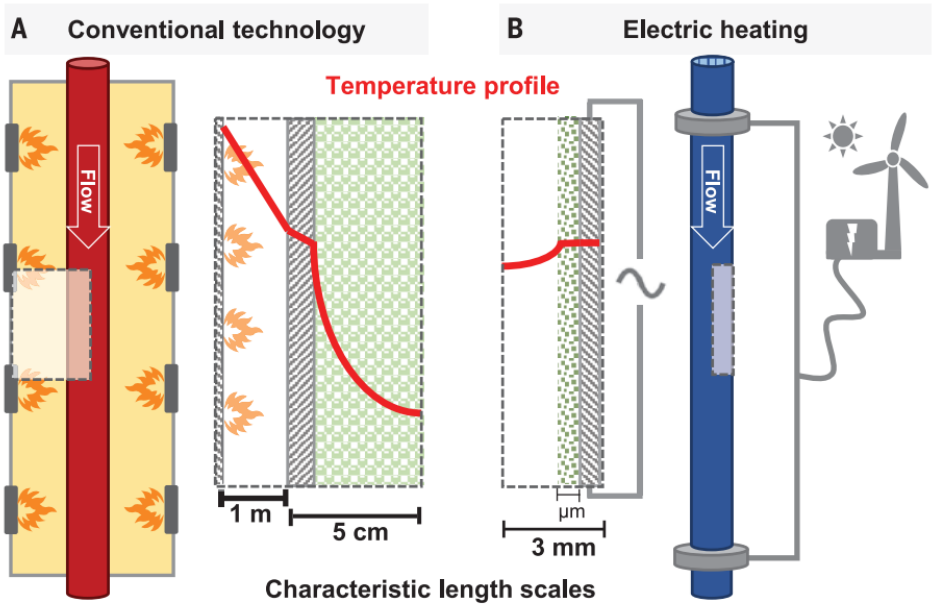

Figure 2.9: Heating principles of SMR. (A) Conventional fired reactor. (B) Electric resistance-heat reactor [142]

In conclusion, SMR is currently the most widely used and cost-effective method for hydrogen production. However, SMR is an inefficient method for production of blue hydrogen because of the poor CO_2 recovery and its highly endothermic reaction [86]. While alternatives burners show some improvements, the use of electrically heated SMR clashes with the use of electrolysis for hydrogen production, which is the true net-zero option for the future.

Partial Oxidation (POX)

Another well known way of producing hydrogen from methane is by partial oxidation. In this process methane will react with a limited amount of oxygen at high temperatures and pressures, resulting in the production of hydrogen and carbon monoxide.

The general reaction equation for higher hydrocarbons is:

$$\mathrm{C_mH_n}\ (g) + m/2\ \mathrm{O_2}\ (g) \longleftrightarrow m\ \mathrm{CO}\ (g) + n/2\ \mathrm{H_2}\ (g)$$

For methane the partial oxidation reaction can be represented as:

$$\mathrm{CH_4}\ (g) + 1/2\ \mathrm{O_2}\ (g) \longleftrightarrow \mathrm{CO}\ (g) + 2\ \mathrm{H_2}\ (g) \qquad (\Delta H_{298K} = -36 kJ/mol)$$

Large scale POX reactors operate at very high temperatures in the range of 1150-1500 °C and pressures between 25-80 bar. The ideal stiochiometry for the partial oxidation is at a methane to oxygen (CH_4/O_2) ratio of 2, resulting in a high yield of syngas [148]. Hydrogen production efficiency in POX is around 70%-80% [82]. The reaction is exothermic meaning that heat is released during the process and no external heating is required.

The main advantage of the POX process is the high feedstock flexibility, it will almost operate with any hydrocarbon feedstock from natural gas to coal. Compared to SMR and ATR, the POX process does not need a catalyst or steam as a reactant, simplifying the gas pre-treatment. Moreover, POX can achieve high carbon capture rates with pre-combustion capture technology. This is because the CO_2 is produced in a more concentrated form, allowing for more efficiently capture. In addition, small-scale POX systems show a high load flexibility due to the fast response time, making the reactor ideal for handling rapidly changing loads [82].

The main drawbacks of POX are the high operating temperatures, the need need for pure oxygen and the low hydrogen yields. POX typically produces less hydrogen compared to SMR and ATR, which can be a limitation for applications that require high hydrogen yields like ammonia production [145]. The process operates at very high temperatures which requires the burning of additional fuel, resulting in a less efficient process [82]. Additionally, POX requires pure oxygen, which increases the operational cost. These factors make POX less efficient and potentially more costly compared to other hydrogen production methods.

A solution to lower the systems operating temperature is to add a catalyst. This catalytic partial oxidation (CPO) shows promising results but is currently still in the research phase. Temperature control is proving challenging, resulting in problems with coke and hot spot formation, which damage the catalyst [145].

Autothermal Reforming (ATR)

Autothermal reforming combines the principles of steam reforming and partial oxidation in a single reactor in the presence of a catalyst. First, methane is partially oxidized exothermically with oxygen. This supplies the heat for the subsequent endothermic steam reforming reaction on the catalyst.

Combining gives the following reaction:

$$\mathrm{CH_4}\ (g) + 1/2\ \mathrm{H_2O}\ (g) + 1/4\ \mathrm{O_2}\ (g) \longleftrightarrow \mathrm{CO}\ (g) + 5/2\ \mathrm{H_2}\ (g) \qquad (\Delta H_{298K} = -77.2 kJ/mol)$$

Operating conditions of ATR depend on what kind of syngas is needed. For high hydrogen yields autothermal reforming typically takes place at high temperatures of around 900-1150 °C and pressures between 1-80 bar [83]. However, syngas selectivity is maximized at temperatures higher then 1200 °C. Other operating parameters are the oxygen/carbon (O/C) and steam/carbon (S/C) ratios which differ slightly from literature but typical values of around 0.45-0.6 (O/C) and 1-2 (S/C) [9] [90]. The gas hourly space velocity (GHSV) is optimal between a range of 1050-14.000 and the performance of the ATR drops significantly when the GHSV is outside these boundaries [48], limiting the volume flexibility.

Carbon capture is easier and more efficient with autothermal reforming (ATR) compared to steam methane reforming (SMR) for producing blue hydrogen. The ATR process takes place in a single reactor which eliminates the need for an external furnace. As a result, all CO_2 emissions are concentrated in the product syngas stream, eliminating the need for separate CO_2 capture systems required

for SMR's flue gas stream. This allows for relative cheaper and higher percentage of CO_2 capture with ATR [114].

Another key advantage of ATR compared to the alternatives is that it has a broad operating range and very high volume flexibility. According to Air Liquide, an ATR can be operated at 30-110% of its nominal capacity, with minor design adjustments. Even an very large unit can be operated with ramp-up and ramp-down rates as fast as 1.5% of its capacity per minute [14]. These are both very important considering the expected intermittency of green hydrogen supply.

Novel new techniques

Besides these three main reactors novel new techniques are developed to enhance the natural gas reforming process. These include the earlier mentioned electrified SMR and the catalytic partial oxidation (CPO). Other techniques like sorbtion enhanced SMR, dry reforming and tri-reforming could increase the flexibility of the process. However, these reactors are not taken into account because off their low technical readiness. The case-study focuses on large scale proven solutions and evaluates how those techniques operate flexible.

2.2.3. Water Gas Shift Reaction

After the reactor the formed carbon monoxide is converted into additional hydrogen and carbon dioxide using steam. This Water Gas Shift Reaction (WGSR) is a moderately exothermic reaction meaning that heat is released during the process. This process is typically conducted in two stages: first, a high-temperature (320-450 °C) stage utilizing an iron-based catalyst, followed by a lower-temperature (150-250 °C) stage using a copper-based catalyst [11].

The somewhat exothermic shift reaction:

$$\mathrm{CO\ (g) + H_2O\ (g)} \longleftrightarrow \mathrm{CO_2\ (g) + H_2\ (g)} \qquad (\Delta H_{298K} = -41.1 kJ/mol)$$

The unfavourable equilibrium of the WGSR at higher temperatures can be overcome by carrying out the reaction in two steps using different catalyst suited to the optimal temperature range each. The first stage uses faster reaction rates at higher temperatures, while the second stages takes advantage of the favorable equilibrium for hydrogen at lower temperatures [111].

The effect of pressure does not effect the equilibrium of the WGSR because there is an equal number of moles on both sides of the reaction. Therefore changing the total pressure does not shift the equilibrium position of the WGSR. However a higher pressure will accelerate the forward reaction rate before equilibrium is established [92].

The inlet feed compositions like CO, H_2 and CO_2 will change depending on the process and operating conditions, thereby affecting the maximum equilibrium CO conversion. For this reason, the water content in the WGSR is an important parameter in obtaining higher or lower CO equilibrium conversions. An increase in the steam to carbon monoxide ratio improves the CO equilibrium conversion, but results in an decrease in efficiency [92]. A research paper shows for a high-temperature iron-based WGSR catalyst for hydrogen production shows a long-term time on stream stability at a steam to CO ratio of 1.5 [29].

2.2.4. Carbon Capture, Transportation and Storage

A crucial step in creating low-carbon blue hydrogen is to capture the CO_2 and prevent the emissions of this green house gas. The system can be split into three stages: CO_2 capture, transport and storage. There are different techniques available for this capturing, transporting and storing of CO_2, with the optimal approach depending on factors like the plant's location and targeted CO_2 capture rate.

Carbon capture techniques

The technique used for CO_2 capture depend on the conditions of the CO_2-containing streams. For blue hydrogen CO_2 can be captured form two types of streams:

1. **Post-combustion CO_2 capture:** This involves capturing CO_2 from combustion flue gas streams, such as those form the (pre)-reformer furnace. These streams are typically at near-atmospheric

pressure and contain low concentration of CO_2, diluted with nitrogen, oxygen, and other combustion products. This represents an important limitation for CO_2 capture. The low CO_2 concentration requires powerful chemical solvents and therefore high energy amounts have to be used to regenerate the solvent.

2. **Pre-combustion CO_2 capture:** Downstream of the water gas shift reactors CO_2 is captured from the process stream. This stream contains high-pressure CO_2 at high concentrations. Thus, the applied equipment to separate CO_2 from the referred stream can be smaller and different solvents can be used with lower energy consumption for refrigeration [108].

The four mature separation techniques found in literature for carbon capture during hydrogen production from natural gas are:

- Absorption
- Adsorption
- Membrane Separation
- Cryogenic separation

Absorption

Absorption of CO_2 can be split in two subcategories. Chemical absorption is used for low CO_2 partial pressures and therefor ideal for post-combustion CO_2 capture. Physical absorption is suitable for high CO_2 partial pressures commonly present in pre-combustion streams.

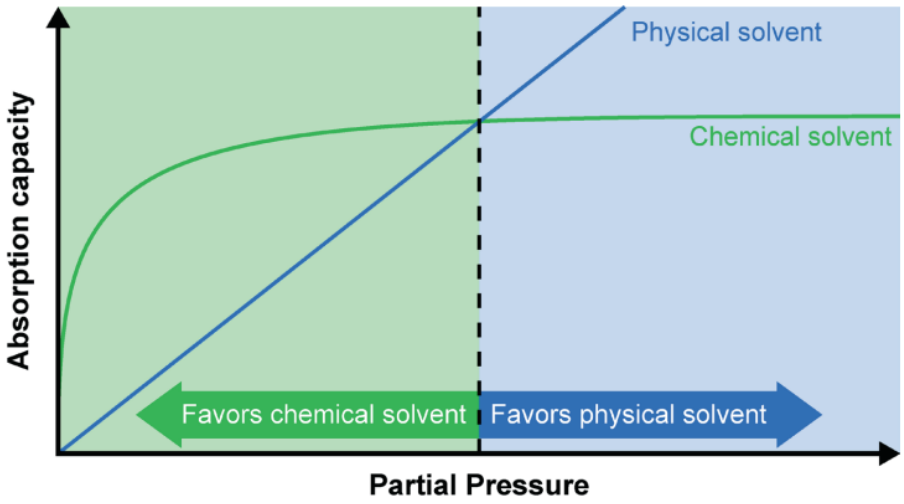

Figure 2.10: Comparison of effectiveness of reactive chemical absorption and physical absorption [153].

Chemical Absorption:

The working principle of chemical absorption is that CO_2 chemically reacts with the solvent, typically an amine-based solution like monoethanolamine (MEA). This forms a reversible chemical bond between the CO_2 and the amine groups in the solvent.

Generally, even with low concentration of CO_2 gas, chemical absorption has a high selectivity ideal for post-combustion CO_2 capture. But the desorption process therefor requires high energy input to reverse the chemical reaction and regenerate the solvent [64].

Physical Absorption:

For physical absorption the CO_2 is absorbed into the solvent through physical intermolecular interactions, without any chemical reactions. It is generally considered to be based on Henry's law, which states that a dissolved gas loading in a physical solvent is proportional to the partial pressure of the gas [97].

This absorption is favored at high CO_2 partial pressures and low temperatures. The solvent desorbs the CO_2 under the condition of lower partial pressure. Since CO_2 is separated from the solvent using a driving force of a pressure difference, it is possible to remove and recover CO_2 with less energy compared to chemical absorption.

This reduced energy need for carbon capture makes pre-combustion CO_2 capture of ATR/POX using physical absorption advantageous compared to post combustion CO_2 capture with chemical absorption needed for SMR.

Adsorption

Adsorption is a process where CO_2 molecules adhere to the surface of a solid absorbent material through physical or chemical interactions. Adsorbents which could be used for CO_2 capture include activated carbon, alumina, metallic oxides and zeolites [113].

Adsorption processes can by grouped in two types regarding the desorption process. By changing the pressure: Pressure Swing Adsorption (PSA) & Vacuum Swing Adsorption (VSA), or by changing the temperature: Temperature Swing Adsorption (TSA) & Electric Swing Adsorption (ESA) [108].

Solid adsorbents are more energy-efficient than absorbents, but scaling them up for large-scale systems presents several challenges. One major issue is the low adsorption capacity of most available adsorbents, which can be problematic at such scales. Additionally, the flue gas streams must be treated to achieve high CO_2 concentrations due to the generally low selectivity of most available adsorbents. For example, zeolites tend to have a stronger affinity for water vapor [64].

Membrane separation

Among the different CO_2-capture technologies, membrane separation is considered one of the most promising solutions due to its energy efficiency and operational simplicity [96]. Membranes are particularly suitable for CO_2 separation due to the inherent high permeability of carbon dioxide molecules.

Carbon dioxide has a smaller kinetic radius compared to lighter gases like oxygen, nitrogen, and methane present in the syngas. Only helium and hydrogen have smaller molecular sizes than CO_2 [33]. This intrinsic property of carbon dioxide, coupled with its high solubility and diffusivity in many membrane materials, makes membranes an attractive technology for efficient CO_2 separation and capture.

Although membrane technology has advantages for capturing CO_2, current CO_2 separation membranes are still insufficient [35]. To be practical for large-scale industrial use, new membranes that effectively balance permeability and selectivity need to be developed, ensuring efficient and cost-effective CO_2 separation processes.

Cryogenic separation

Cryogenic CO_2 separation works by cooling and condensing the CO_2 present in the mixture. An advantage of this technique is that it enables direct production of very pure liquid CO_2, which can be transported or stored via liquid pumping instead of compression of gaseous CO_2, saving energy on the compression steps [146].

The first step of liquefaction is to compress the mixture to a high pressure. Then the compressed mixture is cooled to cryogenic temperatures. This cooling process results in the condensation of CO_2 into a liquid phase, while other components such as hydrogen remain in the gaseous phase. This phase separation is achieved trough a combination of refrigeration cycles, heat exchanger and flash separations.

A disadvantage of cryogenic CO_2 separation is the amount of energy required in refrigeration, especially for diluted gas streams. For this reason cryogenic CO_2 recovery is limited to streams that contain high concentrations of CO_2 with a lower limit of about 50% [33]. It also needs pre-purification of water and heavy hydrocarbons that otherwise freeze on the heat exchangers causing problems in the separation process. So cryogenic separation of CO_2 is most applicable to high pressure gas streams with high concentration of CO_2 in which the liquid CO_2 can directly be stored or shipped away.

Carbon transportation techniques

Transportation of CO_2 is a well-developed process, as its technical requirements align closely with those of transporting other gases [108]. Given that CO_2 is frequently produced in locations separate from where it is utilized or stored, efficient transportation methods are essential. This can be achieved via pipelines, ships, or tanker trucks. Pipelines are generally considered the most cost-effective and reliable method for moving large volumes of CO_2. However, in some situations or locations, transporting CO_2 by ship may offer economic advantages, particularly for long-distance or overseas transportation, as illustrated in Figure 2.11.

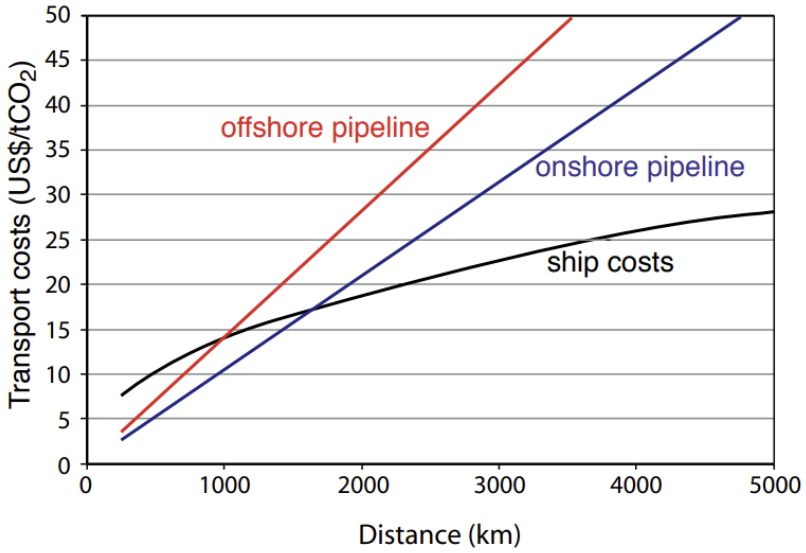

Figure 2.11: Transport costs plotted against distance for offshore pipeline, onshore pipeline and ship costs. Ship costs include intermediate storage facilities, harbour fees, fuel costs, and loading and unloading activities. Costs include also additional costs for liquefaction compared to compression. [147]

For both shipping and pipeline, the carbon dioxide stream needs to be processed before transportation in order to remove impurities and increase the volumetric density. When using pipelines, the carbon dioxide is compressed and the water content is reduced to prevent the formation of acidic compounds that can corrode the pipelines [132]. This water and other volatiles also cause problems for shipping because the carbon dioxide is liquefied by cooling and compression before loading onto specialized CO_2 carrier ships. Removing the water vapor and other volatile impurities is important to prevent dry ice formation in the liquefied CO_2.

Two examples where CO_2 is transported in the Netherlands are the Porthos and Northern Lights projects. In the Porthos porject, CO_2 is transported by pipeline from the harbour of Rotterdam to an empty gas field nearby. In the Northern Lights project, CO_2 is transported by ship from Yara Sluiskil to Norway where it is also stored in an empty gas field.

Carbon storage

The last step is to store the captured and transported CO_2. This carbon storage, also known as carbon sequestration, involves the long term storage of captured CO_2 in secure geological formations or other suitable locations, preventing the release of the green house gas into the atmosphere.

There are several different options for CO_2 storage. The most common is injecting the captured CO_2 into deep underground rock formations such as saline formations or depleted oil and gas reservoirs. Other more unconventional storage options are Basalts, unminable coal seams and organic shales [57]. Once the CO_2 is compressed and injected into the geological formation, the CO_2 becomes trapped trough various mechanisms, such as structural trapping, residual trapping, solubility trapping and mineral trapping [38]. An important step is to choose a secure site and monitor the long-term integrity of the CO_2 storage process to prevent leakage from the storage site.

2.2.5. Hydrogen purification

The last step in the process is hydrogen purification. There are three conventional gas separation methods for large scale separation hydrogen from the process stream. These are membrane separation, pressure swing adsorption and cryogenic distillation.

Separation method for hydrogen	Principle	Hydrogen output		Comments
		Purity	Recovery	
Pressure swing adsorption (PSA)	Partial condensation of gas mixture at low temperatures	99.999%	70-85%	-High energy consumption -Hydrogen lost in purging step
Membrane separation	Differential rate of diffusion of gases through a permeable membrane	92-98%	>85%	-Membrane degradation at high temperatures -Inverse relationship of permeability and selectability
Cryogenic distillation	Partial condensation of gas mixtures at low temperatures	90-98%	95%	-High energy consumption -High operating costs -Prepurification step necessary

Figure 2.12: Comparison of hydrogen purification techniques (adjusted from [42]).

Pressure Swing Adsorption (PSA)

Currently the most widely used technique for the production of high-purity hydrogen from a gas mixture containing 60-90 mol% hydrogen is by using Pressure Swing Adsorption (PSA) [84]. The process uses adsorbent materials like zeolites or activated carbon that selectively adsorbs impurities gases like CO_2, CO, CH_4 and N_2 at high pressures, allowing the hydrogen to pass through and be collected as a high purity product stream. The adsorption occurs in a cyclic process of pressurization, adsorption, depressurization, and purge steps to continuously produce purified hydrogen.

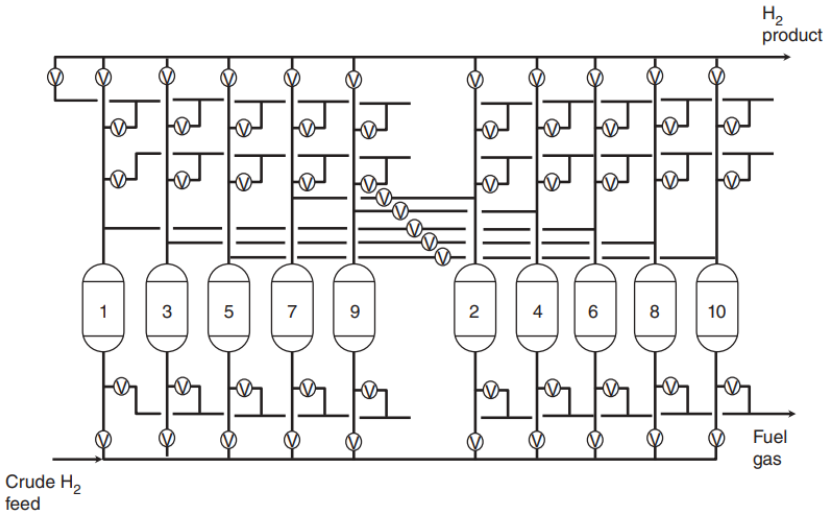

Figure 2.13: Schematic flow diagram for the Poly-bed PSA process

Key performance variables for an industrial hydrogen PSA process are the hydrogen purity, hydrogen recovery rate from the feed gas and hydrogen productivity. In most cases the hydrogen purity is at very high levels (99.995%), needed for applications like fuel cells and ammonia production. The hydrogen recovery rate is typically around 80% to 90% [99] [98]. A small difference in the recovery rate can have a large error of revenue for the hydrogen production facility [84].

Despite its advantages, PSA also has some drawbacks, such as high production cost due to low recovery rates and reduced absorbent capacity over time [13]. The exothermic adsorption of impurities like CO_2, CH_4 en CO releases heat, causing temperature gradients within the adsorption bed. These temperatures variations complicate the desorption process [138].

Membrane separation

Membrane separation of hydrogen from syngas uses semi-permeable membranes that selectively allow hydrogen molecules to permeate based on their size and specific properties. The syngas mixture is fed into a membrane module filled with thousands of hollow fibers made of polymer or carbon molecular sieves. Due to their smaller size, hydrogen molecules permeate through the dense membrane material more easily than larger molecules like CH_4 or CO_2. This process results in a hydrogen-rich permeate stream on one side of the membrane and a waste stream on the retentate side.

Membrane separation offers several advantages as it is more energy-efficient than other separation methods as no heating/cooling is required. Also continuous operation is possible without the need for intermittent cycles or regeneration. However, challenges remain in developing membranes with high selectivity, along with high permeability and stability under harsh conditions [98].

Cryogenic distillation

Cryogenic separation works by partially condensing the syngas mixture at extremely low temperatures. At these conditions, impurities such as CO, CO_2, CH_4 and N_2 condense into liquid form, while hydrogen remains in the gaseous phase. This phase difference allows for the separation of hydrogen from the other components.

The advantages of using Cryogenic separation is that it can be used on a large scale and has a high recovery rate of around 95%. However a disadvantages is the low purity of the hydrogen of around 90-98 % [42]. Additionally, the process is energy intensive and has high capital costs [98].

2.3. Green hydrogen production

Green hydrogen is produced when electricity from renewable sources is used to split water into hydrogen and oxygen through a process called water electrolysis, performed by an electrolyser system. Unlike blue hydrogen, which still emits some greenhouse gases during production, green hydrogen is produced without any greenhouse gas emissions, making it truly a clean fuel for the future [125].

The electrolysis process takes place in an electrolyser unit consisting of an anode and a cathode separated by an electrolyte membrane. When voltage is applied to the electrolyser, water molecules split into hydrogen ions and oxygen ions at the respective electrodes [149]. At the anode, oxygen ions release electrons to form oxygen gas, while at the cathode, hydrogen ions gain electrons to form hydrogen gas.

The overall reaction of water electrolysis:

$$2\ \mathrm{H_2O}\ (\mathrm{l}) \longrightarrow 2\mathrm{H_2}\ (\mathrm{g}) + \mathrm{O_2}\ (\mathrm{g}) \qquad (\Delta H_{STP} = +285.83 kJ/mol)$$

The minimal energy required to continuously split water using only an external power source, such as offshore wind power, at standard temperature and pressure (STP) is equal to the enthalpy change (ΔH) of the water splitting reaction, which is 285.8 kJ/mol (39.34 kWh/kg_{H_2}) [41]. This enthalpy change consist of Gibbs free energy (ΔG) plus the heat generation (TΔS) [94]. The Gibbs free energy represent the minimum electrical energy required for the electrolysis process, which is 237.2 kJ/mol at STP [70]. The additional thermal energy, 48.6 kJ/mol at STP, is needed to keep the process at constant temperature if there is no external heat source. However, in practical applications the energy requirements are higher due to inefficiencies in the system such as electrolysis losses like ohmic, activation and mass transfer losses [93], and system energy requirements for components like pumps and compressors.

The actual amount of energy required to produce hydrogen can be calculated by:

$$\Delta H_{actual,H_2} = \frac{\Delta H_{min,H_2}}{\eta_{system}} \tag{2.7}$$

Where $\Delta H_{actual,H_2}$ is the actual energy required per kilogram of hydrogen (kWh/kg), $\Delta H_{min,H_2}$ is the minimum energy required to split liquid water into gaseous hydrogen and oxygen, based on the Higher Heating Value (HHV) of hydrogen (39.34 kWh/kg under STP conditions). Therefore, the efficiency of the whole system, η_{system}, must also be based on the HHV.

To calculate the amount of hydrogen produced from energy source like offshore wind:

$$m_{H_2} = \frac{E_{available}}{\Delta H_{actual,H_2}} = \frac{E_{available} \times \eta_{system}}{\Delta H_{min,H_2}} \tag{2.8}$$

Here, m_{H_2} is the mass of hydrogen produced (kg) and $E_{available}$ the energy supplied from a source like an offshore wind farm (kWh).

Different electrolysis technologies are available, with the main types being Alkaline Electrolysis (AEL), Proton Exchange Membrane Electrolysis (PEM), and Solid Oxide Electrolysis (SOEC). Each type of electrolyser has distinct advantages and disadvantages depending on their application. For an overview of the main characteristics for the different electrolysers see Appendix A.1.

If electrolysers are only coupled to renewable energy sources, it is important that it is able to operate efficiently over a large load range from 0 to 100% of its designed capacity, as there are periods where there is no electricity produced. Compared to AEL and SOEC, PEM shows good flexibility as they are able to operate between 0-100% of its designed capacity and have a fast response time allowing it to follow the intermittent supply of electricity from renewable sources [122]. However, the catalyst of PEM requires noble metal catalyst and suffers a short lifetime of around 10 years. This creates a lock-in situation and could lead to problems for further up-scaling of green hydrogen production. New technologies are being developed to address the need for noble catalyst while still providing flexible operation. One such technology is the Battolyser, an electrolyser that uses a non-noble Nickel/Iron catalyst and supports 0-100% nominal load operation [95]. However, this technology is still in the development phase and has not yet been proven on large scale.

2.4. Hydrogen storage, transportation and networks

With an increasing amount of hydrogen from renewable sources the need for flexibility-providing facilities only grows. Here the role of flexible blue hydrogen and its cost can be compared with the flexibility offered by storage of hydrogen to see which option is more cost effective. Different storage techniques are available for short term storage to long seasonal storage. However, storage sites also have their limitations regarding their location, size, leakage, cost and efficiency. In addition, the need for flexible blue hydrogen also depends on the ability to cheaply import hydrogen via ammonia and if their is a connected network of suppliers and users [106].

2.4.1. Hydrogen storage

It is difficult to store hydrogen with high efficiency because of the very low density, 1 kg of hydrogen gas occupies 11 m^2 at standard conditions. The density of hydrogen must be increased to make storage of hydrogen at large scale possible. There are four ways of storing hydrogen.

1. As a compressed gas in: Salt caverns, Depleted oil and gas fields, Aquifers, Conventionally mined rock cavern, Pressure vessel or Line packing in pipelines.
2. As a liquid in tanks
3. As a solid by absorbing or reacting with metals or chemical compounds
4. As a chemical by converting it into ammonia for instance

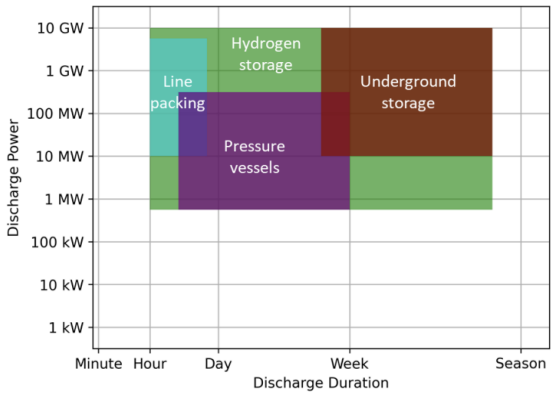

Figure 2.14: Hydrogen storage duration and discharge power [17].

A lot of research goes into reducing the cost of hydrogen generation. However, there has been little attention to the extra cost of hydrogen storage needed in more flexible systems [1]. The lowest levelised cost of hydrogen storage (LCHS) is for line packing with an estimated LCHS of $0.05 per kg hydrogen [17]. In this method hydrogen is pressurised in the pipelines connecting production facilities to end-users. The storage capability of line packing depends strongly on the size of the hydrogen network and it typically provides a very short storage duration of around one day or less.

When a hydrogen network is not available, the next most cost-effective storage option is the use of salt caverns. The cost for this method is approximately $0.14 per kg of hydrogen for a 15-day storage period and around $1.20 per kg of hydrogen for a 120-days storage period. Salt caverns are the best option for long term hydrogen storage due to their low leakage rates. However, this option is geographically limited to areas where suitable salt caverns are available.

If both line packing and salt caverns are not possible, then above ground compressed hydrogen can be used for short term storage. This method has a LCHS of around $0.33 per kg of hydrogen for storage duration of one day. Unlike the other methods, above ground compressed gaseous storage is not location-dependent and can be used everywhere. A major downside to this storage method is it high leakage rate, which is an important parameter for long-term storage. For example, the LCHS for storing hydrogen in above ground storage for 120 days is $25.20 per kg of hydrogen, making it far cheaper to produce hydrogen than to store it for such a long period.

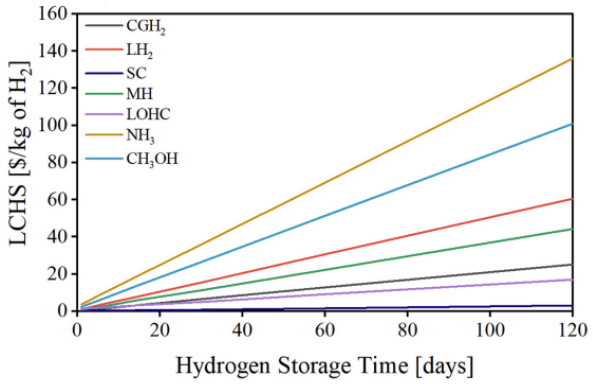

Figure 2.15: Change of levelised cost of hydrogen storage with time. (CGH_2; Compressed gaseous hydrogen, LH_2; Liquid hydrogen, SC; Salt cavern, MH; Metal hydride, $LOHC$; Liquid organic hydrogen carrier, NH_3; Ammonia, CH_3OH; Methanol [1])

Flexible blue hydrogen could reduce the need for long term hydrogen storage. Comparing the extra cost of flexible operation to the reduced cost of hydrogen storage can help to determine if flexible blue hydrogen is economically favorable.

2.4.2. Hydrogen transportation

Transporting hydrogen is needed to connect production sites with end-users. Hydrogen can be transported via pipelines, rail, ships and innovative methods like ammonia or metal hydrides [110].

For short to medium distances, hydrogen pipelines are the most cost effective method for transporting large volumes of hydrogen. Pipelines can continuously supply hydrogen and allow for line-pack storage which also stabilizes a hydrogen network. The cost of transportation of hydrogen by pipeline is around $0.1-1.00 per kg hydrogen per 100 km [110].

For long distances, shipping hydrogen can be more advantageous. Due to hydrogen's low volumetric density, specialized cryogenic ships are required to transport liquid hydrogen at extremely low temperatures (-253 °C). However, handling cryogenic hydrogen is complex and energy-intensive, which increases costs and logistical challenges.

An alternative to cryogenic shipping is to chemically bind the hydrogen, transforming it into ammonia for transportation. Ammonia is easier and cheaper to ship over long distances compared to cryogenic hydrogen, with a Rotterdam-Australia route cost estimations of $0.56 per kg hydrogen [68]. This ammonia can be reconverted to hydrogen at the destination.

Comparing the cost of transportation and import with the ability to produce hydrogen flexible on location can show if importing hydrogen would be more beneficial than importing natural gas for hydrogen production. A recent study shows that importing renewable ammonia from locations with low-cost renewable resources (<$20 MWh) and converting it to hydrogen can be cost competitive with producing local renewable hydrogen in northern Europe using offshore wind ($50 MWh) [2]. However, the development of green ammonia production in countries with the potential for cheap renewable energy remains uncertain, creating a significant uncertainty for blue hydrogen production in the Netherlands.

2.4.3. Hydrogen networks

The need for flexible blue hydrogen also depends on how the hydrogen network will develop in the Netherlands. Currently, hydrogen is produced at the industrial site where hydrogen is needed, mostly by using SMR without carbon capture and storage. However, plans are made to couple the industrial cluster where hydrogen is produced with demand centers and storage facilities, allowing for line packing to balance fluctuations in supply and demand.

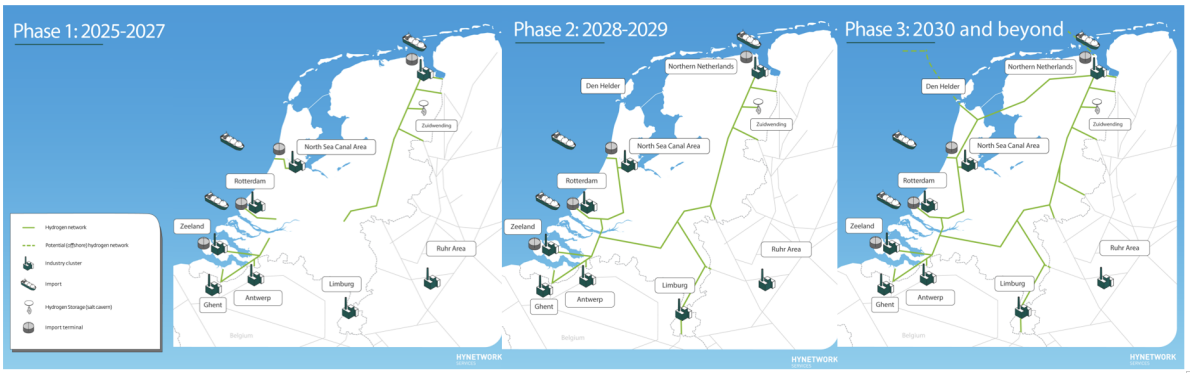

Figure 2.16: Expected development of hydrogen network in the Netherlands [134]

The different scenarios of regional production vs national production using a hydrogen network can be seen in Figure 2.17. Here a simulation shows the possible imbalance in a hydrogen net with the different future scenario's [106].

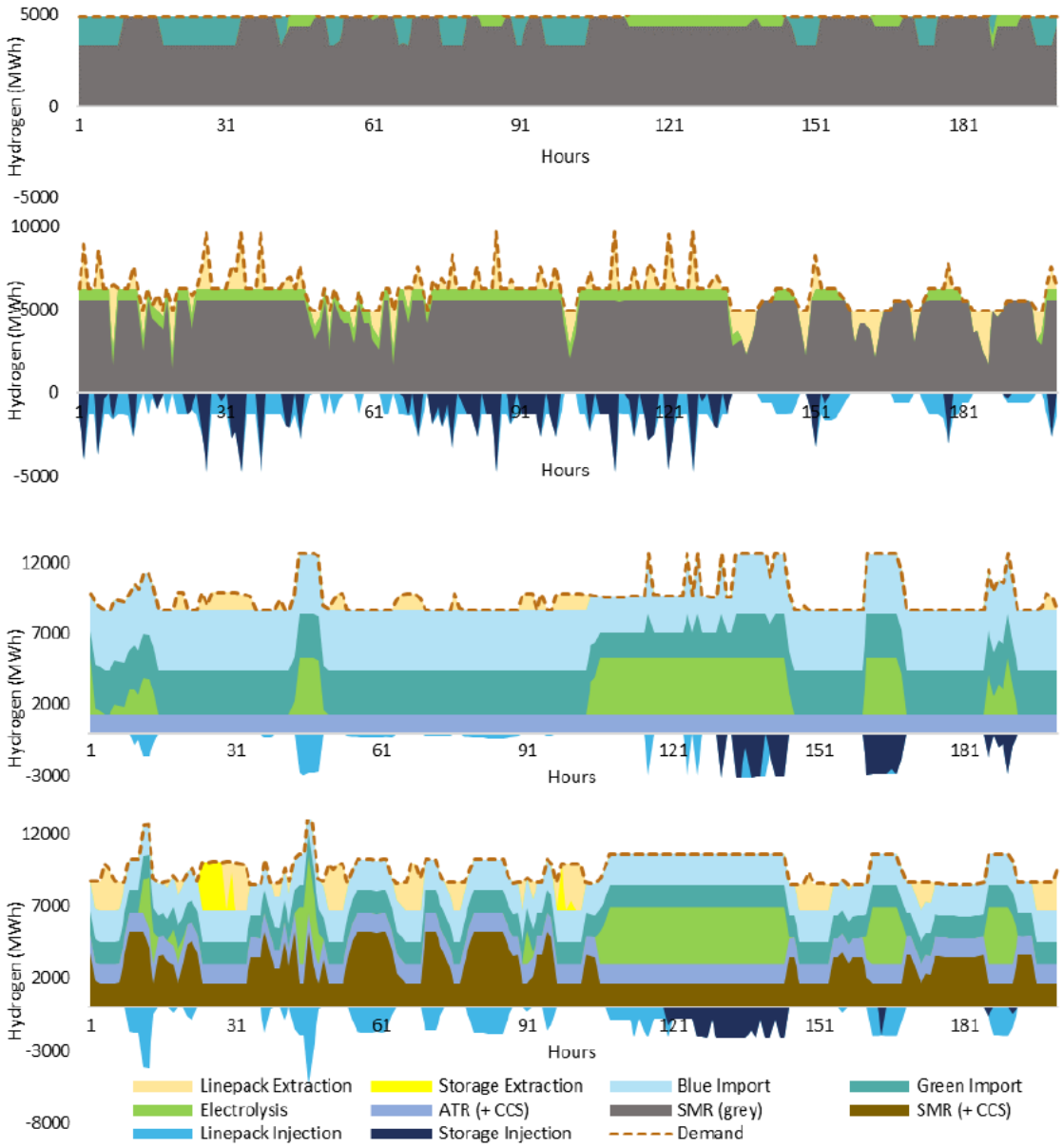

Figure 2.17: Weekly hydrogen balance simulated for a week in October (From above to below: 2027-regional, 2027-national, 2030-cheap NH3 import, 2030-expensive NH3 import) [106]

The research concludes that with rising hydrogen demand and an increasing supply form variable sources after 2030, the system will require more flexibility. In every scenario, all flexibility providing facilities are needed. These include storage, import, and flexible blue hydrogen production, but with different importance [106].

2.5. Ammonia production

For the case study flexible blue hydrogen production is used to balance out the intermittent supply of green hydrogen to ensure a continuous supply of hydrogen for the downstream process of ammonia production. Currently, the production of ammonia is a significant contributor to global greenhouse gas emissions, primarily due to its reliance on hydrogen produced from fossil fuels. In 2020, of the 185 Mt of ammonia produced globally, 72% relied on natural gas-based steam reforming, 26% on coal gasification, about 1% on oil products, and a fraction of a percentage point on electrolysis [56].

To meet energy transition goals, a shift in hydrogen production technologies is needed. Applying Carbon Capture and Storage (CCS) to existing fossil-based methods, combined with increasing the share of hydrogen produced from water electrolysis using renewable energy, will play a key role. For this reason, the case study will use ammonia production as a representative downstream process to demonstrate how flexible blue hydrogen production can stabilize intermittent green hydrogen production, ensuring a reliable hydrogen supply while reducing emissions for ammonia production.

Ammonia production is carried out through the Haber-bosch process. For this case study the hydrogen can be supplied by either natural gas reforming or water electrolysis while the nitrogen is supplied by cryogenic distillation of air. The hydrogen and nitrogen gases are mixed in a stoichiometric ratio of 3:1 and enter an iron-based catalytic reactor at high temperatures of around 450-500 °C and very high pressures of 100-300 bar [118].

The exothermic Haber-Bosch reaction:

$$\mathrm{N_2\ (g)} + 3\ \mathrm{H_2\ (g)} \longleftrightarrow 2\ \mathrm{NH_3\ (g)}$$

At the operating conditions mentioned above, only around 15% of the hydrogen is converted into ammonia in a single pass through the reactor. Ammonia is then separated form the unreacted gases by cooling and condensation. The unreacted gases are recycled back into the reactor. Eventually a conversion of 97% can be achieved [5]. The exothermic heat from the reactor is often used too generate steam for the reforming process.

The need for a continuous supply of hydrogen is because the ammonia synthesis loop is normally designed to always run at its full capacity or close to full capacity. Operating a conventional ammonia synthesis loop at less than 60%-70% capacity is not practical or attractive [116]. However, a lot of research is being done to increase the load flexibility of ammonia plants in order to follow the intermittent supply of green hydrogen. An ammonia synthesis loop coupled with a renewable powered front end may need to handle fast load changes and operate efficiently at low loads of around 20-25% of its nominal capacity [116]. If this is economically not viable than flexible blue hydrogen can be a solution to further decarbonize this industry.

3

Basis of Design

The Basis of Design will clarify which design choices were made for the case study, using information from the literature study. It describes what is inside battery limit of the project and also clearly states whats outside the battery limit. In addition, all assumptions made for the project will be clearly stated. The conceptual process design is developed using the hierarchical Douglas approach for process design [32].

3.1. Process design

3.1.1. Background

A case study of flexible blue hydrogen production is made to compensate for the fluctuating green hydrogen supply ensuring a steady feed for a down stream process like ammonia production. Ammonia production is one of the chemical sectors where green hydrogen can play a key role in replacing fossil fuels. However, the supply of green hydrogen will likely fluctuate due to the intermittent nature of renewable sources. While there are storage options for hydrogen, large-scale storage is not always available. Blue hydrogen can help balance the supply of hydrogen, ensuring consistent and efficient ammonia production.

The consequences of operating a blue hydrogen plant is not well known. Therefore, this case study will focus on the technical aspects of operating a blue hydrogen production plant with regards to its volume flexibility. The entire natural gas reforming process will be inside the battery limit, while the rest of the operating units, like the electrolyser and ammonia production plant, will only provide the boundaries like hydrogen demand and flexibility needed.

3.1.2. Process definition

The best process options for blue hydrogen production in the port of Rotterdam are chosen based on the information found in the literature. Using this information a simple process flow scheme is developed, connecting the different process streams and estimating the process conditions.

Continuous vs batch

The blue hydrogen production process is chosen to operate continuously due to the high maximum production capacity of 22.88 tonnes of hydrogen per hour, required to produce a total of 1 million tonnes of ammonia annually. Natural gas reforming is challenging to run batch-wise because there are a lot of catalytic reaction so the temperature cannot drop below a certain threshold in order to prevent catalyst deactivation. Additionally, the downstream process of ammonia production is run continuously so a constant stream of pure hydrogen is required.

Reactor choice

The first step of designing a process plant for blue hydrogen production is to choose the reactor. The mature choices are between SMR, ATR and POX. As described in the literature, see Chapter 2.2.2, ATR shows the most promising results for the boundaries set by the case study. It has a better hydrogen

yield compared to POX [145]. Additionally, ATR allows for easier carbon capture integration compared to SMR making it more suitable for blue hydrogen production [26]. ATR also allows for more flexible operations because both the exothermic and endothermic reaction occur in the same reactor. This allows for inherent more flexible operations due to a fast ramping speed of 1.5 % per minute, compared with SMR which limits its ramping speed to 5% per hour due to the use of external burners [78] [102]. This fast ramping speed, and the ability to operate at least between 30-100% of its designed capacity, allows ATR to better balance out large fluctuations in hydrogen produced from variable green hydrogen. For these reasons ATR is chosen as the reactor of the process.

The ATR reactor requires three feed streams: steam, methane and oxygen. The oxygen supply can range from direct air as an oxidant to pure oxygen from a cryogenic air separation unit (ASU). Using direct air simplifies the process as there is no need for an expensive ASU, but this introduces a large nitrogen surplus. This surplus requires a cryogenic nitrogen removal unit before the ammonia synthesis loop or a large purge stream from the ammonia synthesis, increasing process complexity. Additionally, using direct air results in large flow rates and equipment size, which raises capital and operational costs. Thus, direct air is generally less efficient and certainly not ideal for ammonia synthesis [101].

For a large-scale ammonia plant as downstream process, oxygen-enriched air is the preferred choice as it can supply the correct stoichiometric ratio of nitrogen to hydrogen for ammonia synthesis. This minimizes the excess nitrogen and avoids unnecessary nitrogen removal equipment downstream, therefor offering a better efficiency than plain air [101]. However, for downstream processes other than ammonia synthesis, pure oxygen is favored because it provides a nitrogen-free syngas, which increases the overall efficiency of the plant. The absence of nitrogen minimizes flow rates, allowing for smaller equipment sizes and lower energy consumption. The focus of this study is flexible blue hydrogen production so the choice is made to use pure oxygen as to not limit the results of the case study on flexible blue hydrogen production only to the downstream process of ammonia production, but flexible blue hydrogen can also be used for ensuring a stable supply of hydrogen to other downstream processes like methanol synthesis or a hydrogen network.

The typical operating conditions for ATR range form 950-1150 °C and 1-80 bar [83]. In this case, an elevated pressure of 40 bar is chosen to ensure compatibility with the downstream ammonia synthesis process, which operates at high pressures between 100-300 bar. This reduces the need for extensive hydrogen compression between the processes. An operating temperature of 1200 °C is used because at this temperature syngas selectivity is maximized [83].

Feed pretreatment

The LNG used as feedstock often contains small amounts of sulfur compounds depending on the source. In this case study the composition of LNG used is from Qatar, see Appendix Figure A.6 and Figure A.7. This sulfur damages the catalysts in the reactor and for that reason need to be removed. This is done by a hydrogenation reactor where the LNG is mixed with hydrogen. After this process the hydrogen sulfide (H_2S) will react with zinc oxide (ZnO) in a seperate reactor. This purified stream will then enter the pre-reformer. The pre-reformer will transform the higher-hydrocarbons into methane to allow for more efficient reactor operations. Both the desulfurization and pre-reformer will increase the feedstock flexibility of the plant.

Water-gas shift reactor

A two staged water gas shift reactor will be used to convert the carbon monoxide (CO) present in the syngas to carbon dioxide (CO_2) and extra hydrogen (H_2). This process takes place after the ATR and uses two catalytic reactors. A high-temperature reactor with an iron catalyst, followed by a low-temperature reactor with a copper catalyst. Two reactors are used to take advantage of both the thermodynamics and the kinetics of the WGS reaction. This results in higher hydrogen yields while lowering the CO levels required for downstream processing.

Carbon capture and storage

Since ATR is the chosen reactor, it will produce a single concentrated source of carbon dioxide. Due to the high operating pressure in the reactor, which is necessary for compatibility with downstream processes, the CO_2 stream will remain under high pressure. Given these conditions, the preferred method for carbon capture is absorption using a physical solvent, as shown in Figure 2.10.

There are many different physical solvents that can be used for CO_2 capture, the main commercially available types found in literature are Selexol, Rectisol, Fluor and Purisol [128]. For this process Selexol is chosen as the solvent for CO_2 capture because of its effectiveness at high pressures and moderate temperatures, combined with its CO_2 selectivity and operational simplicity. Unlike Rectisol and Fluor, Selexol does not require cooling the syngas to cryogenic temperatures, which simplifies the process and reduces energy consumption [64]. In addition, Selexol offers a simpler process compared to Purisol, as it eliminates the need for water washes of the gas stream to recover the solvent [128].

The captured CO_2 is transported by pipeline to an old gas reservoir near the shore of Rotterdam that is refitted as a carbon storage location. The feed requirements of this CO_2 entering the pipelines of this so called Porthos project can be seen in the Appendix by Figure A.4 and A.5.

Hydrogen purification

The last step in blue hydrogen production is to separate and purify the hydrogen from the syngas. This is done using Pressure Swing Adsorption (PSA) because it produces ultra-purified hydrogen (99.99%) needed for ammonia synthesis [88]. The tail-gas from PSA is usually purged in an ATR system because it contains few valuable components and it is at low pressure. Recycling it would require additional compression of the tail-gas.

Process flow diagram

The choices made for blue hydrogen plant result into the block scheme of the process which can be seen in Figure 3.1. This includes the different unit operations needed in order to produce hydrogen from LNG. The pumps, compressors and heat exchangers will be added when this BOD is simulated in Aspen Plus.

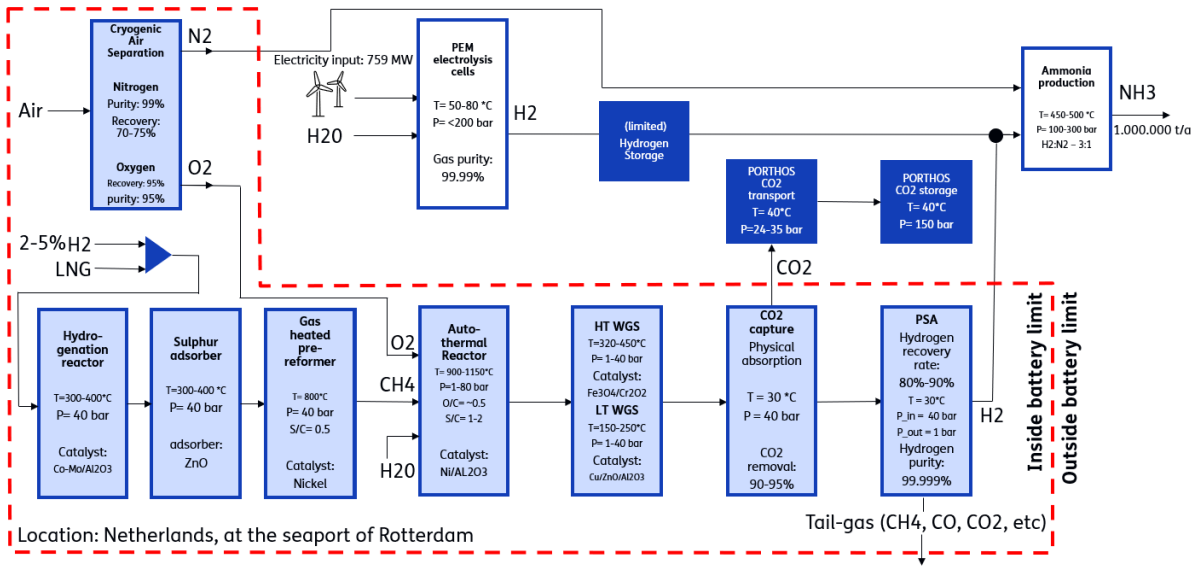

Figure 3.1: Block scheme of the case study

The thermodynamic properties will be integrated into the detailed Aspen Model during simulations and are shown in Appendix A.3. This will include the exact pressures and temperatures used during each process step.

3.1.3. Basic assumptions

This case study is using assumptions about the plant capacity, location, feed streams, available utilities and other relevant information. Here the assumptions are clearly stated in order to provide the information needed to reproduce the case study.

These assumptions are important because they determine the flexibility needed from the blue hydrogen plant. This strongly depends on the amount of green hydrogen produced, the possible hydrogen

storage capacity, if a battery is used, if production is centralized or decentralized, the flexibility and size of the ammonia plant and the fluctuations from the renewable energy produced.

Plant capacity and location

The port of Rotterdam is chosen as the location for the case study. The location must be close to a large source of renewable energy production which is mainly from offshore wind parks in the Netherlands. In addition to prefer a location near the shore, a port is specifically chosen because of the ability to ship in feedstock like LNG and the possibility of exporting CO_2 by ship.

The capacity of the ammonia plant is selected to be equal to 1.000.000 tonnes of ammonia production annually. An average ammonia synthesis plant in Europe produces around 500.000 t/a. However a large plant is chosen for the case study in order to always need a mix of blue and green hydrogen.

The capacity of the blue hydrogen production plant will be sized in such a way that it can deliver 100% of the hydrogen needed for the production of 1.000.000 tonnes of ammonia annually. This will be the maximum capacity of the blue hydrogen plant. Assuming 8000 operating hours per year, this results in a hydrogen production rate of 22.19 t/h when using the theoretical minimum amount of hydrogen needed for ammonia production. However, due to a 97% conversion efficiency under real operating conditions, the plant must produce 22.88 tonnes of hydrogen per hour to meet the full production capacity.

The electrolyser used for green hydrogen production will be a PEM electrolyser. PEM has the advantage of being able to produce hydrogen flexibly, maintaining high efficiencies even at low production capacities. This flexibility is crucial for efficiently producing hydrogen from intermittent renewable sources like the offshore wind farm used in the case study. The amount of green hydrogen produced will depend on the available amount of renewable energy from the offshore wind park, the capacity factor of installed electrolysers and the electrolysers system efficiency.

The ratio between installed electrolyser capacity and offshore wind capacity is assumed to be 78.1%. A study showed this ratio to be optimal for electrolysers coupled to an offshore wind farm, although it may vary in practice due to economic optimization [66]. When the wind farm operates below 78.1% of its capacity, all generated wind energy is fully converted into hydrogen. However, when wind power exceeds this 78.1% capacity, no additional green hydrogen is produced. This ratio increases the utilization of the installed electrolysers and results in the lowest cost per kilogram of hydrogen from the electrolysis.

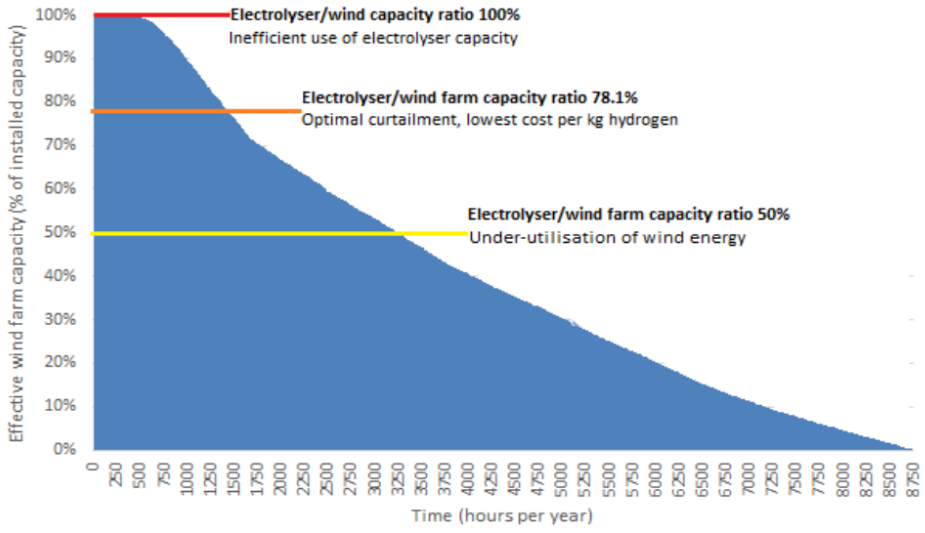

Figure 3.2: Optimal capacity ratio electrolysers coupled to a wind farm [66].

The fluctuating power output from the wind farm coupled to electrolysers will create the imbalance in the hydrogen supply for ammonia production which needs to be balanced by blue hydrogen production.

Utilities

The feed source of the plant is chosen to be Liquefied Natural Gas (LNG). The Netherlands relied heavily on the Groningen Gas field for about half a century and enjoyed relatively cheap gas. However with the closing of the Groningen Gas field and Russian gas imports on a ban the alternative is to import LNG by ship from countries like United States, Qatar or Australia which where the top exporting countries in 2023 [124]. The composition of LNG depends on its geographical origin due to the differences in the natural gas source [77]. For the case study LNG with the feed composition of Qatar is chosen, see Appendix Figure A.6 and A.7. The total amount of sulphur in the LNG is assumed to be a maximum of 30 mg/Nm^3 [104].

An offshore wind farm is used for supplying the electricity needed for water electrolysis. A realistic amount of energy available to connect to the PEM electrolyser will be 759 MW which is equal to the total production of the wind farm Hollandse Kust Noord.

A data set about the windspeed of this parks location enables the calculation of the power output of the wind farm for each hour. The data set contains the hourly windspeed and power production of Hollandse Kust Noord from 1980 until 2019 [71]. A typical production pattern from this wind farm for a month is plotted in Figure 3.3. This data includes a wind turbine power curve, meaning that at very low and very high wind speeds there will be no electricity generation [46].

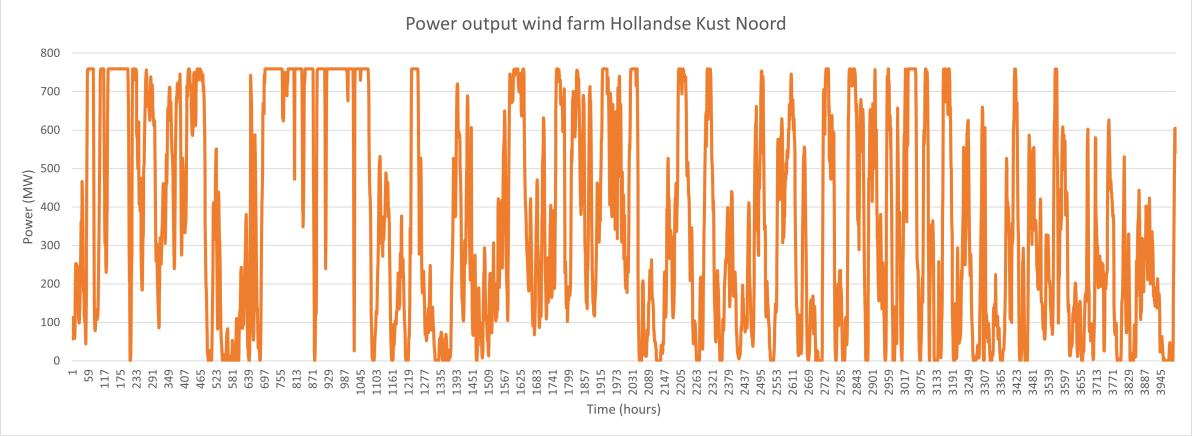

Figure 3.3: Typical power output of the Hollandse Kust Noord wind farm, based on data from the first half of 2019 [71].

Other utilities available at the port of Rotterdam are sea water which can be used for cooling/heating of different processes and have an annual mean sea surface temperature (SST) of 11.5 °C [51]. The water used for steam production is free of salt and assumed to be demineralized.

Air can be used for the production of nitrogen and oxygen using the ASU. It is assumed that the temperature of the air in Rotterdam is constant at 11.8 °C [55]. For simplicity of the model the air only contains 79% nitrogen and 21% oxygen.

Centralized vs decentralised production

The case study uses a decentralized production of hydrogen. Meaning that the electricity produced from the wind farms is only used for the electrolysers and will not be delivered to the electricity grid. In order to produce 100% green electricity the electrolysers will not use electricity from the grid which can be produced using fossil fuels.

The hydrogen produced will all be directly used by the ammonia production plant. This means that in this decentralized scenario no hydrogen will be delivered to or from the hydrogen grid.

Hydrogen storage

The location of hydrogen production is in the harbour of Rotterdam. If the hydrogen production is not coupled to the hydrogen grid, then large scale storage using salt caverns is not possible. Only limited above ground compressed storage or line packing will be possible. The size of this storage is determined during the step of defining the uncertainties.

3.2. Design variations

Three design scenarios will be simulated in order to evaluate the potential of flexible blue hydrogen production. The first design, ATR with CCS, will run continuously while the second design is using the first design only now it runs flexibly due to the implementation of intermittent green hydrogen production. The last design will use design strategies for flexible processes in order to increase the process flexibility of ATR with CCS.

3.2.1. ATR with CCS - Base case - continuous operation

The first case will serve as benchmark for comparing flexible operations of the ATR. There are no uncertainties in throughput for this design and the process plant will continuously deliver 100% of the hydrogen needed for the production of 1 million tonnes ammonia per year.

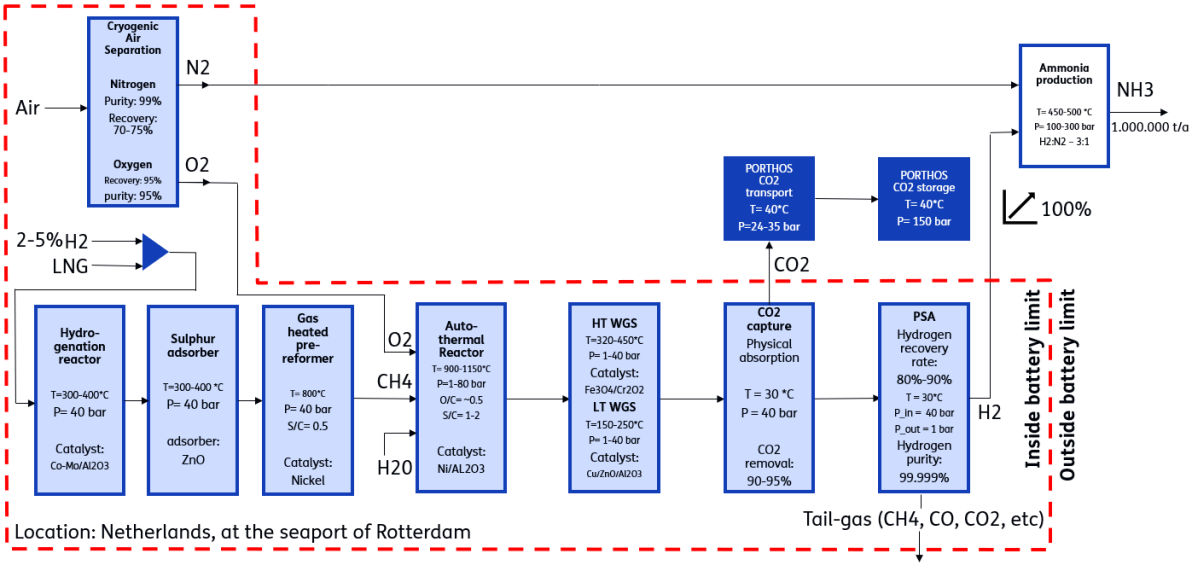

Figure 3.4: Block scheme ATR with CCS operating continuously.

3.2.2. ATR with CCS - Base case - flexible operation

The next step is to include the source of uncertainty. This intermittent production of green hydrogen will result in the need for flexible blue hydrogen production. This process plant will be simulated using the base case of the previous design and lowering the capacity. This will result in less blue hydrogen production, but at what cost?

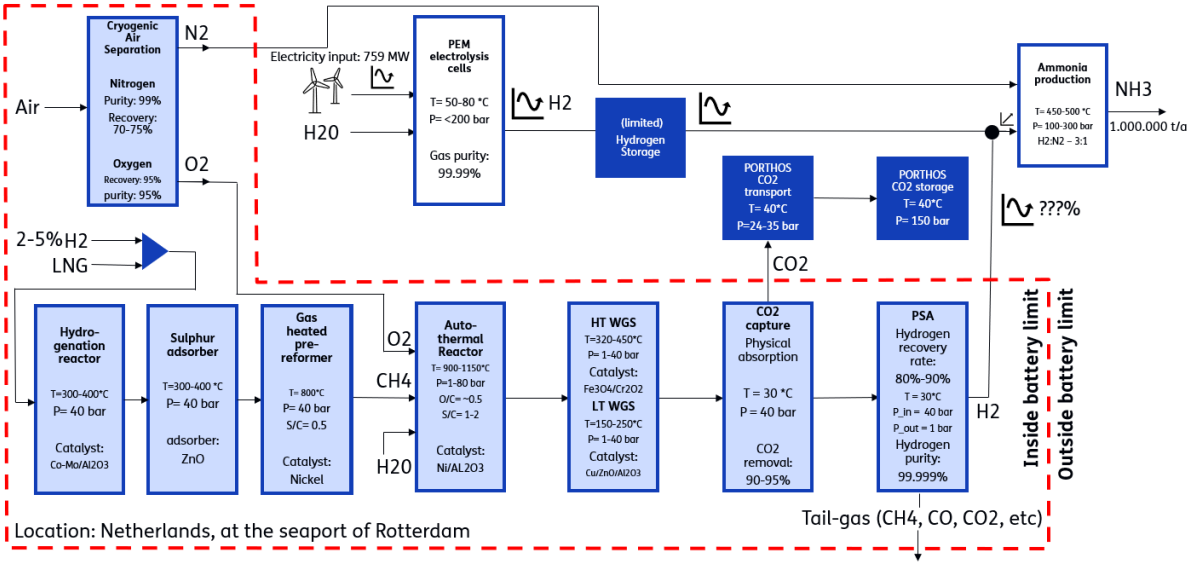

Figure 3.5: Block scheme ATR with CCS operating flexibly.

3.2.3. ATR with CCS - designed for more flexibility

The limitations of flexible blue hydrogen are researched during the simulation of the second case. Once these limitations are known, different techniques can be used to enhance flexibility. These techniques will be included in the final design.

4

Model simulation

This chapter explains the simulation choices made for modeling the blue hydrogen plant in Aspen. It covers the selected processes and configurations used to achieve effective and realistic hydrogen production from natural gas. A block diagram of the entire process is shown in Figure A.15 in the Appendix. The summary of the exact process assumptions of each unit used in the simulation can be found in Table A.3.

4.1. Detailed description process units

Aspen Plus V12 is used for simulating the different case studies on hydrogen production from natural gas because it can model the entire process when all unit operations are specified with their operating temperature and pressure. By inputting this data for each unit the software calculates the energy balances and material flows. This allows it to accurately model all key reactions in the reactors, providing a clear estimate of how much hydrogen is produced form natural gas under different operating conditions.

However, Aspen Plus is designed for steady-state operations and is not able to handle flexible, dynamic operations directly. To simulate flexible operations of the blue hydrogen plant, multiple steady-state simulations are needed to approximate energy and natural gas consumption across the different throughput levels.

4.1.1. Equation of state

The equation of state (EoS) chosen for the simulation in Aspen is the Predictive Redlich-Kwong-Soave (PSRK) EoS. This EoS is used because it accurately predicts the behavior of vapor-liquid equilibrium (VLE) of polar compounds, like H_2O, within a wide temperature and pressure range [81]. This makes a good EoS choice for simulating the process with high pressures and temperatures like autothermal reforming and gas heated pre-reformer.

4.1.2. Pre-feed treatment

The process starts with LNG which is first heated to room temperature using a heat exchanger. The next step in the model is to bring the natural gas to the operating pressure of the plant. This is done using multistage compression with intercooling. Instead of using a single compressor to raise the gas pressure from 1 to 40 bar in one step, a multistage compressor with intercooling is used, which is more efficient [87]. This approach reduces the work required for gas compression and is standard practice in large industrial plants. In Aspen, the compressors are modeled with an isentropic efficiency of 85% with a pressure ratio of around 3.4, reflecting the energy consumption of real compressors compared to an idealized compression process. This multistage compression technique is also applied to compress oxygen and carbon dioxide to their required pressures in the model.

The desulfurization process is modeled in Aspen using a stoichiometric reactor and a separator. In the stoichiometric reactor, all sulfur compounds present in the natural gas react with hydrogen, which is

added with 2% molefrac to the natural gas stream, to form hydrogen sulfide. This hydrogen sulfide is then absorbed by zinc oxide. The absorber is modelled as a separator, where the hydrogen sulfide is removed from the feed stream before entering the pre-refomer.

A small inaccuracy occurs when using a separator instead of an absorber in Aspen because there would be a small amount of steam generated in the reaction between hydrogen sulfide and zinc oxide if an absorber is used instead of a separator. However, this can be neglected because steam is added separately to the pre-refomer in much larger quantities. The small amount of steam produced in this reaction does not impact the accuracy of the model

4.1.3. Gas Heated pre-Reformer

The Gas Heated pre-Reformer (GHR) is modeled using an RGIBBS reactor Aspen. The goal of the pre-reformer is to convert the higher hydrocarbons into methane and pre-heat the gasstream of the autothermal reformer. From a sensitivity analysis in Aspen, by changing the operating temperature of the GHR while keeping the other parameters constant, it is found that at lower temperatures there is a better conversion of higher hydrocarbons but at higher operating temperatures the feed flow of ATR is at higher temperatures which will lead to more hydrogen production. At a temperature of 800 °C and pressure of 40 bar it is found that a steam to carbon ratio of 0.25 to 0.5 is sufficient in converting the higher hydrocarbons into methane.

The increase in temperature and endothermic reactions in the RGIBBS reactor require a lot of energy which should come from the high temperature of the gas leaving the autothermal reformer. To ensure that the GHR does not consume to much energy that could be supplied by the ATR, a heat duty stream (S8) is added and connected to a heat exchanger at the ATR outlet. The outlet temperature of the heat exchanger should be higher than the inlet temperature of the feed to the GHR to ensure an feasible temperature for a heat exchanger. This way the GHR is simulated using a RGIBBS reactor coupled to a heat exchanger at the exit of the ATR just like the industry examples.

4.1.4. Autothermal reforming reactor

The autothermal reactor is modeled in Aspen using two reactors. This is done because the reactor can be split in two parts. The exothermic burner part at the top of the reactor where total combustion of methane with oxygen takes place and the endothermic part concerning the catalysts at the bottom of the reactor where the steam reforming reaction takes place.

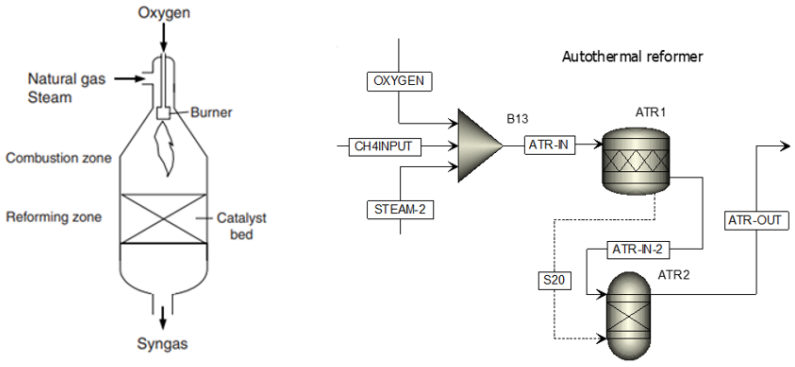

Figure 4.1: Aspen model of autothermal reformer.

An autothermal reactor does not use heat supplied from a outside source like the gas burners used in SMR. The energy needed for the reforming reactions is generated by the burner in the top of the reactor and is simulated by using a stoichiometric reactor (ATR 1) in Aspen where all oxygen supplied reacts with methane. The reaction taking place in the stoichiometric reactor is assumed to only be the total combustion reaction. The excess heat is used for the endothermic part of the reactor and is simulated using an RGIBBS reactor (ATR 2) where the equilibrium is calculated based on the set pressure of 40 bar and the heat duty from the burner which is transferred using a heat stream (S20).

4.1.5. Water-Gas Shift Reactors

The Water-Gas Shift Reaction (WGSR) is modeled using two equilibrium reactors in Aspen, taking into account the different operating temperatures of the high- and low-temperature reactors. An equilibrium reactor is chosen because the catalysts used in the WGSR reactors are highly selective for the desired reaction, minimizing any side reactions. Therefore, it can be assumed that the only reaction occurring is the WGSR, with thermodynamic equilibrium being the main factor that determines the composition of the reaction products. Since temperature strongly affects the equilibrium constant it is necessary to use both the high- and low-temperature reactors to accurately model this section.

4.1.6. CO_2 absorption via Selexol

The Selexol process is modeled as a separate Aspen model. This is done because the recycle streams lead to a lot of errors and long computation time if used in the large model. Therefore in the Apsen simulation of all the unit operations found in Figure A.15 the process is simplified to a separator. Here, 95% of the CO_2 is separated from the stream which is commonly used in ATR. In order to calculate the energy required for the process the same temperature and pressure inlet conditions are taken from the large model and used as input for the Selexol model.

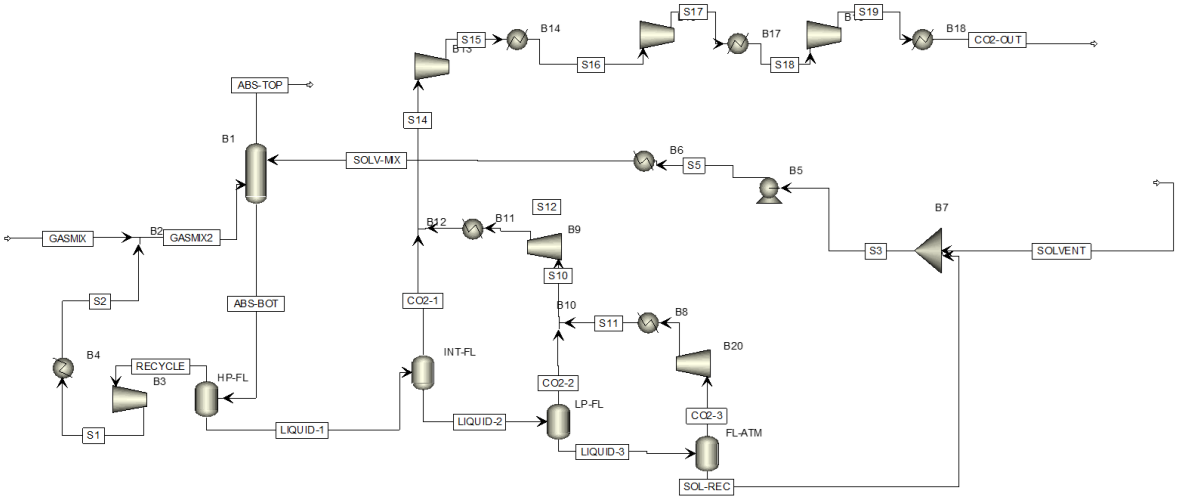

Figure 4.2: Aspen Plus block diagram of Selexol process for CO_2 capture.

The process begins with a high-pressure mixed gas stream, labeled GASMIX, entering the absorber unit which is modeled using a RadFrac model with 9 stages without the use of a condenser or reboiler. Selexol selectively absorbs CO_2 from the gas stream, while the hydrogen passes through. The purified hydrogen-rich gas exits the absorber, while the solvent loaded with CO_2 leaves at the bottom. A calculator is used to remove 95% of the CO_2 from the gas mix by adjusting the flow-rate of Selexol to match the designed specification.

The loaded solvent undergoes multiple stages of depressurization in flash separators to efficiently release the absorbed CO_2. This staged depressurization allows some CO_2 to be released at higher pressures, reducing the energy required for recompression needed to transport the CO_2 through the pressurized pipelines of the Porthos project. The regenerated solvent is recycled back to the absorber. The design currently uses four flash stages, but an optimization study is needed to determine the ideal number of stages, balancing equipment costs with energy savings. This future study can also include temperature swing regeneration as a promising technique to reduce compression cost (CAPEX and OPEX) [153].

Selexol solvent is a mixture of dimethyl ethers of polyethylene glycol ($CH_3O(CH_2CH_2O)_nCH_3$) with n = 3-9 [47]. Due to the unavailability of the pure component properties of the Selexol mixture in Aspen, dimethyl ether of pentaethylene glycol (DEPentaG) was used instead. This so called DEPentaG closely represents the properties of the Selexol mixture and is therefor suitable for the simulation of the carbon capture process in the high-pressure autothermal reforming process [154].

4.1.7. Air Separation Unit

The cryogenic Air Separation Unit (ASU) is simplified in Aspen using a separator to divide air into oxygen, nitrogen and argon. There is a small fraction of 0.001 nitrogen in the oxygen stream just like in a real plant. The energy required for the operation is obtained from literature and used to calculate the process OPEX, with the specific power consumption of 200 kWh/Tonne$_{0_2}$ [10].

4.1.8. Pressure Swing Adsorption

Pressure Swing Adsorption (PSA) is modeled in Aspen using two separators for simplification. Two separators are chosen because approximately 10% of the hydrogen remains in the first waste stream. A second PSA unit is therefore used to extract 90% of the hydrogen from that first waste stream.

Accurate modeling and detailed literature data on the energy consumption of PSA for hydrogen with varying compositions are still limited. In the case of Steam Methane Reforming (SMR), the total energy consumption for conventional PSA-based hydrogen purification is about 9.71 kJ/mol H_2 [129]. However, this process does not include CO_2 capture, resulting in higher concentrations of CO_2 in the hydrogen stream that will require more energy for purification. In this case, with CO_2 capture through the Selexol process reducing impurities in the PSA feed stream, the energy consumption of PSA is expected to be lower than the SMR benchmark. A value of 6.7 kJ/mol is chosen, which is the average between the benchmark of 9.71 kJ/mol and the lowest reported value in the literature study of 3.71 kJ/mol H_2.

5

Techno-Economic Assessment

The Techno-Economic Assessment (TEA) of the three different case studies will give a clear insight in the effects of 'underused CAPEX' on the cost of hydrogen due to flexible operations. The levelised cost of hydrogen (LCOH) is used in order to visualize the effect of underused CAPEX and make it easier to compare with other productions methods. The levelised cost of hydrogen is calculated by making an estimation on the unit cost of the different steps in the process using data available from different sources in literature. With this data a cost estimation on variable OPEX and fixed OPEX can be made using the method proposed by Sinott & Towler [135]. The amount of the consumables used like LNG, oxygen and water are taken from the Aspen Plus simulation.

Capital Cost

In order to provide a more accurate estimate of the current capital cost for the designed autothermal plant, two adjustments need to be made to the costs found in literature. This is because the components prices are based on unit operations at a different capacity and costs from a different time period.

First, the six-tenth rule can be used to estimate the cost of equipment when scaling up or down in size or capacity. The capital cost of the plant at a designed capacity can be calculated by the equation:

$$C_2 = C_1(\frac{S_2}{S_1})^{n_s} \tag{5.1}$$

Where C_2 is the estimated cost of the new equipment, C_1 is the known cost of the reference equipment, S_2 is the size or capacity of the new equipment and S_1 is the size or capacity of the reference equipment. The exponent n_s determines the rate at which costs scale relative to the changes in size or capacity. The six-tenth rule uses $n = 0.6$ as a typical value for many process, however n_s can vary depending on the specific industry, type of equipment, op process being scaled.

The next step, after estimating the cost of the newly sized equipment, is to update the cost to reflect current market prices. This adjustment is typically made using cost indices, which relate present costs to past costs. These indices are based on data for labor, material and energy costs, often published in official economic reports. A common cost index used in the process industries is the Chemical Engineering Plant Cost Index (CEPCI), usually referred to as the CE index.

To adjust historical prices to current values, the following equations is used:

$$C_{present} = C_{past} \times \frac{CEPCI_{present}}{CEPCI_{past}} \tag{5.2}$$

Here $C_{present}$ is the current cost of the equipment, C_{past} is the original cost found in the literature, $CEPCI_{present}$ is the current value of the CEPCI index and $CEPCI_{past}$ is the value of the CEPCI index at the time the original cost what determined.

By using this method, past cost estimates are updated to account for inflation, market changes, and variations in labor and material costs, ensuring a more accurate estimation of the present CAPEX required for the different unit operations of the autothermal process plant.

Table 5.1: Cost and scaling factors for different process components.

Process component	Scaling parameter	Reference capacity	Reference cost (M$)	Scaling factor	Cost year	Source
Desulphurization	Thermal input (MW_{LHV})	413.8	0.66	0.67	2011	[24]
Pre-reformer*	Thermal input (MW_{LHV})	1800	17.5	0.75	2005	[24]
Autothermal reformer	Designed capacity (tonne H_2/day)	607	108	0.75	2020	[103]
Water-Gas Shift Reactor	Designed capacity (tonne H_2/day)	607	61	0.67	2020	[103]
Selexol	Designed capacity (kmol/hr)	28182	52.44	0.67	2020	[6]
Pressure Swing Adsorption	Designed capacity (tonne H_2/day)	607	246	0.6	2020	[103]
Air Separation Unit	Designed capacity (tonne H_2/day)	607	198	0.7	2020	[103]

*There is no data found on the price of a GHR reformer, therefore an adiabatic pre-refomer is used as refrence cost.

The scaling factors used in Table 5.1 are taken from a literature paper on autothermal reforming [25]. However, the reference capacity and cost are mostly based on more recent estimations to provide more accurate results, as shown in the cost year column of Table 5.1.

Using the data from Table 5.1 and applying the six-tenths rule alongside the cost index, we can determine the Inside Battery Limits (ISBL) investment, which represents the cost of the plant itself.

Table 5.2: Cost of Equipment for blue hydrogen plant.

Process component	Cost (M$)
Desulphurization	1.47
Pre-reformer	10.45
Autothermal reformer	134.92
Water-Gas Shift Reactor	76.78
Selexol	47.16
Pressure Swing Adsorption	311.68
Air Separation Unit	248.52
Total ISBL Investment	**830.99** (M$) **756.20** (M_euro)

From this ISBL investment, the Fixed Capital Investment (FCI) can then be calculated. The FCI consists of the total cost of designing, constructing, and installing a plant, as well as the modifications required to prepare the plant site. The fixed capital investment is made up of:

- **Inside Battery Limits (ISBL) Investment**: The cost of the plant itself.
- **Outside Battery Limits (OSBL) Investment**: Covers modifications and improvements to the site infrastructure. For petrochemical projects, this typically ranges from 20–50% of the ISBL investment.
- **Engineering and Construction Costs**: Estimated at approximately 10% of the combined ISBL and OSBL investments for large projects such as the autothermal reforming plant.
- **Contingency Charges**: These account for unexpected costs and are typically a minimum of 10% of the ISBL and OSBL investments.

Using these estimations the FCI can be calculated.

Table 5.3: Breakdown of capital costs assumptions [135].

Capital Expenditure		
Cost Type	**M_euro**	**Assumption**
ISBL Capital costs	756.20	N/A
OSBL Capital costs	151.24	20% of ISBL
Engineering costs	90.74	10% of ISBL + OSBL
Contingency	90.74	10% of ISBL + OSBL
Fixed Capital Investment	**1088.93**	

Fixed Operating Expenditures

Fixed operating expenditures are expenses that stay the same no matter how much the plant produces. These costs do not go down even if production is reduced due to lower throughput of natural gas. They include operating labor, supervision, salary overhead, maintenance, property taxes, rent, general plant overhead and environmental charges. These are necessary expenses to keep the plant running. It is assumed that the cost for sales and marketing is irrelevant for this case study.

Table 5.4: Breakdown of fixed operating costs.

Fixed Operating Expenditures		
Cost Type	**M_euro/yr**	**Assumption**
Labor	1.81	4.8 operators per shift position, 9 shift positions, €42,000/yr per operator
Supervision	0.45	25% of operating labor
Direct overhead	1.13	50% of operating labor + supervision
Maintenance	30.25	4% of ISBL
Property taxes and insurance	7.56	1% of ISBL
Rent of land (and/or buildings)	9.07	1% of ISBL + OSBL
General plant overhead	2.06	65% of total labor
Allocated environmental charges	9.07	1 % of ISBL + OSBL
Total Fixed Cost of Production (FCOP)	**61.57**	

Variable Operating Expenditures

Variable operating expenditures for a blue hydrogen plant are costs that fluctuate based on the plants throughput. These costs increase or decrease depending on how much hydrogen is produced. They include expenses like raw materials, utilities and consumables. Since blue hydrogen production also captures CO_2, the costs of CO_2 transportation and storage also fall under variable expenditures. These costs are directly tied to the plant's throughput and vary with production levels.

Table 5.5: Breakdown of variable cost assumptions.

Variable Cost Assumptions			
Cost Type	**Value**	**Unit**	**Source**
Raw materials			
Liquefied Natural Gas	39.71	Euro/MWh	[34]
	11.03	Euro/GJ	
	0.547	Euro/kg	(LHV = 49.61 MJ/kg)
Water (for steam)	0.9	$/$m^3$	[72]
Utilities			
Cooling water	0.05	$/$m^3$	[72]
Electricity	0.250	Euro/kWh	[131]
CO_2 transportation	1.82	Euro/Tonne_CO_2	[147]
CO_2 storage	35.14	Euro/Tonne_CO_2	[121] [109]
Energy consumption O_2	200	kWh/Tonne_O_2	[10]
Energy consumption PSA	6.7	kJ/mol H_2	[129]
Consumables			
Catalysts		(see appendix)	Figure A.10
Solvents, (Selexol)	4	Euro/L	[7]
Adsorbents, (ZnO)	4	$/kg	

The price of LNG is based on the Title Transfer Facility (TTF) natural gas market, a virtual trading point for gas in the Netherlands [34]. The TTF is a key benchmark for natural gas prices in Europe. The price of LNG have not returned to levels seen before the Ukraine invasion. It is expected that the new LNG liquefaction capacity coming in 2025 and 2026 will bring TTF LNG prices down from 2025 [133]. Therefore, for the purpose of this analysis, the current LNG price is assumed to remain constant over time using the current LNG price.

The cost of CO_2 transportation is based on the cost to transport CO_2 over a short distance using onshore pipeline. This results in the cost of 2 dollar per tonne of CO_2 [147]. Using the exchange rate of 0.91 dollar to euro the cost of CO_2 transportation will result in approximately 1.82 euro per Tonne CO_2. The cost of CO_2 storage is calculated using the total capacity of the underground storage available, 37 million tonnes of CO_2, divided by the total cost of the project which is estimated at 1300 million euro [121]. The cost of CO_2 storage is sometimes included in the CAPEX. However, Porthos has stated that companies will be charged a fee for transporting and storing their carbon emissions through the Porthos network [109]. As a result, these costs vary depending on the amount of CO_2 produced and stored and are therefore calculated as part of the OPEX.

Table 5.6: Breakdown of plant and cash flow assumptions.

Plant and cash flow assumptions		
Cost Type	**Value**	**Unit**
Plant lifetime	20	years
Capital factor	2	%
Actual discount rate	4.25	%
Dollar to euro	0.91	

6

Results & Discussion

6.1. Base case - Continuous operations - Version 1

The first design of the blue hydrogen plant used an adiabatic pre-reformer. The adiabatic pre-reformer was modeled using operating conditions from literature. The operating temperature is 550 °C, pressure of 40 bar and a steam to carbon ratio of 1. The adiabatic pre-reformer was modeled in Aspen using a RGIBBS reactor which calculates the chemical equilibrium based on the given pressure and temperature. After the pre-reformer the feed was pre-heated to 650 °C before entering the autothermal reformer.

This resulted in a plant efficiency (LHV) of 77.02%. This is slightly higher than similar process in literature, this is because in this Aspen simulation there is no pressure loss in the various reactors and pipes. This results in higher efficiencies than real life conditions. However, some processes show that using a gas heated reformer in front of the autothermal reformer can result in higher LHV efficiencies of 80% [67] [30].

Pinch analysis

To see if there is enough high temperature waste heat generated to use a gas heated pre-reformer a pinch analysis is done. The pinch method can be used for designing a heat exchanger network (HEN) in a systematic approach in order to optimize energy recovery and minimize utility consumption. Therefore, this pinch analysis will show the total heating and cooling duty of the autothermal plant with an integrated HEN.

Figure 6.1: The Hot and Cold composite curves of the autothermal plant with adiabatic pre-reformer.

From the pinch analysis it became clear that only a cold utility is necessary for the plant. This means that the plant needs to cool down using techniques like water cooling for 118.8 MW. Because there is excess heat generated by the autothermal reformer at a high temperature a gas heated pre-reformer is used instead of an adiabatic reformer.

6.2. Base case - Continuous operations - Version 2

Using the Aspen model described in Chapter 4 and the techno-economic assessment from Chapter 5 the key performance indicators can be calculated for the blue hydrogen plant which continuously operates at 100% of its capacity.

Process efficiency

Using a gas heated pre-reformer (GHR) increases the plant efficiency (LHV) to 81.45%. This increase in process efficiency compared to a adiabatic pre-reformer is because of two reasons. The first reason is that the gas entering the autothermal reformer have a higher temperature because it is already preheated in the GHR which leads to a higher hydrogen yield. This better heat integration therefore increases the efficiency of the plant. The second reason is that the gas heated reformer already reforms some natural gas into syngas. This leads to a lower oxygen consumption, even though the oxygen-to-carbon ratio stays the same, because there is less methane entering the autothermal reformer. This lower oxygen consumption results in less power consumed by the compressors and the ASU leading to a higher efficiency.

This result is higher than the 80% efficiency (LHV) reported by [67]. The difference could come from the model's simplifications, which do not account for pressure losses of the different units. In addition, the model is optimized for hydrogen production. However, in practice, higher steam-to-carbon ratios may be required in the pre-reformer. Due to limited data, a steam-to-carbon ratio of 0.5 was used in the model, which is sufficient to convert the higher hydrocarbons into methane.

LCOH

The levelised cost of hydrogen is the sum of all the cost made, CAPEX, fixed OPEX and variable OPEX. A breakdown of the Levelised cost of hydrogen for the blue hydrogen plant which runs continuously on 100% of its designed throughput can be seen in Figure 6.2.

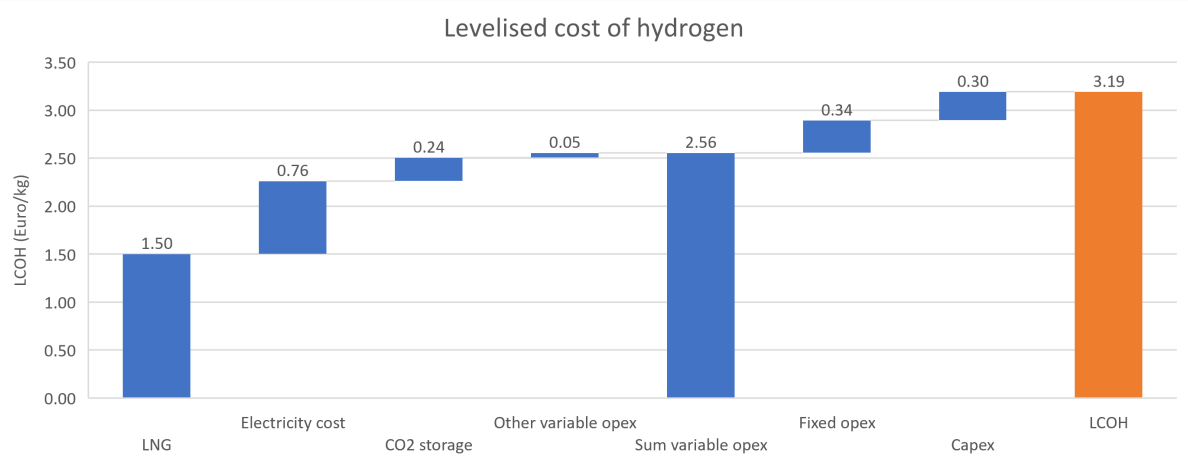

Figure 6.2: Breakdown of the levelised cost of hydrogen for continuous operation.

From the waterfall chart it is clearly visible that the main cost for blue hydrogen is the cost of LNG. Electricity cost is the next large contributor and includes the energy cost of the ASU and PSA but also the cost for compression of CO_2, water and other gasses to the operating pressure of the plant. The cost of CAPEX and fixed OPEX are only a small part of the total cost because of the sizing advantage of a large process plant. Note that the actual LCOH may vary from the calculated value due to uncertainties inherent in a TEA. These uncertainties come from assumptions related to the plant efficiency,

operating conditions, feedstock prices, and capital cost estimations. For blue hydrogen production, the inaccuracy in LCOH calculations using TEA can range from -50% to +60% [107]. Therefore, the data should be interpreted with caution. However, it can still be useful for comparing the change in LCOH between continuous and flexible operations, as the assumptions made in the TEA stay the same.

Carbon intensity

The carbon intensity for this efficient blue hydrogen plant with carbon capture of 95% results in 0.63 kg CO_2-eq/kg H_2, meaning that approximately 0.63 kg of CO_2 is emitted for every kilogram of hydrogen produced. This level of emissions is comparable to other state-of-the-art blue hydrogen plants, such as those in Norway, which report a carbon intensity of around 0.7 kg CO_2-eq/kg H_2 [54]. This low carbon intensity classifies blue hydrogen as a low-carbon alternative, though it still generates some CO_2 emissions compared to true net-zero options, like hydrogen produced via electrolysis using renewable electricity.

6.3. Base case - Flexible operations

Knowing the cost and operating conditions of the base case with continuous operations the next step is to define the uncertainty of the system. The flexibility needed for the process plant can be determined once the uncertainties are clearly defined. In this case, the plant needs to operate flexible in order to balance out the fluctuations in green hydrogen production. This chapter shows the effects of flexible operations on the efficiency, cost and emissions of the blue hydrogen plant.

6.3.1. Define uncertainties

When looking at flexible operations and design of a process plant the first step is to define the uncertainties to which the process plant need to respond. According to Luo et al. [89], questions that can help define the uncertainties are:

1. What are the potential sources of uncertainties
2. What are the boundaries of uncertainties
3. What is the expected frequency of changes in operating parameter, over a given time horizon

Potential sources of uncertainties

In this case study of flexible blue hydrogen the uncertainty introduced is the variable production of green hydrogen. This is compensated using flexible blue hydrogen production to ensure a continuous amount of hydrogen for ammonia synthesis. An important step is to clearly define the uncertainty and the flexibility to which the plant needs to adapt.

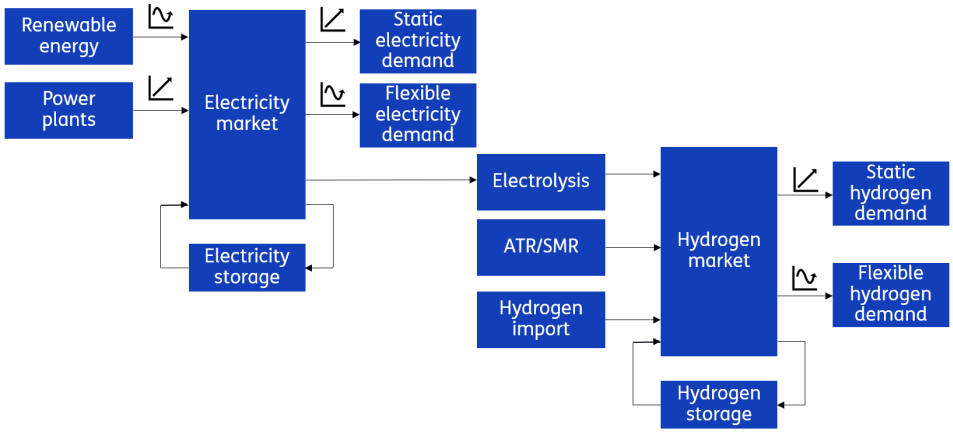

Figure 6.3: Centralised hydrogen system using a hydrogen network.

In Figure 6.3 an overview is given of how a fully centralised hydrogen system could look like with an integrated hydrogen market and electricity market. The variable operating conditions of blue hydrogen production would be different in this situation compared to the case study.

In order to find the uncertainties of the blue hydrogen plant for this case study their are some simplifications and assumptions made. The first assumption is that the hydrogen produced is decentralised. Meaning that there is no use of a hydrogen market or electricity market, all green and blue hydrogen is used for ammonia production. So the next assumption is that the wind farm is directly coupled to the electrolysers without electricity storage and a connection to the grid.

In the case study the source of uncertainty comes from the variable production of green hydrogen from the intermittent source of wind power. However this flexible production could be completely dampened by the use of large-scale green hydrogen storage.

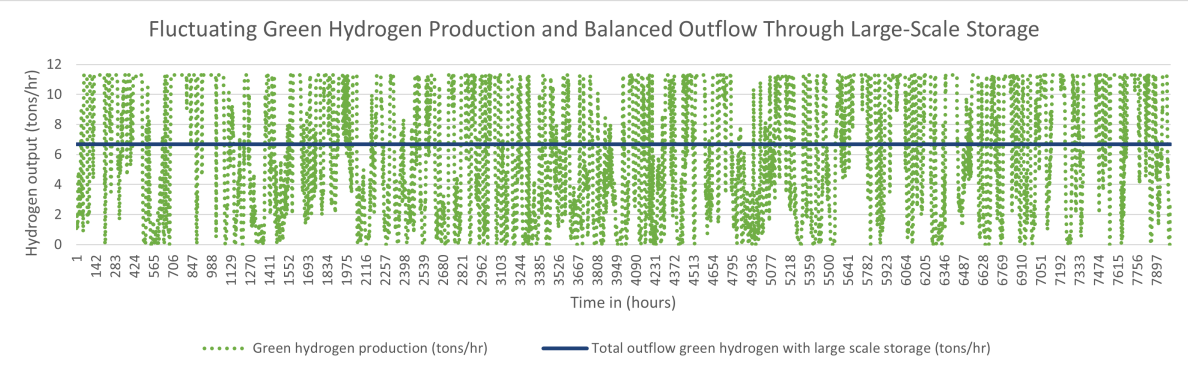

Figure 6.4: Balanced outflow of fluctuating green hydrogen using large-scale storage.

To effectively flatten out the fluctuations in green hydrogen production from an offshore wind farm of a size of 759 MW throughout the year, a total storage capacity of 5350 tons of hydrogen would be needed for this case study, see Figure 6.5. This corresponds to approximately 686,538.46 m^3 at a pressure of 100 bar using a volumetric density of 7.8 kg/m^3 [3]. While underground salt caverns can accommodate this volume of hydrogen, such storage options is not available at the harbor of Rotterdam. In addition, salt caverns are unable to load and unload hydrogen as frequently as necessary to address for the hourly fluctuations in green hydrogen production with a typical duration of storage of 2-4 months [17].

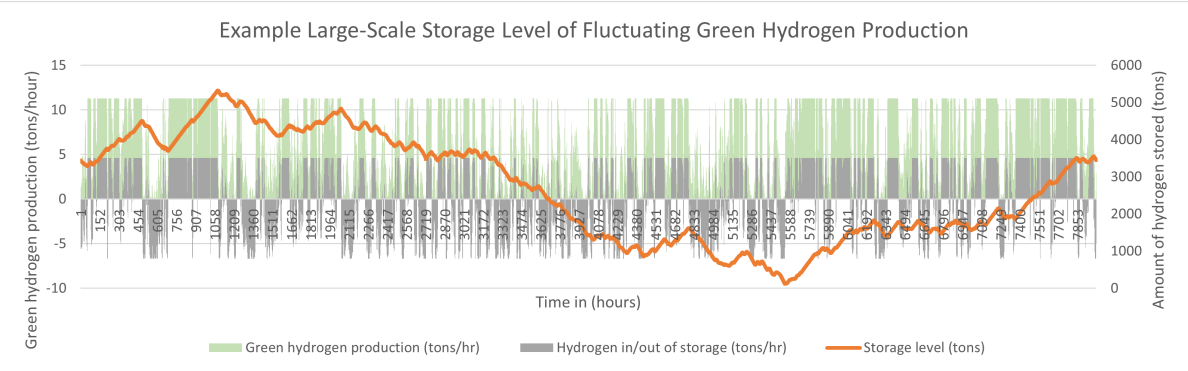

Figure 6.5: Total hydrogen storage needed to keep green hydrogen production stable.

Storage options that are feasible at the harbor for short duration storage, suited for balancing hourly intermittency, consist of above-ground pressurized storage units with a capacity of around 4 tons and storage in pipelines, called line packing, with an estimated capacity of 300 tons [17]. These storage options are used in the case study but do not change the amount of green or blue hydrogen needed. However, they decrease the transient time of the blue hydrogen plant by reducing the need for ramping up or down between varying throughput levels.

The last assumption made is that there is only static hydrogen demand, meaning that the ammonia plant will not operate flexible and needs a continuous supply of hydrogen. These assumptions result in a simplified model which can be seen in Figure 6.6.

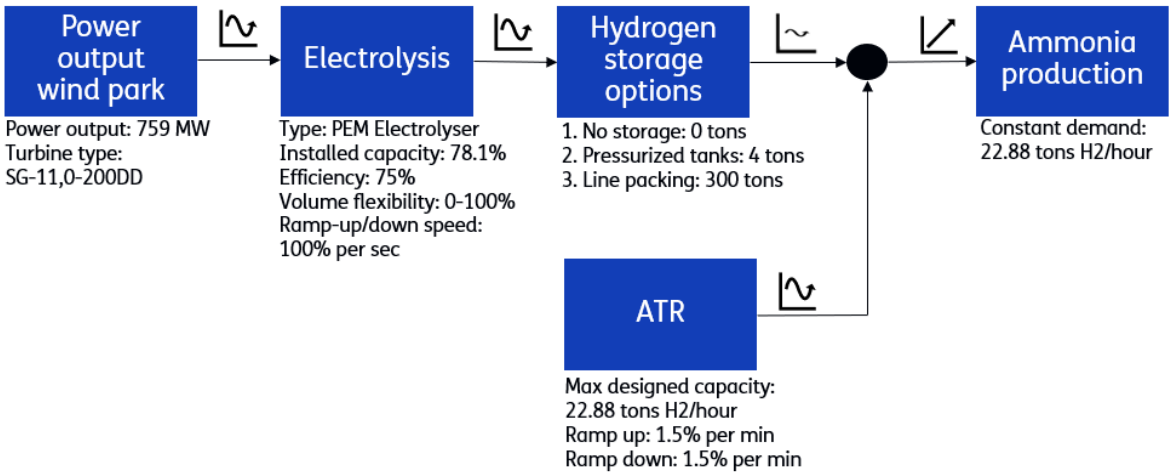

Figure 6.6: Overview of the model for variable blue hydrogen production using ATR to balance intermittent green hydrogen production.

So the uncertainties for this case study come from the intermittent nature of electricity production from wind energy. The different wind speeds result in a variable output of electricity which is coupled to the electrolysers. This results in a variable output of green hydrogen which is a bit dampened by the limited amount of storage. The varying outputs of green hydrogen out of the storage are directly balanced by adjusting the throughput of blue hydrogen, ensuring a constant supply of hydrogen for the ammonia production demand.

Boundaries of uncertainties

The next step is to find what the boundaries of the uncertainties of the system are. In this case the maximum and minimum flow rate of green hydrogen produced from wind energy. The first boundary is the power curve of an offshore wind turbine. At very low or high wind speeds, the wind turbine will not generate any energy, as this depends on the specific turbine. For this case study, the Siemens Gamesa 11.0-200 DD power curve is used to define these limits. The second boundary is the maximum wind power output of the wind farm, in this case 759 MW.

For the electrolyser the characteristics influencing the maximum and minimum flow rate of hydrogen is set by the efficiency of the electrolyser, the ramp-up and down rate, minimum operable hydrogen production rate and installed capacity. The efficiency of the electrolysis system using an PEM electrolyser is set at 75% and this type of electrolyser is characterized for is fast ramping up and down within seconds from 0 to 100%. The volume flexibility is set between 0 and 100% meaning that no battery storage is needed in order to keep a minimum throughput which is necessary for electrolysers types like alkaline electrolysers to prevent gas crossovers. The last boundary of the uncertainty in this case study is the installed electrolyser capacity which is equal to 78.1% of the maximum output of the offshore wind farm. These boundaries lead to a maximum green hydrogen production rate of 11.3 tons per hour, with a minimum flow rate equal to zero.

Expected frequency of changes in operating parameter

The wind speed fluctuates hourly, meaning that the blue hydrogen plant needs to be capable of adjusting its production on an hourly basis to match the changes in green hydrogen production, assuming that there is no storage used.

When using storage the fluctuations are still on an hourly basis. This is due to the limited capacity of the storage compared to the amount of green hydrogen produced. For the pressurized tanks a max storage capacity of 4 tons is used and for line packing a storage capacity of 300 tons is assumed, which would be a pipeline of around 100 km.

Resulting operating condition

With the defined uncertainty the operating conditions of the blue hydrogen plant can be determined. An overview on the formulas used to calculate the blue hydrogen production rate each hour based on the fluctuations in green hydrogen production and its storage used can be found in Appendix A.4. The hourly fluctuations in energy production from the offshore wind park is simulated using the most recent year available from the dataset Hollandse Kust Noord (2019) [71].

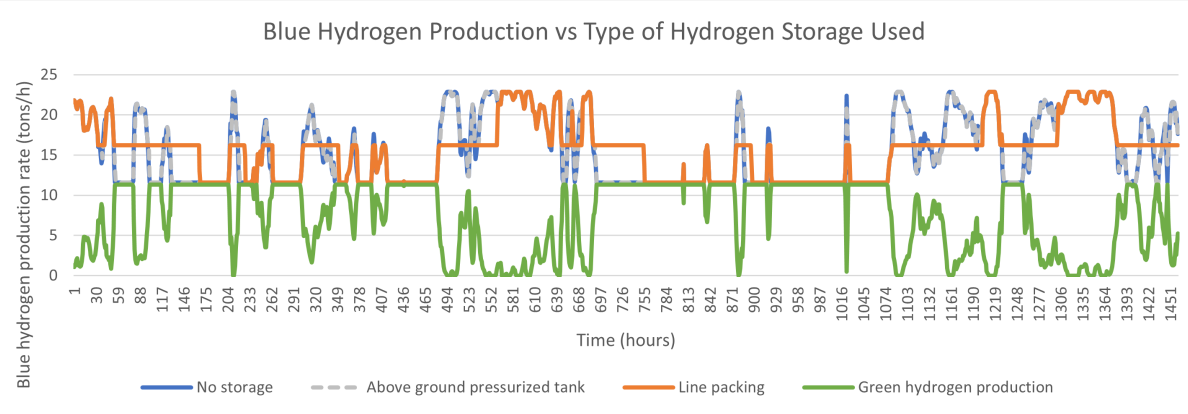

Figure 6.7: Example of difference in blue hydrogen production based on the storage type used for two operating months in 2019.

The next step is to determine the relative throughput range of the blue hydrogen plant.

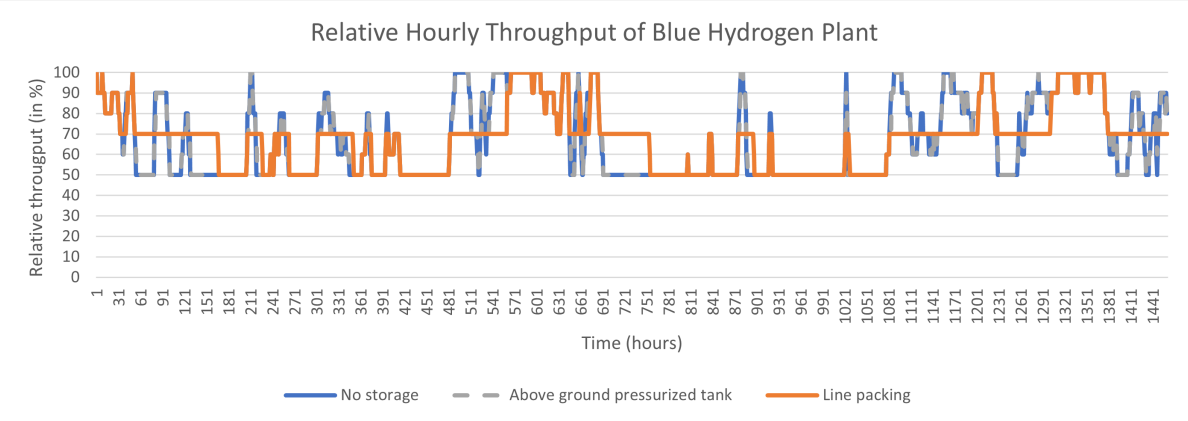

Figure 6.8: Relative throughput of blue hydrogen plant each hour, rounded of to 10%.

The relative throughput is 100% when there is no green hydrogen produced, meaning that the blue hydrogen plants runs at its maximum capacity. When there is maximum green hydrogen production, 11.3 tons in that hour, there still needs to be blue hydrogen produced of 11.6 tons in that hour in order to keep the total hydrogen production to the 22.9 tons of hydrogen needed each hour for ammonia production. This means that the blue hydrogen plant needs to operate between 50-100% of its nominal capacity in this case study.

Rounding the relative throughput to 10% increments between 0 and 100%, the number of hours the blue hydrogen plant will operate at each throughput percentage can be determined, as shown in Table 6.1. This approach of rounding to increments of 10% limits the number of steady-state Aspen simulations required.

Table 6.1: Expected operating conditions blue hydrogen plant for one operating year using different storage types.

Throughput (%)	No storage (hours)	Above ground pressurized tank (hours)	Line packing (hours)
100	1253	1248	613
90	1220	1189	468
80	1054	848	324
70	813	1225	5118
60	622	509	143
50	3038	2981	1334
40	0	0	0
30	0	0	0
20	0	0	0
10	0	0	0
0	0	0	0
Total:	8000	8000	8000

The operating hours depend on the type of storage used. When there is no storage for the green hydrogen then most of the time the blue hydrogen plant runs on 50% of its nominal capacity. This is because most of the time the electrolyser will run at its maximum capacity due to the installed electrolyser capacity of 78.1%.

However, when there is more storage installed, the plant will run mostly on 70% of its nominal capacity. This is because the storage model used, as shown in Appendix A.4, dampens fluctuations in green hydrogen production by supplying the average hourly green hydrogen output, which is around 30% of the total hydrogen demand each hour.

The blue hydrogen plant will need to adjust its hydrogen production rate on an hourly basis, requiring it to ramp up or ramp down its output each hour. A representation on how much it needs to ramp up or down can be seen in Figure 6.9.

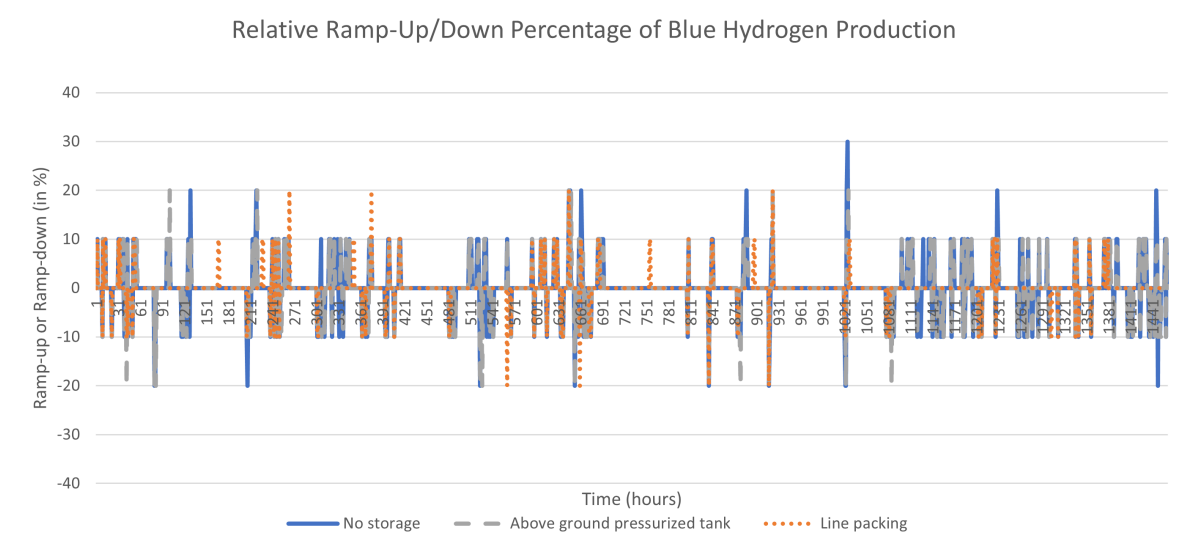

Figure 6.9: Ramp-up and ramp-down of the blue hydrogen plant between each hour following the relative hourly throughput.

The total transient time of the blue hydrogen plant as a result of changing its throughput each hour can be calculated knowing how much percentage the plant needs to ramp up or down each operating year and the ramping up and ramping down speeds. According to HyNet a blue hydrogen plant using

ATR+GHR combination can have a ramp up speed of 1% per minute and a ramp down speed of 6% per minute. [67]. However a report form H-vision mentions that even very large ATR unit can operate with ramp-up and ramp-down rate of 1.5 % per minute [78].

Table 6.2: Transient time of blue hydrogen plant depending on green hydrogen storage used and ramping speeds.

Ramping up/down and Transient time			
	No storage	**Above ground pressurized tank**	**Line packing**
Sum ramping-up (%/operating year)	9310	8760	3400
Sum ramping-down (%/operating year)	-9320	-8770	-3430
(HyNet)			
Ramp-up rate (%/min)	1.5	1.5	1.5
Ramp-down rate (%/min)	-1.5	-1.5	-1.5
Transient time (Hour/operating year)	207	194.8	75.9
(H-vision)			
Ramp-up rate (%/min)	1	1	1
Ramp-down rate (%/min)	-6	-6	-6
Transient time (Hour/operating year)	181.1	170.4	66.2

Using line packing for green hydrogen storage significantly decreases the transient time of a blue hydrogen plant because the there is less need for ramping up or down compared to a situation where there is no storage used. The total volume flexibility needed will not decrease between the different storage options available, only when the storage is large enough and able to rapidly load and unload.

6.3.2. Define flexibility

Now that the uncertainties to which the system needs to respond have been defined, the next step is to define the flexibility. According to Luo et al. [89], the five elements that need to be considered when defining flexibility are:

1. Target: The ability to vary the throughput
2. Range: Between 50-100% of its nominal capacity
3. Hierarchical level: The whole blue hydrogen plant
4. Time scale: Hourly basis
5. Impact: To ensure steady hydrogen supply for ammonia production

This results in the defined flexibility as: The ability to vary the throughput between 50-100% of its nominal capacity of the whole blue hydrogen plant on hourly basis to ensure steady hydrogen supply for ammonia production.

6.3.3. Operating envelope ATR with CCS

An operating envelope is made in order to see if the designed blue hydrogen plant is able to vary its throughput to the required volume flexibility. This operating envelope consists of an upper bound and a lower bound. The upper bound is consistently set at the design capacity of 100%, while the lower bound varies for each unit operation. For example, the lower limit of a compressor is constrained by its surge limit, while for an absorption column, it is determined by weeping. In the Appendix, Figure A.14 provides an overview of the volume flexibility for each unit operation. It is important to note that some strong assumptions were made due to limited data on the flexibility of chemical process equipment.

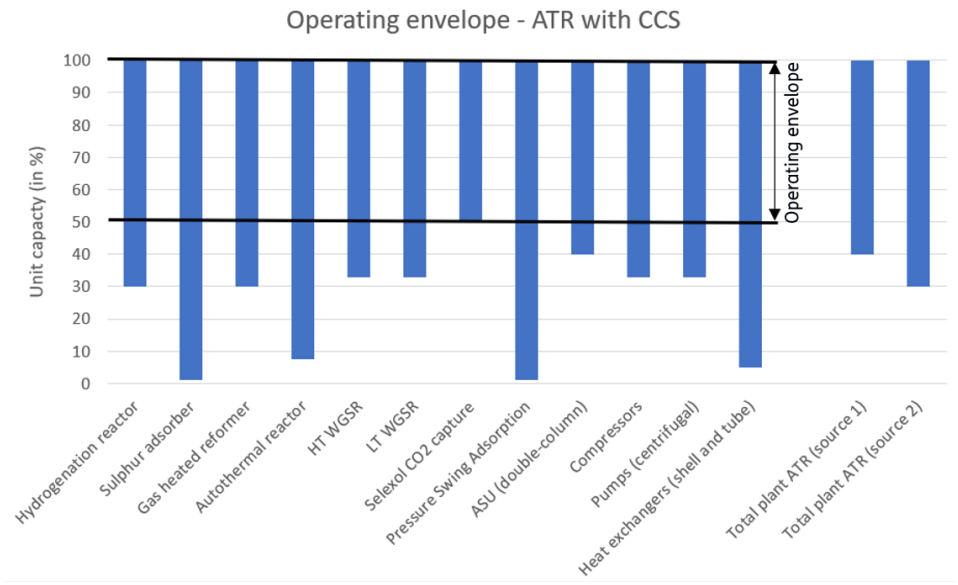

Figure 6.10: Operating envelope ATR with CCS - Base case

From the operating envelope in Figure 6.10 it can be seen that the absorber column in the Selexol process is the bottleneck in the process. If the total volume flexibility of the plant needs to be increased then first the absorber column should be adjusted to handle lower throughput. The total volume flexibility of the plant is estimated to be around 0.5. However, some other sources mention that the volume flexibility of an ATR is equal to 0.6 or 0.7 with minor design adjustments [78] [67].

6.3.4. Apply design strategies for flexibility

For this case study there is no need for an increase in volume flexibility because according to the operating envelope the plant is already capable to handle the uncertainty by operating between 50-100% of its nominal capacity.

6.3.5. KPI's Base case - Flexible operations

The last step is to evaluate flexibility to a reference design. In this case the KPI's of flexible hydrogen production will be compared to the reference design of continuous operations. This will show the effect of varying the throughput on the efficiency of the plant, the levelised cost of hydrogen and the carbon intensity of the hydrogen produced.

Transient state losses

To provide a more accurate estimate of the impact of variable hydrogen production, the time spent in the transient state is taken into account. To quantify the losses during this sub-optimal production phase, a transient loss factor is applied to the total hydrogen produced.

The transient loss factor is calculated by:

$$f_{transient,losses} = 1 - f_{yield,loss} \times \frac{T_{transient}}{N} \tag{6.1}$$

The new total amount of hydrogen produced based on variable throughput can be calculated using the formula:

$$M_t = \textit{Total hydrogen produced per year} = (1 - f_{yield,loss} \times \frac{T_{transient}}{N}) \times \sum_{i=1}^{N} H_i \times t_i \tag{6.2}$$

Where N is the total operating hours of the plant per year, $T_{transient}$ is the number of hours in the transient state per operating year, $f_{yield,loss}$ represents the extent of yield loss during transient hours with 1 indicating 100% loss (no production) and 0 indicating no loss, H_i is the hydrogen production rate in hour i and t_i is the duration of each hour which is usually 1 in the case the production is tracked hourly.

The transient time can be calculated using the formula:

$$T_{transient} = (\sum_{k=1}^{K} \frac{P_{up,k}}{S_{up}}) + (\sum_{k=1}^{K} \frac{P_{down,k}}{S_{down}}) \tag{6.3}$$

Here $T_{transient}$ is the total transient time per operating year, K is the number of ramping events per operating year, $P_{up,k}$ is the percentage increase in throughput required for ramp-up in event k (for example a ramping up of 10% of the throughput is needed between hour 4 and 5), S_{up} is the ramp-up speed of the plant which is defined as the percentage increase in production per unit time, $P_{down,k}$ is the percentage decrease in throughput required for ramp-down in event k, S_{down} is the ramp-down speed of the plant defined as the percentage decrease in production per unit time.

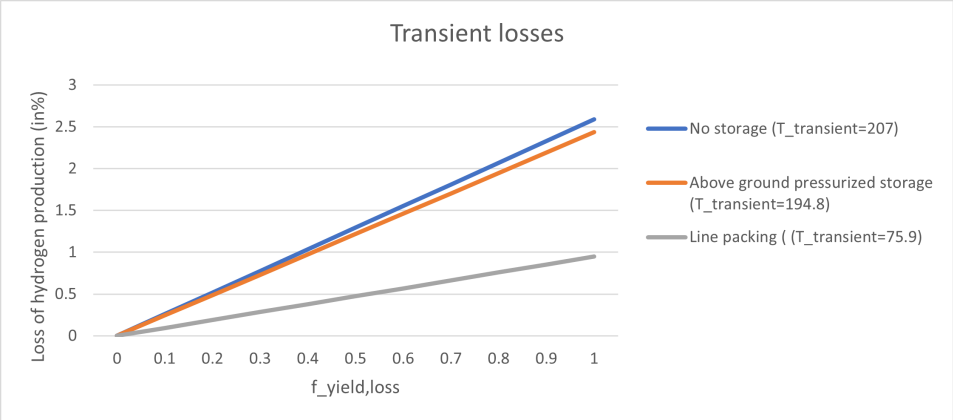

Figure 6.11: Loss of hydrogen production under different yield loss factors and transient times during one operational year of 8000 hours.

From Figure 6.11 is becomes clear that highly flexible chemical processes can suffer large yield losses if a significant portion of the operating year is spent in the transient state and the yield losses are large during production in the transient state. Reducing transient time can be achieved by using processes with faster ramp-up/down speeds or by minimizing the ramping events. Fewer ramping events are possible with large storage or scheduling, allowing operation at set throughput for longer durations and thereby reducing the frequency of changes.

Efficiency

Because the plant operates at lower throughput the efficiency of the compressors will decrease. The assumption made is that at 100% throughput the efficiency of the compressors is the most efficient. However for each 10% drop in capacity, the adiabatic efficiency of the compressors will drop 2%, see appendix Table A.2.

The next efficiency loss simulated in aspen is that of the ASU. The O_2 purity will drop from a purity of 99.9 mol% to a purity of 95.4 mol% because of flexible operations of the ASU [20]. This means that more energy is required to get the same amount of oxygen to the ATR and that more energy is used for the compression step while also more inert nitrogen is entering the system.

The other components remain at their described temperature and pressure and all ratios stay the same in the Aspen simulation of the different throughput's. So local temperature swings and pressure swing due to flexible operations are not taken into account.

Because the hydrogen throughput is adjusted each hour and the electricity consumption is not constant in order to calculate the efficiency of the plant the Formula 2.3 is adjusted to calculate the average plant efficiency over the operating year. The adjusted formula becomes:

$$\eta_{\textit{Plant Efficiency}} = \frac{\sum_{i=1}^{N}(\dot{m}_{H_2,i} \times LHV_{H_2})}{\sum_{i=1}^{N}(\dot{m}_{feul,i} \times LHV_{fuel} + \textit{Power consumption}_i)} \tag{6.4}$$

Without considering the transient state, the plant efficiency would be 81.3%, only 0.15% lower than continuous operation at 100% throughput. This reduction is due to a small loss in electrical efficiency, as the compressors do not operate at peak efficiency and the ASU consumes slightly more energy.

To be more accurate, the hydrogen production loss due to flexible operations can be accounted for by including the losses during transient state. This is done by adding a factor representing the hydrogen production losses in the transient phase, resulting in the following formula:

$$\eta_{\textit{Plant Efficiency}} = \frac{(1 - f_{yield,loss} \times \frac{T_{transient}}{N}) \times \sum_{i=1}^{N}(\dot{m}_{H_2,i} \times LHV_{H_2})}{\sum_{i=1}^{N}(\dot{m}_{feul,i} \times LHV_{fuel} + \textit{Power consumption}_i)} \tag{6.5}$$

When $f_{yield,loss}$ is larger than zero during the transient state then the plant efficiency improves as the time spent in this state decreases. For $f_{yield,loss} = 1$, the efficiency of the ATR plant without storage to buffer the green hydrogen production is 79.25%. With above-ground storage the efficiency increases to 79.37%. When using line pack storage for dampening the fluctuating green hydrogen produced, the ATR plants efficiency becomes 80.57%. This clearly shows that reducing the frequency of changes in throughput by larger storage leads to the ATR plant to operate more efficiently.

LCOH

To find the impact of variable operations on underutilized CAPEX, the levelised cost of hydrogen formula can be used. This formula allows for a comparison between a continuous process operating at maximum capacity and a variable scenario where less hydrogen is produced while maintaining the same equipment cost.

The levelised cost of hydrogen during variable production can be calculated by:

$$LCOH = \frac{\sum_{t=1}^{n} \frac{I_O + A_t}{(1+r)^t}}{\sum_{t=1}^{n} \frac{M_t}{(1+r)^t}} = \frac{\sum_{t=1}^{n} \frac{I_O + F_t + (\sum_{i=1}^{N} O_i \times t_i)_t}{(1+r)^t}}{\sum_{t=1}^{n} \frac{(\sum_{i=1}^{N} H_i \times t_i)_t}{(1+r)^t}} \tag{6.6}$$

The adjusted variables here is that total annual cost, A_t, is split up in the fixed operating cost F_t and the total operational cost which now varies depending on the throughput. For that reason the total operational cost is calculated by taking the sum of the operating cost per hour O_i times duration t_i. The same with the hydrogen produced which varies between the hours based on the throughput, therefore the sum of the hydrogen production rate, H_i, in hour i is taken times the duration of that production rate t_i.

To include the losses during transient state the formula can be adjusted to:

$$LCOH = \frac{\sum_{t=1}^{n} \frac{I_O + F_t + (\sum_{i=1}^{N} O_i \times t_i)_t}{(1+r)^t}}{\sum_{t=1}^{n} \frac{(1 - f_{yield,loss} \times \frac{T_{transient}}{N}) \times (\sum_{i=1}^{N} H_i \times t_i)_t}{(1+r)^t}} \tag{6.7}$$

Using these formulas the levelised cost of hydrogen can be calculated for the ATR with CCS where the throughput is adjusted each hour to balance the varying output of green hydrogen to ensure stable supply of hydrogen for ammonia production. The results can be seen in Figure 6.12.

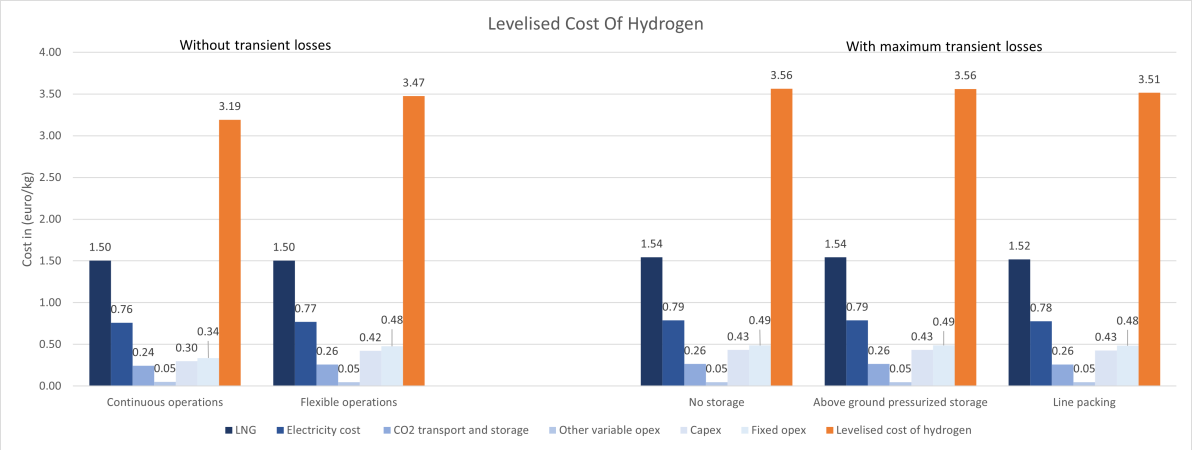

Figure 6.12: Breakdown of LCOH between continuous operations and flexible operations with and without transient losses.

From Figure 6.12 it becomes clear that flexible operations result in an increase in LCOH. Comparing continuous operations with flexible operations it can be seen that the largest increase is due to an increase in the cost of CAPEX and fixed OPEX per kg hydrogen. This is because there is less hydrogen produced using the same large scale plant designed for more production. The second largest increase in LCOH could be due to transient losses, this depends strongly on the yield loss factor and the transient time but can add an extra 9 cents per kg of hydrogen. The next increase in price is due to efficiency losses in the compressors and ASU which increases the electricity cost. The increase in CO_2 transport and storage cost is because there is more CO_2 captured per kg hydrogen produced due to the fact that more nitrogen enters the autothermal reforming reactor changing the compositions in the feed a small bit, resulting in more CO_2 production.

Carbon Intensity

The formula of carbon intensity is adjusted in order to calculate the CI of a plant with varying throughput. The new formula takes the average carbon intensity of the blue hydrogen plant during one operating year. The new formula for carbon intensity for a plant producing flexible:

$$CI = \frac{\sum_{i=1}^{N} C_i \times t_i}{\sum_{i=1}^{N} H_i \times t_i} \tag{6.8}$$

Here C_i is the rate of CO_2 equivalent emitted during that hour in kg/hr. When the plant is operating flexible the carbon intensity is equal to 0.64 kg CO_2-eq/kg H_2 excluding the transient losses. This is a slight increase compared to the 0.63 kg CO_2-eq/kg H_2 with continuous operations.

The previous formula can be adjusted to include the transient losses. The assumption is made that during transient state only hydrogen yield losses occur, but it could be that more CO_2 is produced in the transient state because of unwanted side reactions.

The formula for carbon intensity with transient losses:

$$CI = \frac{\sum_{i=1}^{N} C_i \times t_i}{(1 - f_{yield,loss} \times \frac{T_{transient}}{N}) \times \sum_{i=1}^{N} H_i \times t_i} \tag{6.9}$$

Now the carbon intensity depends on the transient time. When there is no storage used or a small amount using above ground storage, the carbon intensity increases to 0.65 kg CO_2-equivalent emitted per kg hydrogen. When hydrogen is stored using hydrogen packing in pipelines the plant needs to ramp up and down less frequent, resulting in less hydrogen losses and a carbon intensity of 0.64 kg CO_2-eq/kg H_2. These differences are very small compared to the emissions of grey hydrogen production which is around 8 to 12 kg CO_2-eq/kg H_2. This shows that flexible blue hydrogen production can still produce low carbon hydrogen even when transient state losses are taken into account.

6.4. ATR with CCS - Designed for more flexibility

For the last case study, the previous model shown in Figure 6.6 is adjusted so the blue hydrogen plant needs to operate with even larger volume flexibility. There are two situations where the volume flexibility of the blue hydrogen plant needs to increase.

Either the maximum amount of green hydrogen production per hour increases with the same amount of constant hydrogen demand. Or the maximum amount of green hydrogen production per hour is the same as before but the constant hydrogen demand from ammonia production is lower. In both scenario's the amount of blue hydrogen per hour needed to keep a constant supply of hydrogen is lower resulting in a lower throughput of the plant and a higher volume flexibility needed.

For this case study the scenario of an increasing amount of green hydrogen is used based on the trend of more intermittent renewable energy being used to produce flexible green hydrogen.

6.4.1. Define uncertainties

The same sub-questions can be asked in this new case study in order to clearly define the uncertainties. So what are the potential sources of uncertainty? What are the boundaries of uncertainties? What is the expected frequency of changes in the operating parameter?

What are the potential sources of uncertainties

The main source of the uncertainty remains the intermittent power output of the wind park coupled to electrolysers. However in this case the total power output of the wind park is increased to 1400 MW, resulting in a installed electrolyser capacity of 1093.4 MW by using the optimized amount of 78.1% installed capacity.

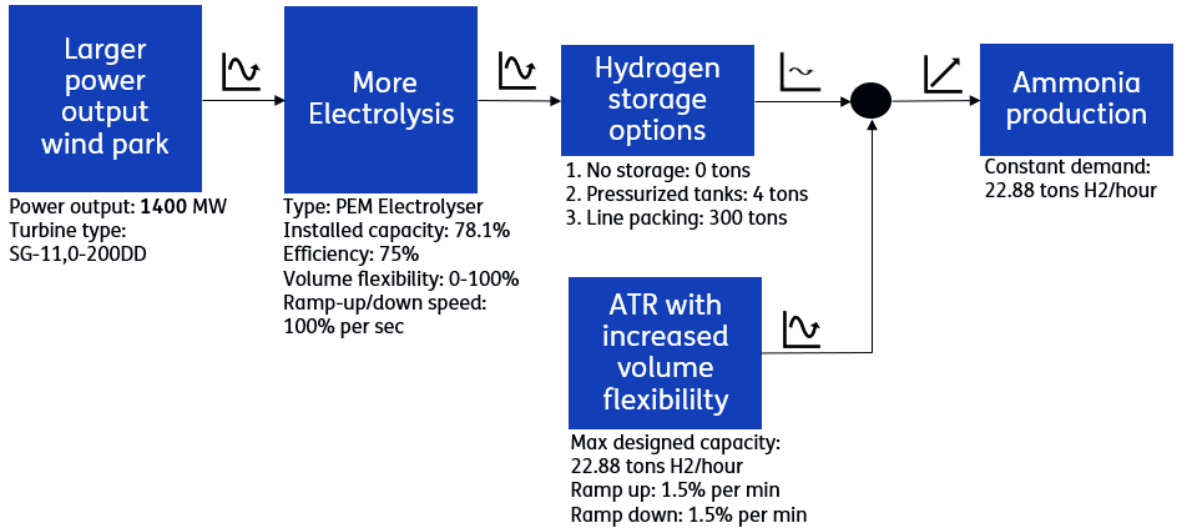

Figure 6.13: New model of ATR with increased volume flexibility in order to balance the increased green hydrogen production.

What are the boundaries of uncertainties

The boundaries of uncertainty, so the maximum and minimum flow rate of green hydrogen, change due to the increase in green hydrogen production in this case study. This leads to an increase in the maximum flow rate of green hydrogen produced. Using the same assumptions and boundaries as the previous case but with an increase in maximum wind power to 1400 MW results in a maximum flow rate of green hydrogen of 20.9 tons per hour. The minimum flow rate of green hydrogen keeps zero when there is no wind power produced.

Expected frequency of changes in operating parameter

The fluctuations are still hourly due to the wind speed fluctuations. The same storage capacity is used as as the previous cases. Meaning there is a case of no storage, 4 tons of above ground pressurized hydrogen storage and a hydrogen pipeline which can hold 300 tons of hydrogen. These storage options are not large enough to balance out the fluctuating green hydrogen in this case study to reduce the frequency of adjusting the throughput of the blue hydrogen plant.

Resulting operating condition

The new operating conditions for the blue hydrogen plant can now be visualized using the increased amount of green hydrogen production while keeping the constant demand for hydrogen the same. This is calculated using the formulas shown in Appendix A.4, using the new maximum power output for the wind farm.

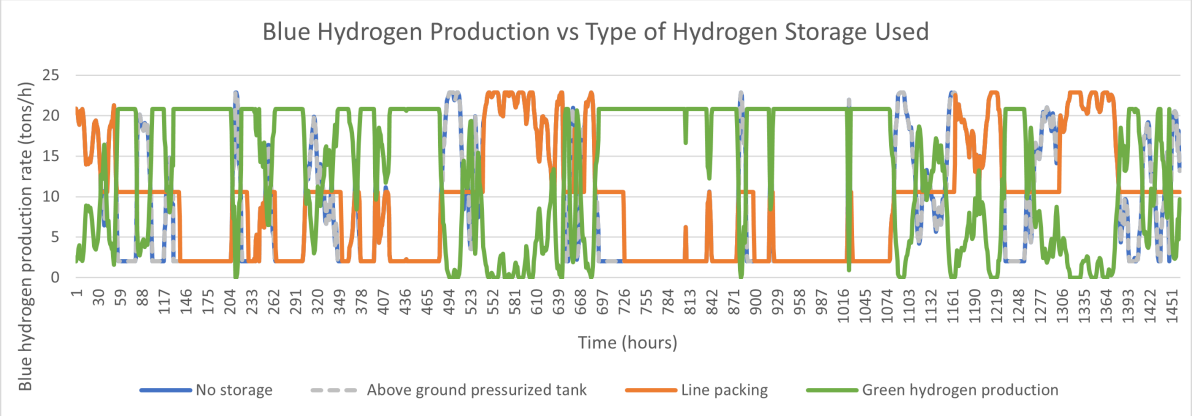

Figure 6.14: New hourly blue hydrogen production rate when there is more green hydrogen produced.

When there is a maximum output of green hydrogen the blue hydrogen plant still needs to deliver some hydrogen. This is no coincidence, the amount of wind power coupled to electrolysers in this case study is chosen so that there is no need for starting up or shutting down the blue hydrogen plant. This cannot be achieved on an hourly basis so is not a viable option for balancing the hydrogen supplied.

The blue hydrogen production shown in Figure 6.14 result in a relative hourly throughput shown in Figure 6.15.

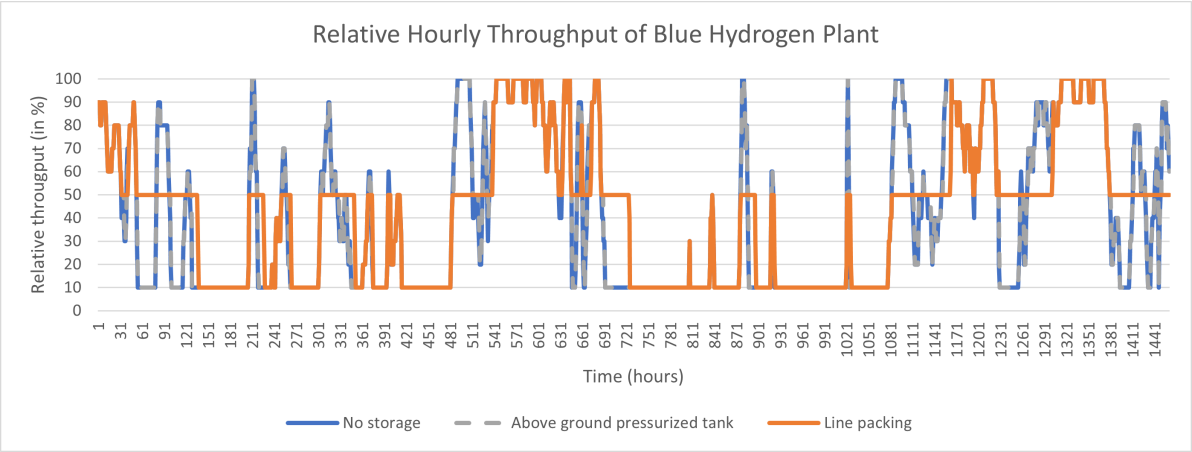

Figure 6.15: New relative hourly throughput of blue hydrogen plant

From Figure 6.15 it can be clearly seen that the blue hydrogen plant needs an increased volume flexibility in order to achieve a throughput of hydrogen of 10% of its nominal capacity.

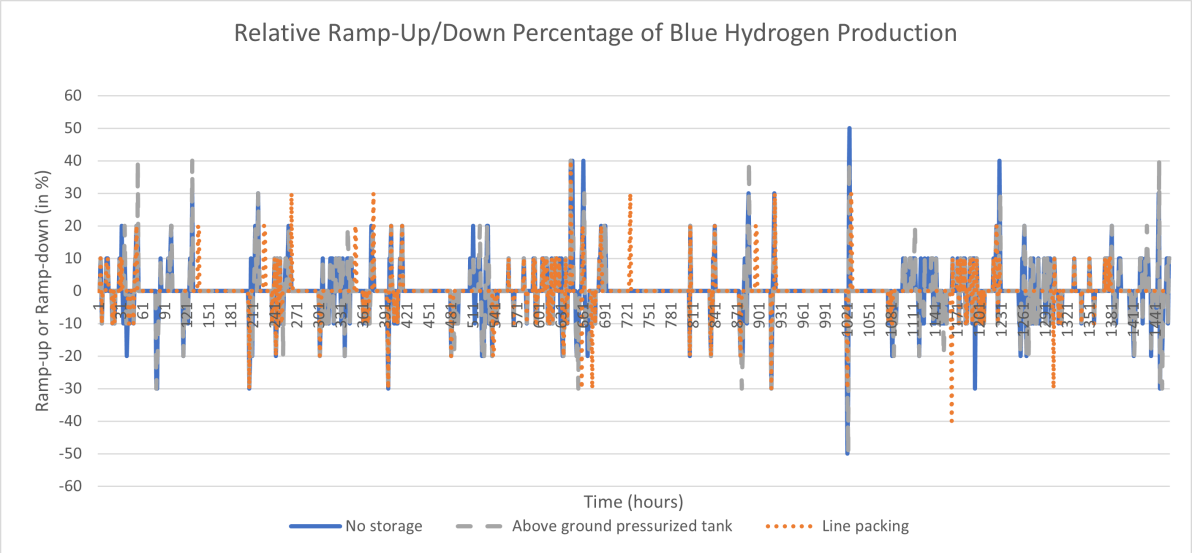

Figure 6.16: Caption

The increased amount of fluctuating green hydrogen also results in a larger and more ramping up or ramping down percentages between the hours for the blue hydrogen plant to balance out the fluctuations. For example, the blue hydrogen plants sometimes needs to ramp from 10% throughput to 60% throughput resulting in an ramp up of 50% in one hour. This will result in longer transient times.

The new operating conditions of the blue hydrogen plant can be seen in Table 6.3.

Table 6.3: New expected operating conditions blue hydrogen plant for one operating year using different storage types.

Throughput (%)	No storage (hours)	Above ground pressurized tank (hours)	Line packing (hours)
100	952	952	570
90	720	716	401
80	663	656	289
70	569	536	237
60	571	475	220
50	444	801	4326
40	437	306	103
30	317	285	95
20	366	340	127
10	2961	2933	1632
0	0	0	0
Total:	8000	8000	8000

Using the ramp-up and ramp-down rates mentioned by HyNet the total transient time can be calculated for this case where ATR needs to produce more flexible [67].

Table 6.4: New total transient time of ATR plant which needs to follow larger fluctuations.

Ramping up/down and Transient time			
	No storage	**Above ground pressurized tank**	**Line packing**
Sum ramping-up (%/operating year)	16530	15940	7380
Sum ramping-down (%/operating year)	-16540	-15950	-7420
(HyNet)			
Ramp-up rate (%/min)	1.5	1.5	1.5
Ramp-down rate (%/min)	-1.5	-1.5	-1.5
Transient time (Hour/operating year)	367.4	354.3	164.4

Using the same amount of storage to dampen out the increased share of fluctuating green hydrogen shows that the difference between no storage and for instance line packing storage becomes smaller when more fluctuations needs to be dampened. In the previous case the transient time of the blue hydrogen plant was around 3 times smaller between no storage and line packing. Now the total transient time is 2 times smaller between no storage and line packing. This is logical as the storage will be full much faster when there is more fluctuating green hydrogen produced with the same amount of storage capacity.

6.4.2. Define flexibility

For this case study the defined flexibility will be: The ability to vary the throughput between 10-100% of its nominal capacity of the whole blue hydrogen plant on hourly basis to ensure steady hydrogen supply for ammonia production.

6.4.3. Apply design strategies for flexibility

In order to achieve the desired volume flexibility a strategy to increase the volume flexibility is needed. Different solutions are possible in order to increase the volume flexibility of the different unit operations. The different strategies found in literature are:

- Parallel units
- Oversizing
- Storage for intermediate production
- Selecting inherent flexible equipment
- Inert gas as method for load regulation

The operating envelope is used to visualize the volume flexibility of each unit operations in order to find the bottleneck, the unit that limits the maximum volume flexibility, and then the best design strategy is used in order to increase the total volume flexibility of the plant. The best design strategy is the one where the total CAPEX and OPEX of the plant remains the lowest while increasing the volume flexibility of the process plant

First bottleneck

The first step is to increase the volume flexibility of the adsorption column used for CO_2 capture. This is the first bottleneck in the process plant which limits the total volume flexibility of the blue hydrogen plant.

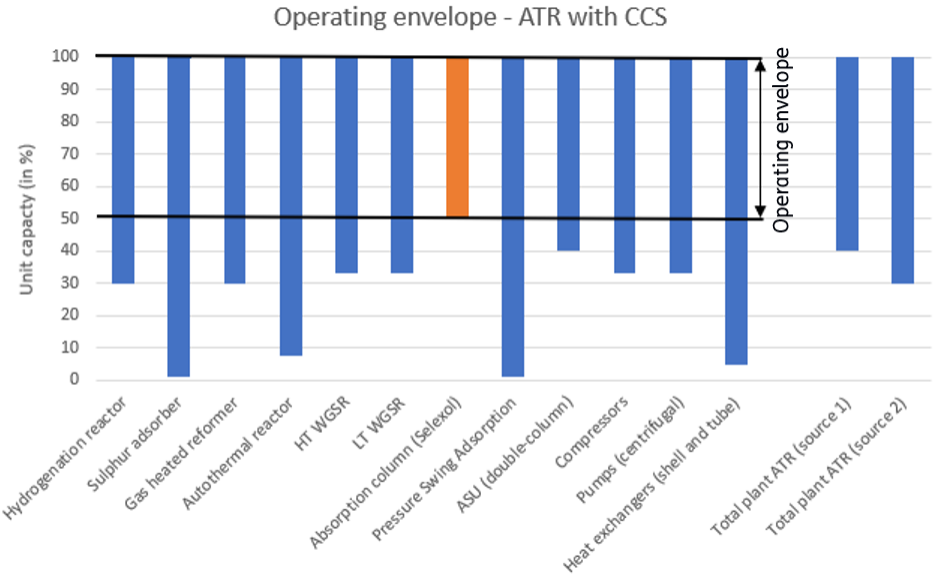

Figure 6.17: First bottleneck of the volume flexibility of the ATR plant.

Two design strategies can be used in this case. The first strategy is to increase the volume flexibility by using parallel absorption columns. The second strategy is to use inherently more flexible equipment. For and absorption column this can be done by using different trays used inside. This strategy will be implemented as it will not require an extra units but does increase the volume flexibility enough.

The standard sieve trays have an expected turndown ratio of 2:1, meaning that it can operate between 50-100% of its designed capacity [75]. However, when using valve trays the turn down ratio can be increased to 4:1 which is a volume flexibility of 25-100% because valve trays will increase the vapor-liquid contact at low flow rates compared to sieve trays [75]. This increase in volume flexibility of the adsorber will come at an increased CAPEX cost of around 20% for the selexol adsrober because the valve trays are more expensive then the sieve trays. OPEX will not change as the pressure drop is comparable with that of sieve trays [75].

Second bottleneck

Now that the volume flexibility of the adsoption column is increased a new bottleneck emerges. This time the bottleneck is the double column Air Separation Unit (ASU) which is capable of operating between 40-100% of the nominal capacity [21].

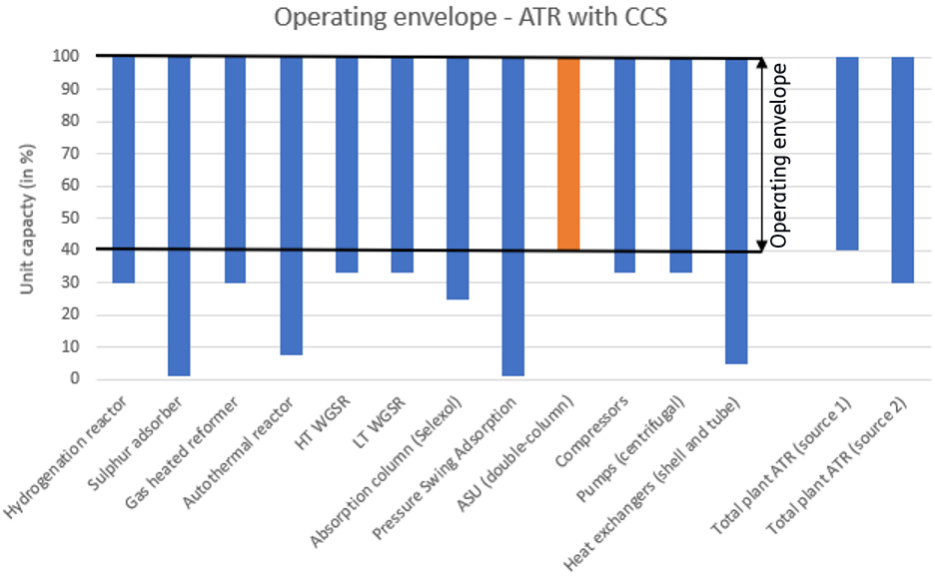

Figure 6.18: Second bottleneck of the volume flexibility of the ATR plant.

One of the design strategies that can be considered in order to increase the volume flexibility of the ASU is to use parallel units. Using two smaller double column ASU's with halve the capacity of the large double column ASU. This could increase the volume flexibility by shutting down one of the parallel ASU's during low oxygen consumption, thereby increasing the volume flexibility to a range of 20-100%. However, this would require two double column ASU's which is very expensive. Also shutting down and starting up a cryogenic air separation unit is not ideal and takes a lot of time and energy.

A better option is to use inherently more flexible equipment. In this case, the most flexible ASU found in literature is already used. Standard industrial ASU's have a operating range between 60-100% of its nominal capacity [73]. However the ASU used in the case study is a double column ASU which increases the operating range to 40-100%.

The last strategy is to use storage for intermediate production. This way the blue hydrogen plant can operate with a larger volume flexibility as it will not be limited by the ASU. If the throughput of the blue hydrogen plant drops lower than 40%, resulting in less oxygen demand, then the ASU will keep producing on its lower bound of 40%. The difference will be stored in large Liquefied Oxygen (LOX) tanks and when the throughput of blue hydrogen increases, thus the oxygen demand, some of the oxygen will be pulled out of the storage. So, the LOX tanks are only needed when the blue hydrogen plant produces between 10-40% of its throughput.

This storage for intermediate production will be implemented as its the cheapest available option. This will result in an increase in CAPEX because large storage tanks are needed. The OPEX will also increase a bit because of the extra energy required for this liquefied oxygen storage. The size of this tank depends on the operating conditions of the blue hydrogen plant. For the most variable case with no hydrogen storage the maximum amount of liquid oxygen storage needed is around 6000 tons, see Appendix A.13. Because the ASU is now independent on the production rate of the blue hydrogen plant it will be removed from the operating envelope, thereby revealing the new bottleneck of the process plant.

Third bottleneck

To lower the throughput even more becomes quite challenging after these two previous solutions as the process plant will not encounter one bottleneck bot several at the same time. Compressors, pumps and reactors all lose efficiency if the throughput becomes to low of its designed capacity.

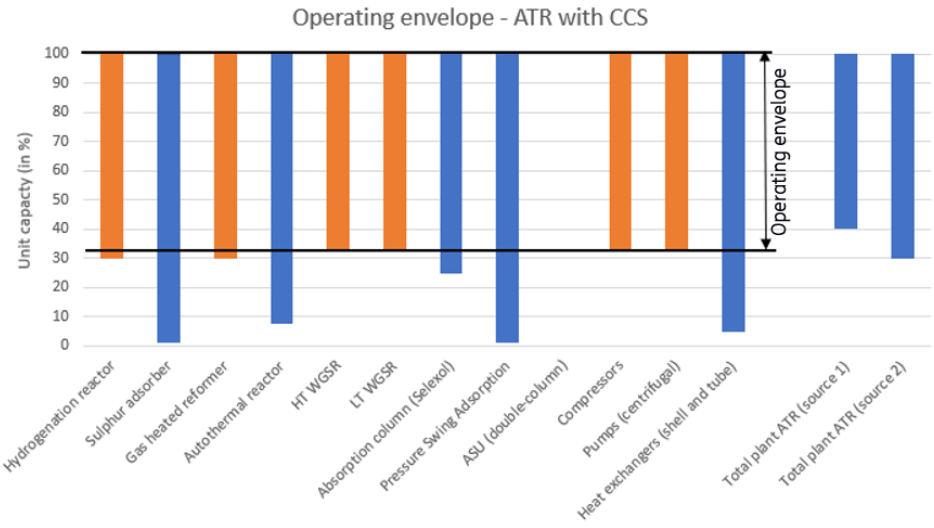

Figure 6.19: Third bottleneck of the volume flexibility of the ATR plant.

One strategy that does not increase the units own volume flexibility but still makes it able to lower the throughput is to use an inert gas when the feed flow rate is below the lower capacity bound. This method for load regulations can be used throughout the whole plant.

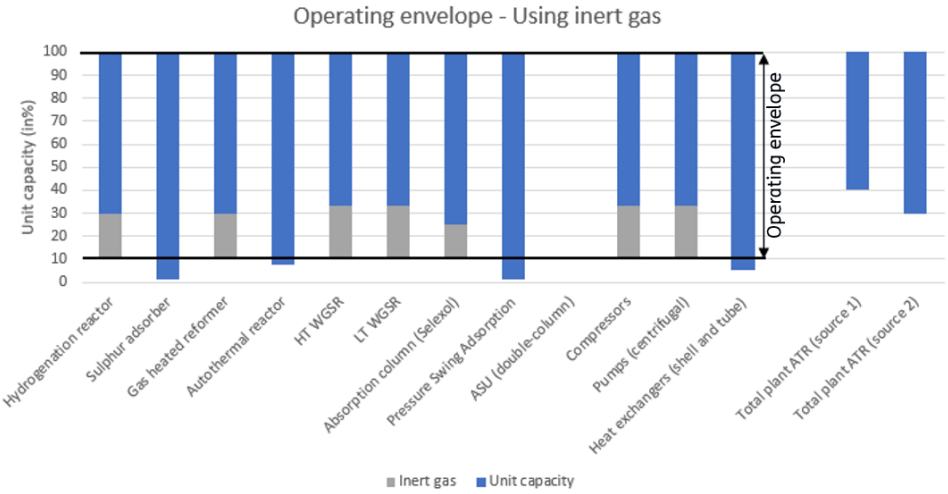

Figure 6.20: Inert gas as technique to increase volume flexibility of the ATR plant.

The amount of inert gas, nitrogen, used in the plant to keep the minimum capacity is either bound by the mass flow rate or the volume flow rate. If 1 kg of LNG is compensated with 1 kg nitrogen then the volumetric flow rate will decrease, thereby lowering the GHSV in the reactors and dropping below the surge limit of the compressors. Therefor, the amount of nitrogen needed is calculated based on the volumetric flow rate. If the plant runs on 20% of the capacity in order to keep the volumetric flow rate constant at the designed 30% capacity, around 9.6 t/h of nitrogen is needed while there is only 6.1 t/h of LNG used less. When the plant is operating at 10% around 19.5 t/h of nitrogen is added to keep the volumetric flow rate above the lower bound of the units capacity.

In order to supply inert gas when the plant is running at its lower capacity a few extra equipment is needed. The plant needs a storage unit for the nitrogen, a separation system to separate the nitrogen from the waste stream in order to reuse it and the nitrogen needs to be pressurized to the pressure at which the plant operates. There is no need for extra equipment to produce the nitrogen as the ASU already supplies enough nitrogen.

Final design for increased volume flexibility

Using these different strategies the volume flexibility of the ATR plant is able to follow the changes in demand of hydrogen as low as 10% of the designed nominal capacity. This range is large enough according the the defined flexibility for this case study.

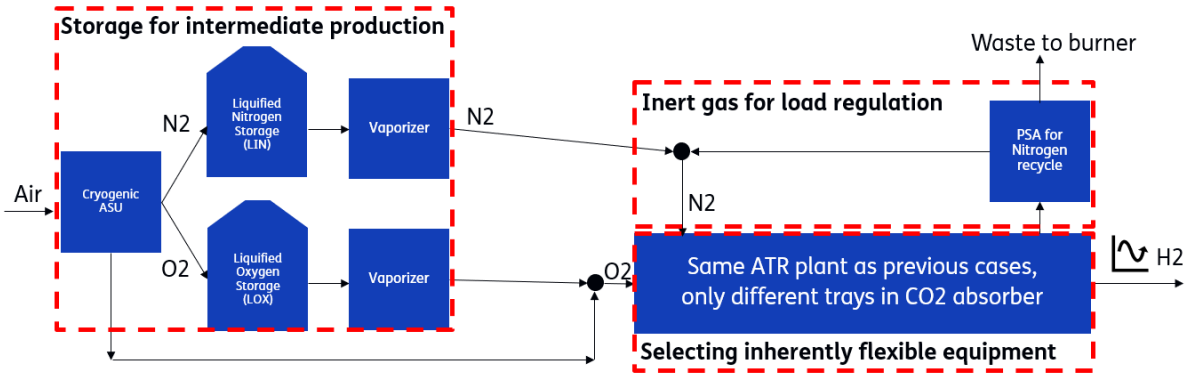

Figure 6.21: Schematic overview of additions for increased volume flexibility.

The new ATR plant, designed to operate with high volume flexibility, requires additional equipment to reduce hydrogen output below 30%. The cost for this equipment are shown in Table 6.5.

To give an illustration on how increased flexibility affects the efficiency, cost and emissions of hydrogen production, estimates of CAPEX and OPEX are made. Although these are rough estimate, less precise than those for the ATR plant itself due to limited reliable data, they still provide valuable insight. There may be some fluctuation in the exact figures, it is clear that the added flexibility will lead to increased total fixed CAPEX and OPEX, as well as higher variable operating cost. These estimations will therefore clearly show how increased flexibility affects the plants KPIs.

The cost for 2500 m^3 liquid gas storage is estimated to be around 0.8 million dollar in 2013, including the vacuum pipes, cryogenic liquid pumps, vaporizers, and pressure regulation appliances [52]. This results in the cost of storage for one 2500 m^3 liquid gas storage tank to 1.13 million dollar in 2024, using the CEPCI index. For the storage of liquid gases an approximation is made that around 6000 tons of liquid oxygen storage is needed and 10,000 tons of liquid nitrogen storage is needed. So for the liquid oxygen storage there are 3 of this 2500 m^3 storage units used and for the liquid nitrogen storage 5 units. The extra cost for the new sieves in the selexol absorber is calculated by taking the price of the old equipment, see Table 5.2, and multiplying it by 20%.

The cost of the nitrogen PSA is hard to predict as its very case specific, depending on factors like feed composition, purity requirements, cycle time, capacity, and throughput. Since the feed entering the nitrogen PSA already consists of 92 mol% nitrogen, and given that both the recovery rate and purity requirements are much lower than for a hydrogen PSA, the nitrogen PSA is assumed to cost roughly half as much as a hydrogen PSA with the same capacity. This gives a new cost estimate for the nitrogen PSA of 31.9 million dollar. This estimate is based on a max recycle capacity of 15.8 tons/hr of nitrogen and a reference cost of 48 million dollar for 18.9 tons/hr hydrogen PSA in 2016 [74]. The cost is then adjusted to today's prices using the CEPCI index and scaled with a factor of 0.6 according to the six-tenth rule.

Table 6.5: Extra equipment cost in order to increase volume flexibility of the ATR plant.

Extra process components	Cost (M$)
Liquid Oxygen storage & vaporizer	3.39
Liquid Nitrogen storage & vaporizer	5.65
PSA for nitrogen	31.79
Extra cost sieve trays	9.43
Total extra ISBL Investment	**50.26** (M$) **45.74** (M_euro)

By adding the values from Table 6.5 to the total ISBL investment in Table 5.2, the new total fixed capital cost of the new plant can be calculated. The same ratios for capital cost, engineering cost, and contingency used in the previous plant are applied here. This increase in capital cost will also lead to a rise in fixed operating costs.

To estimate the additional OPEX for the ATR plant when operating at 10-30% of its designed capacity, several assumptions are made. Nitrogen gas is added to the feed to maintain a constant volume flow rate at 30% capacity. The PSA for nitrogen separation has a recovery rate of 80%, meaning that at 10% or 20% capacity, extra pure nitrogen needs to be produced to compensate for the nitrogen lost during the PSA process. The specific power consumption for producing pure nitrogen is assumed to be 370 kWh/tonne, based on data from a conventional cryogenic ASU process [4].

Additionally, the PSA requires energy for nitrogen recovery. To simulate this, the low pressure waste stream from the hydrogen PSA is repressurized to 40 bar for use in the nitrogen PSA. The recycled nitrogen is then repressurized to the plants operating conditions, adding to the overall electricity consumption. This process is simulated in Aspen, and the energy requirements depend on the feed flow rate of the nitrogen added. For simplicity, boil-off rates from the liquefied gas storage tanks are assumed to be zero.

6.4.4. KPI's Design for more flexibility

The ATR plant is now capable of operating between 10% and 100% of its nominal capacity, as defined by the flexibility required for this case study. This adjustment increases the plants volume flexibility from 0.5 to 0.9. However, this increased flexibility comes with trade-offs. The impact on efficiency, cost and emissions will be analyzed using the different KPIs, based on the assumptions made in the previous chapter.

Process efficiency

The process efficiency of the new ATR plant is calculated the same way as the flexible case. The efficiency is lower compared to the previous cases because there is more energy consumption for the same amount of hydrogen produced. Especially when the plant is running on 10% or 20% of the designed capacity. During these hours there is extra energy required for the nitrogen loop to keep the volumetric flow rate above the lower limit.

Table 6.6: Efficiency of ATR designed for increased volume flexibility.

	No Storage	Above Ground Storage	Line Packing
Efficiency	80.78%	80.79%	81.00%

The reason for the larger difference between the efficiency of the blue hydrogen plant which follows the fluctuations of green hydrogen directly, meaning no storage, and the blue hydrogen plant which needs to follow a dampened green hydrogen output by using storage in hydrogen pipelines, line packing, is because of the difference in hours operating between the less efficient 10-30% throughput. When looking at Table 6.3, it can be seen that using line packing result in the blue hydrogen plant operating more on a constant 50% of its throughput which is more efficient compared to 10% or 20%. This shows that when the plant is designed for more flexibility it could be wise to introduce scheduling in order to minimize the amount of hours spend on less efficient throughput, in this case between 10 and 30%.

Because of the increase in frequency of fluctuations, the transient time for the blue hydrogen plant also increases compared to the previous flexible case.

Table 6.7: Efficiency including transient losses of ATR designed for increased volume flexibility, assuming $f_{yield,loss}$ =1 .

	No Storage	Above Ground Storage	Line Packing
Transient Time (hours)	367.40	354.30	164.40
Efficiency (including transient losses)	77.07%	77.21%	79.34%

The data shows that if the hydrogen yield during transient state is low, then the efficiency of the plant will also decrease a lot. Therefore, when using the ATR flexibly to balance out the large intermittent supply of green hydrogen, it is important to understand the yield loss when the plant is in transient state. If the yield loss is large, then ATR is not efficient when operating very flexible. However, if the loss is small, then the ATR can produce hydrogen flexible with reasonable efficiency.

LCOH

Although the plant designed for increased flexibility operates reasonably efficiently, the LCOH rises significantly due to higher CAPEX and fixed OPEX while reducing the total amount of hydrogen produced.

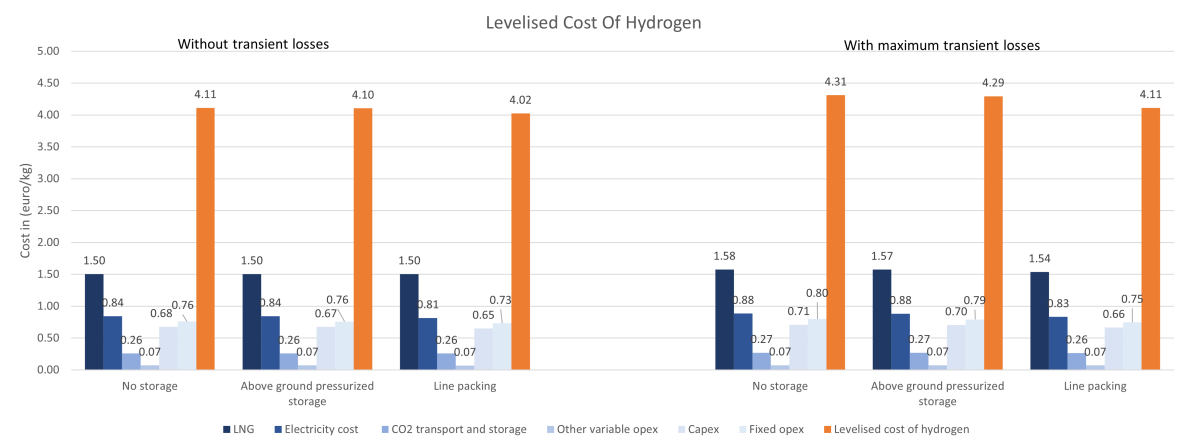

Figure 6.22: Breakdown of levelised cost of hydrogen for ATR designed for flexibility comparing 3 different operating conditions.

For each operating condition of the ATR plant designed for flexibility, the LCOH increases significantly from from the reference cost of 3.19 euro per kg hydrogen for the ATR plant operating continuously at 100% to a cost of at least 4.02 euro per kg hydrogen. The reason of this increase is again mainly due to underused CAPEX, as the plant requires extra investments to operate at 10% of its designed capacity while producing less hydrogen. Therefore, the cost of CAPEX and Fixed OPEX together increases to at least 1.38 euro per kg hydrogen, compared to 0.64 for the the base case operating continuously, as shown in Figure 6.2.

The transient state losses are also higher than in the previous flexible case due to increased flexibility needed to manage the larger fluctuations in intermittent green hydrogen production. If the yield loss during transient state is large, these losses could add up to an additional 20 cents per kilogram of hydrogen, depending on how flexible the blue hydrogen plant needs to operate.

In addition, the variable operating cost also increase as there is more electricity needed for the recompression of the inert nitrogen when operating at low throughput. This extra electricity cost can be reduced when the plant operates above 30% of its capacity for longer periods of time, as seen in the electricity cost column of Figure 6.22, where the difference in electricity cost between the operating conditions of using no storage and line packing is 3 cents per kg hydrogen.

Carbon Intensity

It is found, using the formula for calculating the carbon intensity from the previous chapter, that for the ATR designed for a larger volume flexibility that the carbon intensity depends on the operating conditions of the plant. If the amount of hours spend between 10-30% of its maximum throughput per operating year is larger then the carbon intensity will increase. This is because operating between these points will dilute the reactor with nitrogen and therefore decrease the amount of hydrogen produced per kg CO_2 emitted.

Table 6.8: Carbon intensity of ATR designed for increased volume flexibility.

	No Storage	Above Ground Storage	Line Packing
Carbon intensity	0.64	0.64	0.63
Carbon intensity (with transient losses)	0.67	0.67	0.65

However, just like the previous case this difference is relatively small compared to using different techniques for hydrogen production. Grey hydrogen, made from natural gas without carbon capture and storage, emits between 9 to 12 kg CO_2-equivalent per kg hydrogen. So, even if the ATR plant is operating very flexible it is still able to produce hydrogen with low emissions.

6.5. Summary results

Collecting all the different results a summary can be made of the effect of flexible hydrogen production on the different KPI's.

	Case 1: ATR with CCS continuous operations	Case 2: ATR with CCS flexible operations	Case 3: ATR with CCS designed for more flexibility
Volume Flexibility (-)	0.5	0.5	0.9
Efficiency (%)	81.45	79.25-81.36	77.07-81.00
LCOH (€/kg)	3.19	3.47-3.57	4.02-4.31
CI (KG CO2-eq/kg H2)	0.63	0.63-0.65	0.63-0.67

7

Conclusion

The main research question of this thesis was:

"What is the potential of flexible natural gas reforming with carbon capture and storage for balancing the intermittent supply of green hydrogen to ensure continuous ammonia production in the harbour of Rotterdam?"

In order to find the potential a few sub-question are answered first:

What will the overall process design of blue hydrogen in combination with electrolysis be for large scale NH_3 production?

For large-scale NH_3 production, Autothermal Reforming (ATR) with Carbon Capture and Storage (CCS) using a Gas Heated pre-Reformer (GHR) is recommended as most suitable process design. This process is efficient and cost-effective because the ATR reactor can be scaled to large capacities, while the integration of the GHR utilizes the high-grade heat from the reformed gas downstream of the ATR reducing overall energy consumption. Crucially, ATR produces a single concentrated CO_2 stream, allowing efficient pre-combustion CO_2 capture, which allows high capture rates. This is essential for decarbonizing the future energy system.

Additionally, the ATR process is well-suited to balance fluctuations in green hydrogen production from wind powered PEM electrolysis. With the ability to ramp production up or down rapidly, ATR ensures a stable hydrogen supply for the ammonia synthesis loop, even as renewable energy production fluctuate.

What is the possible volume flexibility of the process and how can it be increased?

The initial volume flexibility of the ATR with CCS is equal to 0.5, allowing operation between 50-100% of its designed capacity. To increase this flexibility, several design strategies are recommended: using inherent flexible equipment, adding storage for intermediate production and using inert gas as a method for load regulation.

The first step to increase the volume flexibility is to adjust the trays in the CO_2 absorber column, which raises the plants volume flexibility to 0.6. Next, decoupling the Air Separation Unit (ASU) from the blue hydrogen plant by using liquid oxygen storage further increases the volume flexibility to around 0.7. Further increasing the volume flexibility beyond 0.7 becomes increasingly difficult as multiple units like reactors, compressors and absorbers encounter limitations. To address this, inert gas can be introduced for load regulation, potentially raising the plants volume flexibility to 0.9. However, this approach brings some trade-offs, affecting the cost and efficiency of the process.

Which key performance indicators can be used to evaluate the effect of flexible operations?

In order to evaluate the effects of flexible operations, it is useful to compare the Key Performance Indicators (KPIs) of a traditional process, which operates continuously at maximum production capacity, with the same process using flexible operations. KPIs used to compare the effects flexible blue hydrogen production are the plants efficiency, Levelised Cost of Hydrogen (LCOH) and Carbon Intensity

(CI). These three KPIs provide insights into the effects of flexible operations on efficiency, cost and emissions giving a full picture on the impact of flexibility.

In highly flexible chemical processes, the frequency of production changes is much higher, resulting in the plant spending a significant amount of time in the transient state. To accurately represent the effects of flexibility, the losses due to the the plant operating in less favorable conditions should be included to the mentioned KPIs to give a more accurate representation of the effect of flexible operations.

It is found that for flexible process parameters like ramping speed, amount of frequency changes and losses during transient state become very important. A chemical process is better suited for flexible operations, meaning a process with a lot of frequency changes, when either it has a high ramping speed or low yield loss during transient state.

How will the economy of the process be impacted by the need for flexibility? What will be the impact of 'underused CAPEX' on the overall process?

The impact on the economy of the blue hydrogen process depends on the level of flexibility required during operation. The plant has its lowest production cost when operating at maximum capacity, as this fully utilized the CAPEX and ensures the process is running at its most efficient point. This result in a blue hydrogen cost of 3.19 euro per kg.

When the plant varies production within its 'base' volume flexibility, meaning the flexibility it already has without additional equipment, three types of losses affect the economy of the process. The first loss is underused CAPEX which is the largest and depends on the reduced amount of hydrogen produced compared with operating at maximum capacity. The second is the loss of hydrogen produced when the plant is operating in transient state. If these losses are significant, they can further impact the economy of the process, especially when the time spent in transient state and the yield losses during these periods are large. The third loss is related to efficiency reduction in process equipment, such as compressors, which require more energy when operating off their optimal design conditions. When operating between its base volume flexibility the cost of blue hydrogen increases to somewhere between 3.47 and 3.57 depending on the operating conditions and transient losses. This is an increase of around 30 cent per kg hydrogen as a result of flexible production.

If the blue hydrogen plant needs to operate more flexibly, in this case with a larger volume flexibility, there will be an additional loss to the economy of the process. As increasing the volume flexibility by lowering its minimum capacity will require extra equipment which increases the CAPEX while the plant is designed to produce less hydrogen. This will increase the production cost of hydrogen the most. For this flexible case the levelised cost of hydrogen is somewhere between 4.02 and 4.31 euro per kg. This is an increase of at least 83 cents per kg which is more than two times larger then the previous flexible case where there was no additional equipment needed and more hydrogen produced.

Conclusion to main research question:
This research shows that flexible natural gas reforming with carbon capture and storage can effectively balance the intermittent supply of green hydrogen ensuring a stable hydrogen supply for downstream process. In this case study, Autothermal Reforming with Carbon Capture and Storage using a Gas Heated Pre-Reformer provides the lowest cost for blue hydrogen while maintaining the ability to quickly adapt to demand variations. When operating flexible, varying the throughput each hour, the blue hydrogen plant is still able to produce low carbon hydrogen efficiently.

However, there is a trade-off between cost and flexible production as a consequence of underused CAPEX. The cost of flexible blue hydrogen is competitive with alternatives such as above ground storage when the plant operates within its base volume flexibility. If the plant needs to increase its volume flexibility beyond this base, then the cost of blue hydrogen rises significantly, making alternatives like hydrogen storage or imports more economically viable to balance out the intermittent supply of green hydrogen.

As the hydrogen economy grows and the need for renewable energy integration increases, the role of flexible hydrogen production through natural gas reforming with CCS is likely to grow. Further research on optimizing process flexibility will be critical in making the hydrogen system more resilient and economically feasible transitioning towards a sustainable energy future.

8

Recommendations

Design chemical processes with flexibility in mind

As flexible chemical processes become increasingly important for a sustainable future with intermittent power and feedstock supply, it is crucial for future chemical processes to adapt. Designing inherently flexible plants allows systems to better handle uncertainties. Processes that are designed to operate continuously at maximum capacity limit their ability to adapt to fluctuations in energy availability and material demand, hindering integration with renewable energy sources.

This case study shows that using inherently more flexible equipment, such as autothermal reforming instead of steam methane reforming, can provide increased volume and load flexibility without significant efficiency losses when operating within its designed base volume flexibility range. Therefore, building knowledge on the flexibility of different chemical processes is essential. Not only focusing on metrics like cost and energy consumption but also on other metrics such as volume flexibility and ramping speed.

Use experiments to verify the feasibility of flexible chemical processes

The lack of experimental data, let alone real-time data from industry, makes it hard to verify the feasibility of flexible chemical processes. While models and simulations provide a useful insight, experimental verifications is needed to better understand the practical challenges of operating under fluctuation conditions. For this reason there are three suggested experiments to verify the potential of flexible natural gas reforming proceses:

- **Data on the effects of varying throughput on catalyst performance:** Experiments should be conducted to assess catalyst degradation, activity and selectivity under variable load conditions. A low TRL 2-3 experiment, such as varying load on a lab-scale Water Gas Shift Reactor, could demonstrate the feasibility of flexible operation in natural gas reforming. Not only for this case study using autothermal reforming, but also for alternatives like e-SMR which can also produce varying amounts of syngas based on the amount of electricity available. Such experiments could provide insights into how well these thermochemical process operate under load variability.
- **Study the effects of inert gas for load regulation in reactors:** The use of inert gases, like nitrogen, for load regulation could improve a plants volume flexibility. However, the effects of this technique on the performance of a reactor is not well known. A TRL 4 proof-of-concept experiment on lab scale could help evaluate how inert gases influence reactor operation and flexibility.
- **Measure transient state losses to assess economic impacts:** A TRL 6 demonstration to measure losses during transient state will give a better understanding on the potential added economic loss of flexible operations in a real operational environment. Transient state, which occur during start-up, shut-down and load changes, can result in significant inefficiencies, both in terms of product yield and energy consumption. By quantifying transient state losses through experiments, it becomes more clear what the potential losses of flexible operations are and whether implementing strategies to reduce these losses is advantageous.

Integration and optimization study flexible blue hydrogen

Blue hydrogen can play a key role in balancing fluctuations in hydrogen production. Further research is needed to optimize its integration with other technologies. This case study provides a simplified overview of how blue hydrogen can stabilize fluctuations in green hydrogen production. One area for optimization is determining the optimal balance between blue and green hydrogen production, considering that electrolysers also produce oxygen. It could be interesting so see if this oxygen can be used for autothermal reforming, thereby reducing the need for an expensive ASU.

A more detailed study could look at the ideal amount of flexible blue hydrogen production in combination with a broader system that includes storage, both fluctuating and constant hydrogen demand, variable green hydrogen production and potential hydrogen imports. The goal would be to minimize costs and emissions while ensuring a stable, resilient hydrogen supply. This integrated approach could provide valuable insights into how best to design hydrogen systems that balance flexibility, cost-effectiveness, and sustainability.

Integrating electrolysers oxygen to ATR for ammonia synthesis

Another interesting case is to explore the possibility of integrating the oxygen produced from electrolysers with air to supply the right amount of oxygen-enriched air to the ATR for the downstream process of ammonia synthesis. A feasibility study should be conducted to compare the overall cost and energy consumption of this approach with a conventional case that relies on oxygen from an ASU. This would help to see if integrating electrolysers into the process of ATR offers a more cost-effective and sustainable solution for ammonia production.

Future study on flexibility in hydrogen demand

In the case study, blue hydrogen is used to ensure a stable hydrogen supply for the downstream process of ammonia synthesis. However, this approach may not be necessary if downstream processes can operate efficiently and cost-effectively with intermittently produced hydrogen.

Therefore, it would be interesting to study the flexibility of downstream hydrogen processes, like ammonia synthesis, methanol production and steel manufacturing, and find ways to increase the flexibility of these process. This would help the integration of intermittent green hydrogen production, especially in locations without large-scale hydrogen infrastructure.

Life Cycle Assessment

A Life Cycle Assessment (LCA) is recommended to evaluate the full environmental impact of flexible natural gas reforming processes. It will provide insights into the emissions and resource use across the whole process chain, from raw materials to disposables. By applying a LCA, the effects of flexibility on overall sustainability can be quantified, such as the effect of underused equipment. The LCA will allow for a better comparison on emissions between different hydrogen production technologies. Showing a detailed assessment of their environmental performance, including trade-offs in emissions and resource use.

References

[1] Zainul Abdin, Kaveh Khalilpour, and Kylie Catchpole. “Projecting the levelized cost of large scale hydrogen storage for stationary applications”. In: *Energy Conversion and Management* 270 (2022), p. 116241. ISSN: 0196-8904. DOI: https://doi.org/10.1016/j.enconman.2022.116241. URL: https://www.sciencedirect.com/science/article/pii/S0196890422010184.

[2] International Renewable Energy Agency and Ammonia Energy Association. *Innovation Outlook: Renewable Ammonia*. Abu Dhabi and Brooklyn: International Renewable Energy Agency, 2022. URL: https://www.irena.org/-/media/Files/IRENA/Agency/Publication/2022/May/IRENA_Innovation_Outlook_Ammonia_2022.pdf.

[3] Joakim Andersson and Stefan Grönkvist. “Large-scale storage of hydrogen”. In: *International Journal of Hydrogen Energy* 44.23 (2019), pp. 11901–11919. ISSN: 0360-3199. DOI: https://doi.org/10.1016/j.ijhydene.2019.03.063. URL: https://www.sciencedirect.com/science/article/pii/S0360319919310195.

[4] Mathew Aneke and Meihong Wang. “Potential for improving the energy efficiency of cryogenic air separation unit (ASU) using binary heat recovery cycles”. In: *Applied Thermal Engineering* 81 (2015), pp. 223–231. ISSN: 1359-4311. DOI: https://doi.org/10.1016/j.applthermaleng.2015.02.034. URL: https://www.sciencedirect.com/science/article/pii/S1359431115001428.

[5] Max Appl. “Ammonia”. In: *Ullmann’s Encyclopedia of Industrial Chemistry*. John Wiley Sons, Ltd, 2006. ISBN: 9783527306732. DOI: https://doi.org/10.1002/14356007.a02_143.pub2. eprint: https://onlinelibrary.wiley.com/doi/pdf/10.1002/14356007.a02_143.pub2. URL: https://onlinelibrary.wiley.com/doi/abs/10.1002/14356007.a02_143.pub2.

[6] Husain E. Ashkanani et al. “Levelized Cost of CO2 Captured Using Five Physical Solvents in Pre-combustion Applications”. In: *International Journal of Greenhouse Gas Control* 101 (2020), p. 103135. ISSN: 1750-5836. DOI: https://doi.org/10.1016/j.ijggc.2020.103135. URL: https://www.sciencedirect.com/science/article/pii/S1750583620305600.

[7] Husain E. Ashkanani et al. “Levelized Cost of CO2 Captured Using Five Physical Solvents in Pre-combustion Applications”. In: *International Journal of Greenhouse Gas Control* 101 (2020), p. 103135. ISSN: 1750-5836. DOI: https://doi.org/10.1016/j.ijggc.2020.103135. URL: https://www.sciencedirect.com/science/article/pii/S1750583620305600.

[8] Asia Industrial Gases Association. *Hydrogen Pressure Swing Adsorber (PSA) Mechanical Integrity Requirements*. Version 08-2018. 2018. URL: https://www.asiaiga.org/uploaded_docs/en_AIGA_100_18_Hydrogen_PSA_Mechanical_Integrity_Ver_08-2018.pdf.

[9] Mohammad Azarhoosh, H. Ebrahim, and Seyed Pourtarah. “Simulating and Optimizing Hydrogen Production by Low-pressure Autothermal Reforming of Natural Gas using Non-dominated Sorting Genetic Algorithm-II”. In: *Chemical and Biochemical Engineering Quarterly* 29 (Dec. 2015), pp. 519–531. DOI: 10.15255/CABEQ.2014.2158.

[10] T. Banaszkiewicz, M. Chorowski, and W. Gizicki. “Comparative Analysis of Oxygen Production for Oxy-combustion Application”. In: *Energy Procedia* 51 (2014). 7th Trondheim Conference on CO2 capture, Transport and Storage (2013)., pp. 127–134. ISSN: 1876-6102. DOI: https://doi.org/10.1016/j.egypro.2014.07.014. URL: https://www.sciencedirect.com/science/article/pii/S1876610214008765.

[11] Erlisa Baraj, Karel Ciahotný, and Tomáš Hlinčík. “The water gas shift reaction: Catalysts and reaction mechanism”. In: *Fuel* 288 (2021), p. 119817. ISSN: 0016-2361. DOI: https://doi.org/10.1016/j.fuel.2020.119817. URL: https://www.sciencedirect.com/science/article/pii/S0016236120328131.

[12] A. Basile, S. Liguori, and A. Iulianelli. “2 - Membrane reactors for methane steam reforming (MSR)”. In: *Membrane Reactors for Energy Applications and Basic Chemical Production*. Ed. by Angelo Basile et al. Woodhead Publishing Series in Energy. Woodhead Publishing, 2015, pp. 31–59. ISBN: 978-1-78242-223-5. DOI: 10.1016/B978-1-78242-223-5.00002-9. URL: https://www.sciencedirect.com/science/article/pii/B9781782422235000029.

[13] Basile et al. *12.2.2 Pressure Swing Adsorption*. Institution of Engineering and Technology (The IET), 2017. ISBN: 978-1-78561-100-1. URL: https://app.knovel.com/hotlink/khtml/id:kt011AKX94/hydrogen-production-separation/pressure-swing-adsorption.

[14] Rajat Bhardwaj, Robert de Kler, and Octavian Partenie. *Enabling a Low-Carbon Economy via Hydrogen and CCS*. Project Report. TNO, 2020. URL: https://www.sintef.no/globalassets/project/elegancy/deliverables/elegancy_d5.2.2_rotterdam_h2-production_integration.pdf.

[15] Svenja Bielefeld, Miloš Cvetković, and Andrea Ramírez. “Should we exploit flexibility of chemical processes for demand response? Differing perspectives on potential benefits and limitations”. English. In: *Frontiers in Energy Research* 11 (2023). ISSN: 2296-598X. DOI: 10.3389/fenrg.2023.1190174.

[16] Bruns et al. “A systematic approach to define flexibility in chemical engineering”. In: *Journal of Advanced Manufacturing and Processing* 2 (July 2020). DOI: 10.1002/amp2.10063. URL: https://aiche.onlinelibrary.wiley.com/doi/epdf/10.1002/amp2.10063.

[17] Andrew Burke, Joan Ogden, and Lewis Fulton. “Hydrogen Storage and Transport: Technologies and Cost”. In: (Feb. 2024). URL: https://escholarship.org/content/qt83p5k54m/qt83p5k54m_noSplash_8bb1326c13cfb9aa3d0d376ec26d3e06.pdf?t=s9oa2u.

[18] Maximilian Cegla et al. “Flexible process operation for electrified chemical plants”. In: *Current Opinion in Chemical Engineering* 39 (2023), p. 100898. ISSN: 2211-3398. DOI: https://doi.org/10.1016/j.coche.2023.100898. URL: https://www.sciencedirect.com/science/article/pii/S2211339823000023.

[19] Chao Chen and Aidong Yang. “Power-to-methanol: The role of process flexibility in the integration of variable renewable energy into chemical production”. In: *Energy Conversion and Management* 228 (2021), p. 113673. ISSN: 0196-8904. DOI: https://doi.org/10.1016/j.enconman.2020.113673. URL: https://www.sciencedirect.com/science/article/pii/S0196890420311997.

[20] Mao Cheng et al. “Flexible cryogenic air separation unit—An application for low-carbon fossil-fuel plants”. In: *Separation and Purification Technology* 302 (2022), p. 122086. ISSN: 1383-5866. DOI: https://doi.org/10.1016/j.seppur.2022.122086. URL: https://www.sciencedirect.com/science/article/pii/S1383586622016410.

[21] Mao Cheng et al. “Flexible cryogenic air separation unit—An application for low-carbon fossil-fuel plants”. In: *Separation and Purification Technology* 302 (2022), p. 122086. ISSN: 1383-5866. DOI: https://doi.org/10.1016/j.seppur.2022.122086. URL: https://www.sciencedirect.com/science/article/pii/S1383586622016410.

[22] Thomas S. Christensen. “Adiabatic prereforming of hydrocarbons — an important step in syngas production”. In: *Applied Catalysis A: General* 138.2 (1996), pp. 285–309. ISSN: 0926-860X. DOI: 10.1016/0926-860X(95)00302-9. URL: https://doi.org/10.1016/0926-860X(95)00302-9.

[23] Thomas S. Christensen. “Adiabatic prereforming of hydrocarbons — an important step in syngas production”. In: *Applied Catalysis A: General* 138.2 (1996). Chemical Engineering and Catalysis, pp. 285–309. ISSN: 0926-860X. DOI: https://doi.org/10.1016/0926-860X(95)00302-9. URL: https://www.sciencedirect.com/science/article/pii/0926860X95003029.

[24] Schalk Cloete et al. “Cost-effective clean ammonia production using membrane-assisted autothermal reforming”. In: *Chemical Engineering Journal* 404 (2021), p. 126550. ISSN: 1385-8947. DOI: https://doi.org/10.1016/j.cej.2020.126550. URL: https://www.sciencedirect.com/science/article/pii/S1385894720326784.

[25] Schalk Cloete et al. “Cost-effective clean ammonia production using membrane-assisted autothermal reforming”. In: *Chemical Engineering Journal* 404 (2021), p. 126550. ISSN: 1385-8947. DOI: https://doi.org/10.1016/j.cej.2020.126550. URL: https://www.sciencedirect.com/science/article/pii/S1385894720326784.

[26] G. Collodi. “Hydrogen Production via Steam Reforming with CO2 Capture”. In: *Chemical Engineering Transactions* 19 (Apr. 2010), pp. 37–42. DOI: 10.3303/CET1019007. URL: https://www.cetjournal.it/index.php/cet/article/view/CET1019007.

[27] Collodi and Guido. “Hydrogen Production via Steam Reforming with CO2 Capture”. In: vol. 19. Jan. 2010, pp. 37–42. ISBN: 978-88-95608-11-2. DOI: 10.3303/CET1019007. URL: https://www.aidic.it/cet/10/19/007.pdf.

[28] Paul Cosgrove, Tony Roulstone, and Stan Zachary. “Intermittency and periodicity in net-zero renewable energy systems with storage”. In: *Renewable Energy* 212 (2023), pp. 299–307. ISSN: 0960-1481. DOI: https://doi.org/10.1016/j.renene.2023.04.135. URL: https://www.sciencedirect.com/science/article/pii/S0960148123006018.

[29] Devaiah Damma and Panagiotis G Smirniotis. “Recent advances in iron-based high-temperature water-gas shift catalysis for hydrogen production”. In: *Current Opinion in Chemical Engineering* 21 (2018). Energy and environmental engineering • Reaction engineering and catalysis, pp. 103–110. ISSN: 2211-3398. DOI: https://doi.org/10.1016/j.coche.2018.09.003. URL: https://www.sciencedirect.com/science/article/pii/S2211339818300121.

[30] Vegar Atland Daniel Jakobsen. “Concepts for Large Scale Hydrogen Production”. MA thesis. NTNU, 2016. URL: http://hdl.handle.net/11250/2402554.

[31] Louis Patrick Dansereau et al. “Framework for margins-based planning: Forest biorefinery case study”. In: *Computers Chemical Engineering* 63 (2014), pp. 34–50. ISSN: 0098-1354. DOI: https://doi.org/10.1016/j.compchemeng.2013.12.006. URL: https://www.sciencedirect.com/science/article/pii/S0098135413003840.

[32] J. M. Douglas. *Conceptual Design of Chemical Processes*. McGraw-Hill, 1988.

[33] Armin D. Ebner and James A. Ritter. “State-of-the-art Adsorption and Membrane Separation Processes for Carbon Dioxide Production from Carbon Dioxide Emitting Industries”. In: *Separation Science and Technology* 44.6 (2009), pp. 1273–1421. DOI: 10.1080/01496390902733314. URL: https://doi.org/10.1080/01496390902733314.

[34] Trading Economics. *EU Natural Gas*. Accessed: 2024-10-13. 2024. URL: https://tradingeconomics.com/commodity/eu-natural-gas.

[35] Tomohisa Yoshioka Eiji Kamio and Hideto Matsuyama. “Recent Advances in Carbon Dioxide Separation Membranes: A Review”. In: *Journal of Chemical Engineering of Japan* 56.1 (2023), p. 2222000. DOI: 10.1080/00219592.2023.2222000. URL: https://doi.org/10.1080/00219592.2023.2222000.

[36] European Commission, Directorate-General for Climate Action. *Going climate-neutral by 2050 – A strategic long-term vision for a prosperous, modern, competitive and climate-neutral EU economy*. Publications Office, 2019. URL: https://data.europa.eu/doi/10.2834/02074.

[37] Konrad L. Fischer and Hannsjörg Freund. “Intensification of load flexible fixed bed reactors by optimal design of staged reactor setups”. In: *Chemical Engineering and Processing - Process Intensification* 159 (2021), p. 108183. ISSN: 0255-2701. DOI: https://doi.org/10.1016/j.cep.2020.108183. URL: https://www.sciencedirect.com/science/article/pii/S0255270120306450.

[38] S. Flude and J. Alcade. *Carbon capture and storage has stalled needlessly – three reasons why fears of CO leakage are overblown*. 2020. URL: https://theconversation.com/carbon-capture-and-storage-has-stalled-needlessly-three-reasons-why-fears-of-co2-leakage-are-overblown-138396.

[39] Alessandro Franco and Caterina Giovannini. “Routes for Hydrogen Introduction in the Industrial Hard-to-Abate Sectors for Promoting Energy Transition”. In: *Energies* 16.16 (2023). ISSN: 1996-1073. DOI: 10.3390/en16166098. URL: https://www.mdpi.com/1996-1073/16/16/6098.

[40] Christian Frilund et al. “Desulfurization of Biomass Syngas Using ZnO-Based Adsorbents: Long-Term Hydrogen Sulfide Breakthrough Experiments”. In: *Energy & Fuels* 34.3 (2020), pp. 3316–3325. DOI: 10.1021/acs.energyfuels.9b04276. URL: https://doi.org/10.1021/acs.energyfuels.9b04276.

[41] Anna Godula-Jopek. *Hydrogen Production: By Electrolysis*. Wiley, 2015. Chap. 2, pp. 33–62. URL: https://public.ebookcentral.proquest.com/choice/publicfullrecord.aspx?p=1956440.

[42] G. J. Grashoff, C. E. Pilkington, and C. W. Corti. “The Purification of Hydrogen”. In: *Platinum Metals Review* 27.4 (1983), pp. 157–169. ISSN: 0032-1400. DOI: https://doi.org/10.1595/003214083X274157169. URL: https://technology.matthey.com/content/journals/10.1595/003214083X274157169.

[43] Katharina Großmann, Peter Treiber, and Jürgen Karl. “Steam methane reforming at low S/C ratios for power-to-gas applications”. In: *International Journal of Hydrogen Energy* 41.40 (2016), pp. 17784–17792. ISSN: 0360-3199. DOI: 10.1016/j.ijhydene.2016.08.007. URL: https://www.sciencedirect.com/science/article/pii/S0360319916323321.

[44] I.E. Grossmann and C.A. Floudas. “Active constraint strategy for flexibility analysis in chemical processes”. In: *Computers Chemical Engineering* 11.6 (1987), pp. 675–693. ISSN: 0098-1354. DOI: https://doi.org/10.1016/0098-1354(87)87011-4. URL: https://www.sciencedirect.com/science/article/pii/0098135487870114.

[45] I.E. Grossmann, K.P. Halemane, and R.E. Swaney. “Optimization strategies for flexible chemical processes”. In: *Computers Chemical Engineering* 7.4 (1983), pp. 439–462. ISSN: 0098-1354. DOI: https://doi.org/10.1016/0098-1354(83)80022-2. URL: https://www.sciencedirect.com/science/article/pii/0098135483800222.

[46] Grothe et al. “Analyzing Europe’s Biggest Offshore Wind Farms: A Data Set with 40 Years of Hourly Wind Speeds and Electricity Production”. In: *Energies* 15.5 (2022). ISSN: 1996-1073. DOI: 10.3390/en15051700. URL: https://www.mdpi.com/1996-1073/15/5/1700.

[47] Wanjun Guo et al. “Simulation and energy performance assessment of CO2 removal from crude synthetic natural gas via physical absorption process”. In: *Journal of Natural Gas Chemistry* 21.6 (2012), pp. 633–638. ISSN: 1003-9953. DOI: https://doi.org/10.1016/S1003-9953(11)60412-X. URL: https://www.sciencedirect.com/science/article/pii/S100399531160412X.

[48] M.H. Halabi et al. “Modeling and analysis of autothermal reforming of methane to hydrogen in a fixed bed reformer”. In: *Chemical Engineering Journal* 137.3 (2008), pp. 568–578. ISSN: 1385-8947. DOI: 10.1016/j.cej.2007.05.019. URL: https://www.sciencedirect.com/science/article/pii/S138589470700352X.

[49] Norman Hall. *Minimum Velocities in Heat Exchangers: Part 2*. May 2016. URL: https://www.deppmann.com/blog/monday-morning-minutes/minimum-velocity-heat-exchangers-part-2/.

[50] Matthias Heitmann, Gerhard Schembecker, and Christian Bramsiepe. “Framework to decide for a volume flexible chemical plant during early phases of plant design”. In: *Chemical Engineering Research and Design* 128 (2017), pp. 85–95. ISSN: 0263-8762. DOI: https://doi.org/10.1016/j.cherd.2017.09.028. URL: https://www.sciencedirect.com/science/article/pii/S0263876217305464.

[51] Peter Herman and Olivier Beauchard. *De staat van de Noordzee*. Accessed: 2024-11-19. 2015. URL: https://www.noordzeeloket.nl/beheer/@168108/staat-noordzee-2015/.

[52] Yukun Hu et al. “Peak and off-peak operations of the air separation unit in oxy-coal combustion power generation systems”. In: *Applied Energy* 112 (2013), pp. 747–754. ISSN: 0306-2619. DOI: https://doi.org/10.1016/j.apenergy.2012.12.001. URL: https://www.sciencedirect.com/science/article/pii/S0306261912008781.

[53] IEA. *Renewables 2023*. Licence: CC BY 4.0. IEA. 2024. URL: https://www.iea.org/reports/renewables-2023.

[54] IEA. *Share of renewable electricity generation by technology, 2000-2028*. https://www.iea.org/data-and-statistics/charts/share-of-renewable-electricity-generation-by-technology-2000-2028. Licence: CC BY 4.0. Paris: IEA, 2024.

[55] Koninklijk Nederlands Meteorologisch Instituut. *Jaar 2023*. Accessed: 2024-11-19. 2023. URL: https://www.knmi.nl/nederland-nu/klimatologie/maand-en-seizoensoverzichten/2023/jaar.

[56] International Energy Agency. *Ammonia Technology Roadmap*. Licence: CC BY 4.0. Paris, 2021. URL: https://www.iea.org/reports/ammonia-technology-roadmap.

[57] International Energy Agency. *CO2 storage resources and their development*. Licence: CC BY 4.0. Paris, 2022. URL: https://www.iea.org/reports/co2-storage-resources-and-their-development.

[58] International Energy Agency. *Global Hydrogen Review 2022*. International Energy Agency. 2022. URL: https://iea.blob.core.windows.net/assets/c5bc75b1-9e4d-460d-9056-6e8e626a11c4/GlobalHydrogenReview2022.pdf.

[59] International Energy Agency. *Global Hydrogen Review 2024*. Licence: CC BY 4.0. 2024. URL: https://www.iea.org/reports/global-hydrogen-review-2024.

[60] International Energy Agency. *Towards hydrogen definitions based on their emissions intensity*. Tech. rep. Licence: CC BY 4.0. Paris: IEA, 2023. URL: https://www.iea.org/reports/towards-hydrogen-definitions-based-on-their-emissions-intensity.

[61] International Energy Agency (IEA). *Global Hydrogen Review 2023*. Tech. rep. Licence: CC BY 4.0. Paris: IEA, 2023. URL: https://www.iea.org/reports/global-hydrogen-review-2023.

[62] International Renewable Energy Agency (IRENA). *Making the breakthrough: Green hydrogen policies and technology costs*. Abu Dhabi: International Renewable Energy Agency, 2021. URL: https://www.irena.org/-/media/Files/IRENA/Agency/Publication/2020/Nov/IRENA_Green_Hydrogen_breakthrough_2021.pdf.

[63] Andrea Isella, Raffaele Ostuni, and Davide Manca. "Towards the decarbonization of ammonia synthesis – A techno-economic assessment of hybrid-green process alternatives". In: *Chemical Engineering Journal* 486 (2024), p. 150132. ISSN: 1385-8947. DOI: 10.1016/j.cej.2024.150132. URL: https://www.sciencedirect.com/science/article/pii/S1385894724016188.

[64] Daniel Jansen et al. "Pre-combustion CO2 capture". In: *International Journal of Greenhouse Gas Control* 40 (2015). Special Issue commemorating the 10th year anniversary of the publication of the Intergovernmental Panel on Climate Change Special Report on CO2 Capture and Storage, pp. 167–187. ISSN: 1750-5836. DOI: https://doi.org/10.1016/j.ijggc.2015.05.028. URL: https://www.sciencedirect.com/science/article/pii/S1750583615001917.

[65] Brian Jenkins et al. "Techno-Economic Analysis of Low Carbon Hydrogen Production from Offshore Wind Using Battolyser Technology". In: *Energies* 15.16 (2022). ISSN: 1996-1073. DOI: 10.3390/en15165796. URL: https://www.mdpi.com/1996-1073/15/16/5796.

[66] Catrinus J. Jepma and Miralda van Schot. *On the economics of offshore energy conversion: smart combinations*. Converting offshore wind energy into green hydrogen on existing oil and gas platforms in the North Sea. Energy Delta Institute (EDI), Feb. 2017. URL: https://projecten.topsectorenergie.nl/storage/app/uploads/public/5d0/263/410/5d026341016a2991247120.pdf.

[67] Johnson Matthey et al. *HyNet Low Carbon Hydrogen Plant: BEIS Hydrogen Supply Competition*. Accessed: 15-10-2024. 2021. URL: https://assets.publishing.service.gov.uk/media/621369ddd3bf7f4f027607af/Phase_2_Report_-_Progressive_Energy_-_HyNet_Low_Carbon_Hydrogen__3_.pdf.

[68] Charles Johnston et al. "Shipping the sunshine: An open-source model for costing renewable hydrogen transport from Australia". In: *International Journal of Hydrogen Energy* 47.47 (2022), pp. 20362–20377. ISSN: 0360-3199. DOI: https://doi.org/10.1016/j.ijhydene.2022.04.156. URL: https://www.sciencedirect.com/science/article/pii/S0360319922017281.

[69] Gregory Mark Joseph H. Saleh and Nicole C. Jordan. "Flexibility: a multi-disciplinary literature review and a research agenda for designing flexible engineering systems". In: *Journal of Engineering Design* 20.3 (2009), pp. 307–323. DOI: 10.1080/09544820701870813. eprint: https://doi.org/10.1080/09544820701870813. URL: https://doi.org/10.1080/09544820701870813.

[70] Hou Junbo and Yang Min. *Green Hydrogen Production by Water Electrolysis.* CRC Press, 2024. ISBN: 9781032438078. URL: https://search.ebscohost.com/login.aspx?direct=true&db=nlebk&AN=3772477&site=ehost-live&authtype=sso&custid=s1131660.

[71] Fabian Kächele, Oliver Grothe, and Mira Watermeyer. *Dataset for the Paper: "Analyzing Europe's Biggest Offshore Wind Farms: a Data set With 40 Years of Hourly Wind Speeds and Electricity Production"*. Accessed: 2024-10-10. 2022. URL: https://doi.org/10.6084/m9.figshare.19139648.v1.

[72] Mary Katebah, Ma'moun Al-Rawashdeh, and Patrick Linke. "Analysis of hydrogen production costs in Steam-Methane Reforming considering integration with electrolysis and CO2 capture". In: *Cleaner Engineering and Technology* 10 (2022), p. 100552. ISSN: 2666-7908. DOI: https://doi.org/10.1016/j.clet.2022.100552. URL: https://www.sciencedirect.com/science/article/pii/S2666790822001574.

[73] Robert Kender et al. "Improving the load flexibility of industrial air separation units using a pressure-driven digital twin". In: *AIChE Journal* 68.7 (2022), e17692. DOI: https://doi.org/10.1002/aic.17692. eprint: https://aiche.onlinelibrary.wiley.com/doi/pdf/10.1002/aic.17692. URL: https://aiche.onlinelibrary.wiley.com/doi/abs/10.1002/aic.17692.

[74] Yaser Khojasteh Salkuyeh, Bradley A. Saville, and Heather L. MacLean. "Techno-economic analysis and life cycle assessment of hydrogen production from natural gas using current and emerging technologies". In: *International Journal of Hydrogen Energy* 42.30 (2017), pp. 18894–18909. ISSN: 0360-3199. DOI: https://doi.org/10.1016/j.ijhydene.2017.05.219. URL: https://www.sciencedirect.com/science/article/pii/S0360319917322036.

[75] Henry Z. Kister. *Distillation Design*. McGraw-Hill, Inc., 1992. Chap. 6, p. 266. URL: https://aussiedistiller.com.au/books2/Distillation%20Design.pdf.

[76] Christoph kost et al. "Levelised cost of electricity renewable energy technologies". In: (2021). URL: https://www.ise.fraunhofer.de/en/publications/studies/cost-of-electricity.html.

[77] Kuczyński et al. "Impact of Liquefied Natural Gas Composition Changes on Methane Number as a Fuel Quality Requirement". In: *Energies* 13.19 (2020). ISSN: 1996-1073. DOI: 10.3390/en13195060. URL: https://www.mdpi.com/1996-1073/13/19/5060.

[78] Steven Lak. *Blue Hydrogen as Accelerator and Pioneer for Energy Transition in the Industry: Feasibility Study Report*. H-Vision Feasibility Study Report. July 2019. URL: https://www.h-vision.nl/en/publications.

[79] Christian Langner et al. "Novel Reformulations for Modeling Uncertainty and Variations in a Framework for Chemical Process Design". In: *Industrial & Engineering Chemistry Research* 62.46 (2023), pp. 19715–19739. DOI: 10.1021/acs.iecr.3c01584. URL: https://doi.org/10.1021/acs.iecr.3c01584.

[80] Peter G. Levi and Jonathan M. Cullen. "Mapping Global Flows of Chemicals: From Fossil Fuel Feedstocks to Chemical Products". In: *Environmental Science & Technology* 52.4 (2018). PMID: 29363951, pp. 1725–1734. DOI: 10.1021/acs.est.7b04573. eprint: https://doi.org/10.1021/acs.est.7b04573. URL: https://doi.org/10.1021/acs.est.7b04573.

[81] Xinyu Li et al. "Equation of State Associated with Activity Coefficient Model Based on Elements and Chemical Bonds". In: *Processes* 11.5 (2023). ISSN: 2227-9717. DOI: 10.3390/pr11051499. URL: https://www.mdpi.com/2227-9717/11/5/1499.

[82] Ke Liu et al. "Hydrogen and Syngas Production and Purification Technologies". In: John Wiley & Sons, Incorporated, 2010. Chap. 3.2.2 Homogeneous POX. URL: https://ebookcentral-proquest-com.tudelft.idm.oclc.org/lib/delft/detail.action?docID=468763.

[83] Ke Liu et al. "Hydrogen and Syngas Production and Purification Technologies". In: John Wiley & Sons, Incorporated, 2010. Chap. 3.2.1 ATR. URL: https://ebookcentral-proquest-com.tudelft.idm.oclc.org/lib/delft/detail.action?docID=468763.

[84] Ke Liu et al. “Hydrogen and Syngas Production and Purification Technologies”. In: John Wiley & Sons, Incorporated, 2010. Chap. 10 Pressure Swing Adsorption Technology for Hydrogen Production. URL: https://ebookcentral-proquest-com.tudelft.idm.oclc.org/lib/delft/detail.action?docID=468763.

[85] Ke Liu et al. “Hydrogen and Syngas Production and Purification Technologies”. In: John Wiley & Sons, Incorporated, 2010. Chap. 6 Water-Gas Shift technologies. URL: https://ebookcentral-proquest-com.tudelft.idm.oclc.org/lib/delft/detail.action?docID=468763.

[86] Nan Liu. *THE SHELL BLUE HYDROGEN PROCESS*. Tech. rep. Shell Global, 2020. URL: http://media.hydrocarbonengineering.com/whitepapers/files/The-Shell-Blue-Hydrogen-Process.pdf.

[87] Ignacio López-Paniagua et al. “Step by Step Derivation of the Optimum Multistage Compression Ratio and an Application Case”. In: *Entropy* 22.6 (2020). ISSN: 1099-4300. DOI: 10.3390/e22060678. URL: https://www.mdpi.com/1099-4300/22/6/678.

[88] Mauro Luberti and Hyungwoong Ahn. “Review of Polybed pressure swing adsorption for hydrogen purification”. In: *International Journal of Hydrogen Energy* 47.20 (2022), pp. 10911–10933. ISSN: 0360-3199. DOI: https://doi.org/10.1016/j.ijhydene.2022.01.147. URL: https://www.sciencedirect.com/science/article/pii/S0360319922002877.

[89] Jisiwei Luo, Jonathan Moncada, and Andrea Ramirez. “Development of a Conceptual Framework for Evaluating the Flexibility of Future Chemical Processes”. In: *Industrial & Engineering Chemistry Research* 61.9 (2022), pp. 3219–3232. DOI: 10.1021/acs.iecr.1c03874. eprint: https://doi.org/10.1021/acs.iecr.1c03874. URL: https://doi.org/10.1021/acs.iecr.1c03874.

[90] Michiel Makkee, Jacob A. Moulijn, and Annelies E. van Diepen. “Autothermal Reforming Process”. In: *Chemical Process Technology*. Second. Address (optional): Publisher, May 2013. Chap. 5.2.3. ISBN: 978-1-444-32025-1.

[91] Charles Maxwell. *Towering skills*. Accessed: 2024-10-04. 2024. URL: https://toweringskills.com/financial-analysis/cost-indices/.

[92] D. Mendes et al. “The water-gas shift reaction: from conventional catalytic systems to Pd-based membrane reactors—a review”. In: *Asia-Pacific Journal of Chemical Engineering* 5.1 (2010), pp. 111–137. DOI: https://doi.org/10.1002/apj.364. eprint: https://onlinelibrary.wiley.com/doi/pdf/10.1002/apj.364. URL: https://onlinelibrary.wiley.com/doi/abs/10.1002/apj.364.

[93] Jan van der Merwe et al. “A study of the loss characteristics of a single cell PEM electrolyser for pure hydrogen production”. In: *2013 IEEE International Conference on Industrial Technology (ICIT)*. 2013, pp. 668–672. DOI: 10.1109/ICIT.2013.6505751.

[94] Pierre Millet. “Chapter 2 - Fundamentals of water electrolysis”. In: *Electrochemical Power Sources: Fundamentals, Systems, and Applications*. Ed. by Tom Smolinka and Jurgen Garche. Elsevier, 2022, pp. 37–62. ISBN: 978-0-12-819424-9. DOI: https://doi.org/10.1016/B978-0-12-819424-9.00002-1. URL: https://www.sciencedirect.com/science/article/pii/B9780128194249000021.

[95] F. M. Mulder et al. “Efficient electricity storage with a battolyser, an integrated Ni–Fe battery and electrolyser”. In: *Energy Environ. Sci.* 10 (3 2017), pp. 756–764. DOI: 10.1039/C6EE02923J. URL: http://dx.doi.org/10.1039/C6EE02923J.

[96] S.-i. Nakao et al. In: *Advanced CO2 capture technologies: absorption, adsorption, and membrane separation methods*. SpringerBriefs in Energy. Springer, 2019. Chap. 5. Membrane for CO2 Separation, pp. 65–83. DOI: 10.1007/978-3-030-18858-0_5.

[97] S.-i. Nakao et al. “Advanced CO2 capture technologies: absorption, adsorption, and membrane separation methods”. In: *Advanced CO2 capture technologies: absorption, adsorption, and membrane separation methods*. Springer, 2019. Chap. 3.1.1 Physical Absorption. DOI: 10.1007/978-3-030-18858-0.

[98] Ahmad Naquash et al. “Hydrogen Purification through a Membrane–Cryogenic Integrated Process: A 3 E’s (Energy, Exergy, and Economic) Assessment”. In: *Gases* 3.3 (2023), pp. 92–105. ISSN: 2673-5628. DOI: 10.3390/gases3030006. URL: https://www.mdpi.com/2673-5628/3/3/6.

[99] Ahmad Naquash et al. “Separation and purification of syngas-derived hydrogen: A comparative evaluation of membrane- and cryogenic-assisted approaches”. In: *Chemosphere* 313 (2023), p. 137420. ISSN: 0045-6535. DOI: https://doi.org/10.1016/j.chemosphere.2022.137420. URL: https://www.sciencedirect.com/science/article/pii/S0045653522039133.

[100] Andrea Nava et al. “Carbon-negative “emerald hydrogen” from electrified steam methane reforming of biogas: System integration and optimization”. In: *International Journal of Hydrogen Energy* 88 (2024), pp. 1237–1255. ISSN: 0360-3199. DOI: https://doi.org/10.1016/j.ijhydene.2024.09.171. URL: https://www.sciencedirect.com/science/article/pii/S0360319924038801.

[101] Klaus Noeker and Joachim Johanning. *Autothermal Reforming: A Flexible Syngas Route with Future Potential*. Tech. rep. Thyssenkrupp Industrial Solutions, 2010. URL: https://ucpcdn.thyssenkrupp.com/_legacy/UCPthyssenkruppBAIS/assets.files/download_1/ammonia_2/autothermal_reforming_syngas_2010_paper.pdf.

[102] Northern Gas Networks. *H21 Leeds City Gate*. Tech. rep. Northern Gas Networks, 2016. URL: https://www.northerngasnetworks.co.uk/wp-content/uploads/2017/04/H21-Report-Interactive-PDF-July-2016.compressed.pdf.

[103] A.O. Oni et al. “Comparative assessment of blue hydrogen from steam methane reforming, autothermal reforming, and natural gas decomposition technologies for natural gas-producing regions”. In: *Energy Conversion and Management* 254 (2022), p. 115245. ISSN: 0196-8904. DOI: https://doi.org/10.1016/j.enconman.2022.115245. URL: https://www.sciencedirect.com/science/article/pii/S0196890422000413.

[104] OPAP. *Gas Products LNG*. Accessed: 2024-10-13. 2024. URL: https://www.opap.ir/en-single.php?pid=421.

[105] Mohammad Ostadi et al. “Flexible and synergistic methanol production via biomass gasification and natural gas reforming”. In: *Cleaner Chemical Engineering* 10 (2024), p. 100120. ISSN: 2772-7823. DOI: https://doi.org/10.1016/j.clce.2024.100120. URL: https://www.sciencedirect.com/science/article/pii/S2772782324000056.

[106] Bert den Ouden et al. *Hydrogen Spot Market Simulation, Policy Report*. Policy Report. Institution Address: TNO, HyXchange, and Berenschot, Feb. 2024. URL: https://hyxchange.nl/document-library/.

[107] Jan Overbeek. “Cost-effective Hydrogen Production: A comparison of uncertainties in the levelized cost of hydrogen for the dominant hydrogen production pathways”. MA thesis. Utrecht, Netherlands: Utrecht University, 2020. URL: https://studenttheses.uu.nl/bitstream/handle/20.500.12932/35845/Master's%20Thesis%20Energy%20Science%20-%20Overbeek,%20Jan%20-%20%204012968.pdf?sequence=1.

[108] J.C.M. Pires et al. “Recent developments on carbon capture and storage: An overview”. In: *Chemical Engineering Research and Design* 89.9 (2011). Special Issue on Carbon Capture Storage, pp. 1446–1460. ISSN: 0263-8762. DOI: https://doi.org/10.1016/j.cherd.2011.01.028. URL: https://www.sciencedirect.com/science/article/pii/S0263876211000554.

[109] Port of Rotterdam. *102 million euros in funding on the horizon for Porthos carbon storage project*. Accessed: 2024-10-14. 2020. URL: https://www.portofrotterdam.com/en/news-and-press-releases/102-million-euros-in-funding-on-the-horizon-for-porthos-carbon-storage-project.

[110] Fazil Qureshi et al. “A State-of-The-Art Review on the Latest trends in Hydrogen production, storage, and transportation techniques”. In: *Fuel* 340 (2023), p. 127574. ISSN: 0016-2361. DOI: https://doi.org/10.1016/j.fuel.2023.127574. URL: https://www.sciencedirect.com/science/article/pii/S0016236123001874.

[111] Byron Smith R.J., Muruganandam Loganathan, and Murthy Shekhar Shantha. “A Review of the Water Gas Shift Reaction Kinetics”. In: *International Journal of Chemical Reactor Engineering* 8.1 (2010). DOI: 10.2202/1542-6580.2238. URL: https://doi.org/10.2202/1542-6580.2238.

[112] Federico Zardi Raffaele Ostuni. “Method for load regulation of an ammonia plant”. Type of Patent (e.g., Utility Patent) US 9,463,983 B2. Oct. 2016.

[113] Federica Raganati, Francesco Miccio, and Paola Ammendola. “Adsorption of Carbon Dioxide for Post-combustion Capture: A Review”. In: *Energy & Fuels* 35.16 (2021), pp. 12845–12868. ISSN: 0887-0624. DOI: 10.1021/acs.energyfuels.1c01618. URL: https://doi.org/10.1021/acs.energyfuels.1c01618.

[114] M. Riemer and V. Duscha. “Carbon capture in hydrogen production-Review of modelling assumptions”. In: *Energy* 2004 (2022), p. 2965.

[115] J. Riese and M. Grunewald. “Flexibility for Absorption and Distillation Columns”. In: *Chemical Engineering Transactions* 69 (2018), pp. 787–792. DOI: 10.3303/CET1869132.

[116] Maurizio RIZZI. “Control of an Ammonia Synthesis Loop at Partial Load”. United States Patent Application Publication US 20230331569A1 (United States Patent, Trademark Office). 2023. URL: https://patentimages.storage.googleapis.com/17/85/87/0f3bc99a53d0e9/US20230331569A1.pdf.

[117] K. Roh et al. “Flexible operation of switchable chlor-alkali electrolysis for demand side management”. In: *Applied Energy* 255 (2020), p. 113880. DOI: 10.1016/j.apenergy.2019.113880.

[118] Kevin Hendrik Reindert Rouwenhorst et al. “Ammonia Production Technologies”. English. In: *Techno-Economic Challenges of Green Ammonia as Energy Vector*. Ed. by Agustin Valera-Medina and Rene Banares-Alcantara. Elsevier, 2021, pp. 41–83. DOI: 10.1016/B978-0-12-820560-0.00004-7.

[119] P. Saha et al. “Grey, blue, and green hydrogen: A comprehensive review of production methods and prospects for zero-emission energy”. In: *International Journal of Green Energy* 21.6 (2023), pp. 1383–1397. DOI: 10.1080/15435075.2023.2244583.

[120] Joseph H. Saleh, George Mark, and Norman C. Jordan. “Flexibility: a multi-disciplinary literature review and a research agenda for designing flexible engineering systems”. In: *Journal of Engineering Design* (2009). DOI: 10.1080/09544820701870813. URL: https://doi.org/10.1080/09544820701870813.

[121] Sascha Ranevska. *Rising Costs Challenge Dutch CO2 Capture Project Porthos*. Accessed: 2024-10-14. 2024. URL: https://carbonherald.com/rising-costs-challenge-dutch-co2-capture-project-porthos/.

[122] O. Schmidt et al. “Future cost and performance of water electrolysis: An expert elicitation study”. In: *International Journal of Hydrogen Energy* 42.52 (2017), pp. 30470–30492. ISSN: 0360-3199. DOI: https://doi.org/10.1016/j.ijhydene.2017.10.045. URL: https://www.sciencedirect.com/science/article/pii/S0360319917339435.

[123] Tim Seifert et al. “Capacity Flexibility of Chemical Plants”. In: *Chemical Engineering & Technology* 37.2 (2014), pp. 332–342. DOI: https://doi.org/10.1002/ceat.201300635. eprint: https://onlinelibrary.wiley.com/doi/pdf/10.1002/ceat.201300635. URL: https://onlinelibrary.wiley.com/doi/abs/10.1002/ceat.201300635.

[124] Shell. *LNG Outlook 2023*. Accessed: 2024-06-13. 2023. URL: https://www.shell.com/what-we-do/oil-and-natural-gas/liquefied-natural-gas-lng/lng-outlook-2023/_jcr_content/root/main/section_599628081_co/promo_copy_copy/links/item0.stream/1676487838925/410880176bce66136fc24a70866f941295eb70e7/lng-outlook-2023.pdf.

[125] S. Shiva Kumar and Hankwon Lim. “An overview of water electrolysis technologies for green hydrogen production”. In: *Energy Reports* 8 (2022), pp. 13793–13813. ISSN: 2352-4847. DOI: https://doi.org/10.1016/j.egyr.2022.10.127. URL: https://www.sciencedirect.com/science/article/pii/S2352484722020625.

[126] Adam P. Simpson and Andrew E. Lutz. “Exergy analysis of hydrogen production via steam methane reforming”. In: *International Journal of Hydrogen Energy* 32.18 (2007), pp. 4811–4820. ISSN: 0360-3199. DOI: https://doi.org/10.1016/j.ijhydene.2007.08.025. URL: https://www.sciencedirect.com/science/article/pii/S036031990700482X.

[127] Adam P. Simpson and Andrew E. Lutz. “Exergy analysis of hydrogen production via steam methane reforming”. In: *International Journal of Hydrogen Energy* 32.18 (2007), pp. 4811–4820. ISSN: 0360-3199. DOI: 10.1016/j.ijhydene.2007.08.025. URL: https://doi.org/10.1016/j.ijhydene.2007.08.025.

[128] Kathryn H. Smith et al. “Physical solvents and techno-economic analysis for pre-combustion CO2 capture: A review”. In: *International Journal of Greenhouse Gas Control* 118 (2022), p. 103694. ISSN: 1750-5836. DOI: https://doi.org/10.1016/j.ijggc.2022.103694. URL: https://www.sciencedirect.com/science/article/pii/S1750583622001128.

[129] Chunfeng Song et al. “Optimization of steam methane reforming coupled with pressure swing adsorption hydrogen production process by heat integration”. In: *Applied Energy* 154 (2015), pp. 392–401. ISSN: 0306-2619. DOI: https://doi.org/10.1016/j.apenergy.2015.05.038. URL: https://www.sciencedirect.com/science/article/pii/S0306261915006480.

[130] Chunshan Song and Xiaoliang Ma. *Desulfurization Technologies*. John Wiley & Sons, Ltd, 2009. Chap. 5, pp. 219–310. ISBN: 9780471719755. DOI: 10.1002/9780470561256.ch5. URL: https://doi.org/10.1002/9780470561256.ch5.

[131] Statistics Netherlands (CBS). *Prices of natural gas and electricity*. Accessed: 2024-10-14. 2024. URL: https://www.cbs.nl/en-gb/figures/detail/856666ENG.

[132] Rickard Svensson et al. “Transportation systems for CO2—-application to carbon capture and storage”. In: *Energy conversion and management* 45.15-16 (2004), pp. 2343–2353.

[133] Gülbahar Tezel. *Onderzoek langetermijnbehoefte LNG in Nederland*. Tech. rep. Strategy, March 2024. URL: https://www.rijksoverheid.nl/documenten/rapporten/2024/05/08/bijlage-4-strategy-onderzoek-langetermijnbehoefte-lng-in-nederland-eindrapport.

[134] *The Hydrogen Network Netherlands: a Vital Building Block for the Energy Transition*. 2024. URL: https://www.hynetwork.nl/en.

[135] Gavin Towler and Ray Sinnott. “Chapter 7 - Capital cost estimating”. In: *Chemical Engineering Design (Third Edition)*. Ed. by Gavin Towler and Ray Sinnott. Third Edition. Butterworth-Heinemann, 2022, pp. 239–278. ISBN: 978-0-12-821179-3. DOI: https://doi.org/10.1016/B978-0-12-821179-3.00007-8. URL: https://www.sciencedirect.com/science/article/pii/B9780128211793000078.

[136] United Nations Framework Convention on Climate Change. *Paris Agreement*. Accessed: Insert date. 2015. URL: https://unfccc.int/sites/default/files/resource/parisagreement_publication.pdf.

[137] Jack Walden. *Blue Hydrogen Production Technology Review*. Tech. rep. Bacton Energy Hub Hydrogen Supply Special Interest Group, 2022. URL: http://www.progressive-energy.com.

[138] B. Wang. “Zeolite deactivation during hydrocarbon reactions: characterisation of coke precursors and acidity, product distribution”. PhD thesis. University College London, Dec. 2007. URL: https://core.ac.uk/download/pdf/1683015.pdf.

[139] Margrete Hånes Wesenberg. “Gas Heated Steam Reformer Modelling”. PhD thesis. Trondheim, Norway: Norwegian University of Science and Technology, Apr. 2006. URL: https://ntnuopen.ntnu.no/ntnu-xmlui/bitstream/handle/11250/248060/122646_FULLTEXT01.pdf.

[140] Margrete Hanes Wesenberg. “Gas Heated Steam Reformer Modelling”. PhD thesis. NTNU, 2006. URL: http://hdl.handle.net/11250/248060.

[141] K. C. Wilson. “Centrifugal Pumps”. In: *Slurry Transport Using Centrifugal Pumps*. Boston, MA: Springer US, 2006, pp. 190–226. ISBN: 978-0-387-23263-8. DOI: 10.1007/0-387-23263-X_9. URL: https://doi.org/10.1007/0-387-23263-X_9.

[142] Sebastian T. Wismann et al. “Electrified methane reforming: A compact approach to greener industrial hydrogen production”. In: *Science* (2019). DOI: 10.1126/science.aaw8775.

[143] Sebastian T. Wismann et al. “Electrified methane reforming: Elucidating transient phenomena”. In: *Chemical Engineering Journal* (2021). DOI: 10.1016/j.cej.2021.131509. URL: https://www.sciencedirect.com/science/article/pii/S1385894721030904.

[144] Sebastian Thor Wismann. “Electrically heated steam methane reforming”. PhD thesis. 2019.

[145] Ababay Ketema Worku et al. “Recent Advances and Challenges of Hydrogen Production Technologies via Renewable Energy Sources”. In: *Advanced Energy and Sustainability Research* 5.5 (2024), p. 2300273. DOI: https://doi.org/10.1002/aesr.202300273. eprint: https://onlinelibrary.wiley.com/doi/pdf/10.1002/aesr.202300273. URL: https://onlinelibrary.wiley.com/doi/abs/10.1002/aesr.202300273.

[146] Gang Xu et al. “An Improved CO_2 Separation and Purification System Based on Cryogenic Separation and Distillation Theory”. In: *Energies* 7.5 (2014), pp. 3484–3502. ISSN: 1996-1073. DOI: 10.3390/en7053484. URL: https://www.mdpi.com/1996-1073/7/5/3484.

[147] Byeong-Yong Yoo et al. “New CCS system integration with CO2 carrier and liquefaction process”. In: *Energy Procedia* 4 (2011). 10th International Conference on Greenhouse Gas Control Technologies, pp. 2308–2314. ISSN: 1876-6102. DOI: https://doi.org/10.1016/j.egypro.2011.02.121. URL: https://www.sciencedirect.com/science/article/pii/S1876610211003183.

[148] A.P. York, T. Xiao, and M.L. Green. “Brief Overview of the Partial Oxidation of Methane to Synthesis Gas”. In: *Topics in Catalysis* 22 (2003), pp. 345–358. DOI: 10.1023/A:1023552709642.

[149] Mingquan Yu, Eko Budiyanto, and Harun Tüysüz. “Principles of Water Electrolysis and Recent Progress in Cobalt-, Nickel-, and Iron-Based Oxides for the Oxygen Evolution Reaction”. In: *Angewandte Chemie International Edition* 61.1 (2022), e202103824. DOI: 10.1002/anie.202103824. eprint: https://onlinelibrary.wiley.com/doi/pdf/10.1002/anie.202103824. URL: https://onlinelibrary.wiley.com/doi/abs/10.1002/anie.202103824.

[150] Qi Zhang, Ignacio E. Grossmann, and Ricardo M. Lima. “On the relation between flexibility analysis and robust optimization for linear systems”. In: *AIChE Journal* 62.9 (2016), pp. 3109–3123. DOI: https://doi.org/10.1002/aic.15221. eprint: https://aiche.onlinelibrary.wiley.com/doi/pdf/10.1002/aic.15221. URL: https://aiche.onlinelibrary.wiley.com/doi/abs/10.1002/aic.15221.

[151] Yongning Zhao et al. “Optimal operation of compressor units in gas networks to provide flexibility to power systems”. In: *Applied Energy* 290 (2021), p. 116740. ISSN: 0306-2619. DOI: https://doi.org/10.1016/j.apenergy.2021.116740. URL: https://www.sciencedirect.com/science/article/pii/S030626192100252X.

[152] Ronny Tobias Zimmermann, Jens Bremer, and Kai Sundmacher. “Load-flexible fixed-bed reactors by multi-period design optimization”. In: *Chemical Engineering Journal* 428 (2022), p. 130771. ISSN: 1385-8947. DOI: https://doi.org/10.1016/j.cej.2021.130771. URL: https://www.sciencedirect.com/science/article/pii/S1385894721023561.

[153] L.F. Zubeir. “Carbon capture with novel low-volatile solvents : experiments and modeling”. English. Proefschrift. Phd Thesis 1 (Research TU/e / Graduation TU/e). Chemical Engineering and Chemistry, Oct. 2016. ISBN: 978-90-386-4152-2.

[154] Lawien F. Zubeir et al. “Novel pressure and temperature swing processes for CO2 capture using low viscosity ionic liquids”. In: *Separation and Purification Technology* 204 (2018), pp. 314–327. ISSN: 1383-5866. DOI: https://doi.org/10.1016/j.seppur.2018.04.085. URL: https://www.sciencedirect.com/science/article/pii/S138358661733839X.

A

Appendix

A.1. Literature review

Flexibility test & index

The analysis of the flexibility of chemical processes is closely related to the solution of optimization problems under uncertainty [150]. Grossmann et al. developed an optimization model to quantify process flexibility by solving the flexibility test problem and flexibility index problem.

The flexibility test determines if a given process design is flexible enough to handle a specified range of uncertain parameters variations while still meeting all the constraints. The solution to the flexibility test problem defines the feasible region in the space of the uncertainty parameters θ over which the process can operate while meeting all the constraints as seen in figure A.1.

Different type of design variables can be used according to Grossman et al., ranging from process parameters (feed flowrates, temperatures, pressures, etc) to equipment sizes (reactor volumes, heat exchanger areas, etc) or structural decisions (existence/non-existence of units, interconnection between units, process flowsheet configuration).

The flexibility test problem, which need to be solved, can be stated as follows: For a given design variable d, determine whether by proper adjustment of the control variables z, the inequalities $f_j(d, z, \theta) \leq 0$, $j \in J$, hold for all $\theta \in T = \{\theta : \theta^L \leq \theta \leq \theta^U\}$. Here, T denotes the uncertainty space that is modelled using the expected extreme values (θ^L, θ^U) and takes the form of an N_θ-dimensional hyperbox.

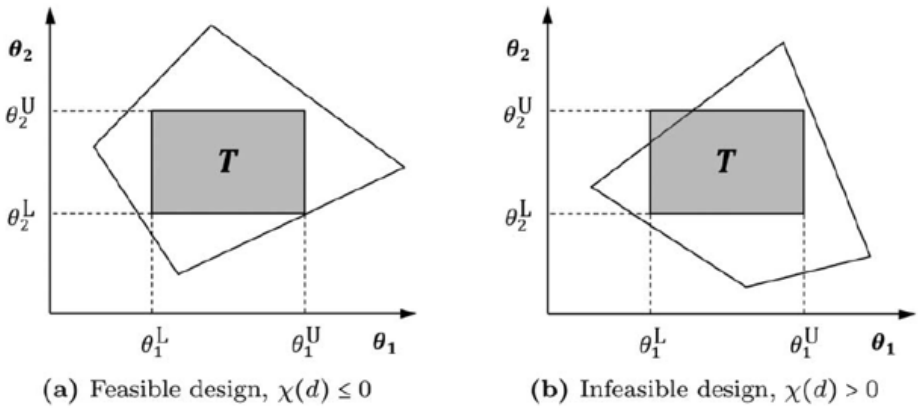

Figure A.1: Geometric interpretation of the flexibility test: examples of feasible and infeasible design with respect to a given uncertainty space T [150].

The flexibility index can be used as a metric to quantify the flexibility of a chemical plant. The flexibility

index, often denoted as $F(d)$, is a scalar value ≥ 0 which scales a geometric shape that is used to model the expected uncertainty space in the (hyper-)space of the uncertain parameters.

The flexibility index quantifies the maximum range of uncertain parameter variation over which feasible operation is possible. It also provides the bounds of the parameters within which feasible operation is guaranteed. Additionally, it allows for the identification of the ”worst-case” conditions that limit the flexibility of the process.

The flexibility index problem can be stated as follows: For a given design variables d, find the largest δ such that by proper adjustment of the control variables z, the inequalities $f_j(d, z, \theta) \leq 0$, $j \in J$, hold for all $\theta \in T(\delta)$. This maximum δ is referred to as the flexibility index $F(d)$.

A higher flexibility index indicates a larger feasible operating region and thus more flexibility to handle uncertainties. If the index is greater or equal to 1 ($F(d) \geq 1$), then the process can be operated for all expected variations.

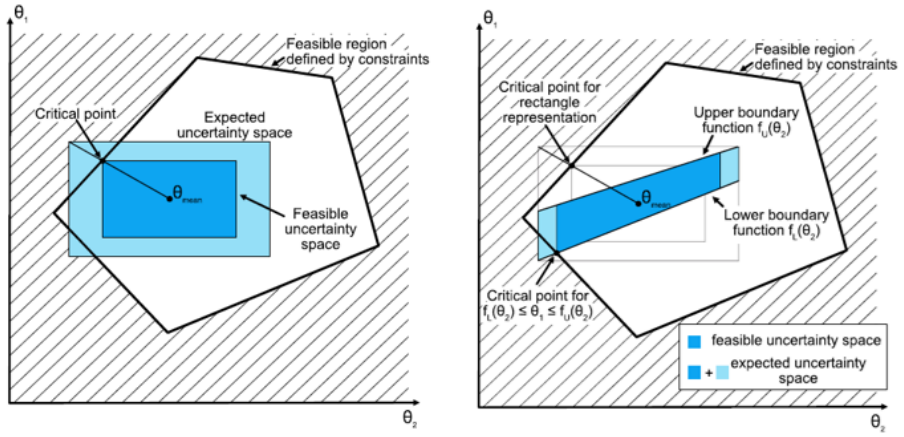

(a) (hyper-)rectangle with respect to expected variations and maximum scaled (hyper-)rectangle inscribed within the feasible region in the space of two uncertain parameters.

(b) Reformulated model of the uncertainty space based on boundary functions to capture a dependency between the two uncertain parameters.

Figure A.2: Visualization of the flexibility index for two uncertain parameters using the (hyper-)rectangle approach (a) and the approach based on boundary functions (b) to model the expected uncertainty space [79]

Both the flexibility test and flexibility index can be solved by reformulating the bilevel formulations, which involve two level of optimization problems integrated within each other, into single-level mixed-integer nonlinear programs (MINLPs) using an active constraints strategy with binary variables to activate the limiting constraints [44]. Older methods used by Grossmann where nonlinear programs (NLPs) instead of MINLPs. It is an active research field on how to solve these problems [150].

The in-depth research into these methods aims to improve chemical process design by enhancing flexibility. The goal in chemical process design is to produce a plant design that is optimal with respect to cost and performance. For that reason, for a design’s flexibility to be considered ”optimal” requires that the economic advantages of flexibility are balanced in relation to its cost [45]. An example of a trade-off curve can be seen in Figure A.3. This curve shows the potential use of a quantitative metric for flexibility given by solving the flexibility index problem.

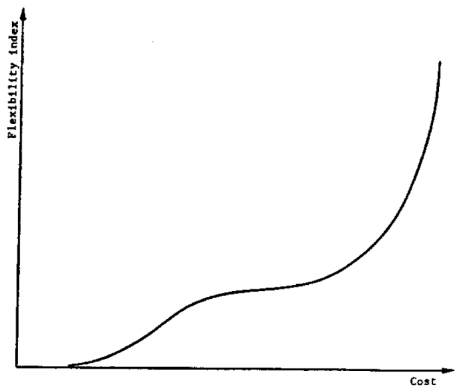

Figure A.3: Trade-off curve between flexibility and cost [45]

Although the flexibility index offers a clear measurable insight into the flexibility of a chemical plant, its practical application on a large scale proves challenging due to the complexity of the calculations. While existing examples, often limited to scenarios like heat exchangers networks or basic pump and pipe system, show promise, extending this method to an entire process plant would be to complex and time-consuming for answering the simpler research sub-questions.

Green hydrogen production

Table A.1: Main characteristics of AEL, PEM and SOEC, adjusted from [122].

	AEL	**PEM**	**SOEC**
Cathode	Ni, Ni-Mo alloys	Pt, Pt-Pd	Ni/YSZ
Anode	Ni, Ni-Co alloys	RuO_2, IrO_2	LSM/YSZ
System efficiency (kWh/kgH_2)*	50-78	50-83	45-55
System efficiency (%$_{HHV}$)*	50-79	47-79	72-87
Operating Temperature (°C)	60-80	50-80	650-1000
Operating Pressure (bar)	<30	<200	<25
Gas purity (%)	>99.5	99.99	99.9
Load flexibility (% of nominal capacity)	10-100	0-100	30-100
System response	Seconds	Milliseconds	Seconds
Cold-start time (min)	<60	<20	<60
Stack lifetime (h)	60000-90000	20000-60000	<10000
Maturity	Mature	Commercial	Demonstration

*(Source: [62])

A.2. Figures

CO_2 specifications

Component	Mole Base
CO_2	≥ 95%
H_2O	≤ 70 ppm
Sum [H_2+N_2+Ar+CH_4+CO+O_2]	≤ 4%
H_2	≤ 0.75%
N_2	≤ 2.4%
Ar	≤ 0.4%
CH_4	≤ 1%
CO	≤ 750 ppm
O_2	≤ 40 ppm
Total sulfur-contained compounds (COS, DMS, H_2S, SOx, Mercaptan)	≤ 20 ppm Of which H_2S ≤ 5 ppm
Total NOx	≤ 5 ppm
Total aliphatic hydrocarbons (C2 to C10)[i]	≤ 1200 ppm
Total aromatic hydrocarbons (C6 to C10, incl. BTEX)[i]	≤ 0.1 ppm
Total volatile organic compounds[ii] (excl. methane, total aliphatic HC (C2 to C10), methanol, ethanol, and aldehydes)	≤ 10 ppm
Total aldehyde compounds	≤ 10 ppm
Ethanol	≤ 20 ppm
Methanol	≤ 620 ppm
Hydrogen cyanide (HCN)	≤ 2 ppm
Total amine compounds	≤ 1 ppm
Total glycol compounds	Follow dew point specification
Ammonia (NH_3)	≤ 3 ppm
Total carboxylic acid and amide compounds	≤ 1 ppm
Total phosphorus-contained compounds	≤ 1 ppm
Toxic compounds[iii]	
Dew point limit value measurement (for all liquids, i.e. for complete CO_2 composition)	< -10 °C (at 20 bara)

Note i: Specification values are molecular based
Note ii: VOC definition according to Dutch policy
Note iii: Toxic compounds: although CO_2 and other gases like i.e. H_2 and N_2 can form a risk of asphyxiation, Porthos would like to know other components within the stream which impose a risk on personal safety to be taken into account in Porthos HSE policy

Figure A.4: CO_2 specifications for the pipelines of the Porthos project.

Pressure						
Downstream design pressure	Pdd	X-845-0x	Porthos		36,0	bar (g)
Range of operating pressure		X-845-0x	Porthos		24-35	bar (g)
Downstream max. operating pressure	MOPd	X-845-0x	Porthos		35,0	bar (g)
Downstream max. incidental pressure (process safety to avoid 2 phase CO2, lower than the MIP acc. NEN-3650-1)	MIPd	X-845-0x	Porthos		40,0	bar (g)
Upstream design pressure	Pdu	pipeline tag-number	client		xx	bar (g)
Upstream max. operating pressure at the feeding point	MOPu		client		xx	bar (g)
					setpoint	
Pressure Relief Valve (if aplicable)		tag-number	client		xx	bar (g)
Pressure alarming and recording (NEN 3650-1)		PARxx	client		36,7	bar (g)
High Pressure Shut Down (HPSD)		tag-number	client		38,0	bar (g)
HPSD action: open V-C02, close V-C01						
Temperature				Min.	Max.	
Downstream design temperature	Tdd	X-845-0x	Porthos	-45	50,0	°C
Downstream max. operating temperature	MOTd	X-845-0x	Porthos	NA	40,0	°C
temporary for extreme circumstances, after consultation with CCP-Porthos					50,0	°C
Downstream max. incidental temperature	MITd	X-845-0x	Porthos	-49,5	55,0	°C
Upstream design temperature	Tdu	pipeline tag-number	client	xx	xx	°C
Upstream max. operating temperature	MOTu		client	NA	40,0	°C
Upstream min. operating temperature			client	8	NA	°C
					setpoint	
Temperature alarm		tag-number	client		43 and 50	°C
High Temperature Shut Down (HTSD)		tag-number	client		52,0	°C
HTSD action: open V-C02, close V-C01						
Low Temperature Shut Down (LTSD)		tag-number	client		5,0	°C
LTSD action: open V-C02, close V-C01						
Flow					setpoint	
Reverse Flow Trip (RFT)		tag-number	client		client to decide	
RFT action: close V-C01						

Figure A.5: Pressure and temperature specifications for CO_2 transport in pipelines of the Porthos project.

Source \ Composition	Methane C_1	Ethane C_2	Propane C_3	C_{4+}	Nitrogen N_2
Australia NWS	87.33	8.33	3.33	0.97	0.04
Australia Darwin	87.64	9.97	1.96	0.33	0.1
Algieria–Skikda	91.4	7.35	0.57	0.05	0.63
Algieria–Bethioua	89.55	8.2	1.3	0.31	0.64
Algieria–Arzew	88.92	8.42	1.58	0.37	0.71
Brunei	90.12	5.34	3.02	1.48	0.04
Egypt–Idku	95.31	3.58	0.74	0.35	0.02
Egypt–Damietta	97.25	2.49	0.12	0.12	0.02
Indonesia–Badak	90.14	5.46	2.98	1.41	0.01
Libya	81.39	12.44	3.51	0.64	2.02
Malaysia–Bintulu	91.69	4.64	2.6	0.93	0.14
Nigeria	91.7	5.52	2.17	0.58	0.03
Norway	92.03	5.75	1.31	0.45	0.46
Oman	90.68	5.75	2.12	1.25	0.2
Peru	89.06	10.26	0.1	0.01	0.57
Qatar	90.91	6.43	1.66	0.73	0.27
Russia–Sakhalin	92.54	4.47	1.97	0.95	0.07
Trynidad	96.78	2.78	0.37	0.06	0.01
USA–Alaska	99.7	0.09	0.03	0.01	0.17
Yemen	93.17	5.92	0.77	0.12	0.02

Figure A.6: LNG compositions from various export sources [77].

Composition	Mole fraction
Methane	0.9091
Ethane	0.0643
Propane	0.0166
Butane	0.0073
Nitrogen	0.002679
Hydrogen sulfide	0,000007
Methyl mercaptan	0,000007
Diethyl sulfide	0,000007
Lower Heating Value (LHV)	**49.61 (MJ/kg)**

Figure A.7: LNG composition used in Aspen Plus.

Figure A.8: NG price Netherlands, from [34].

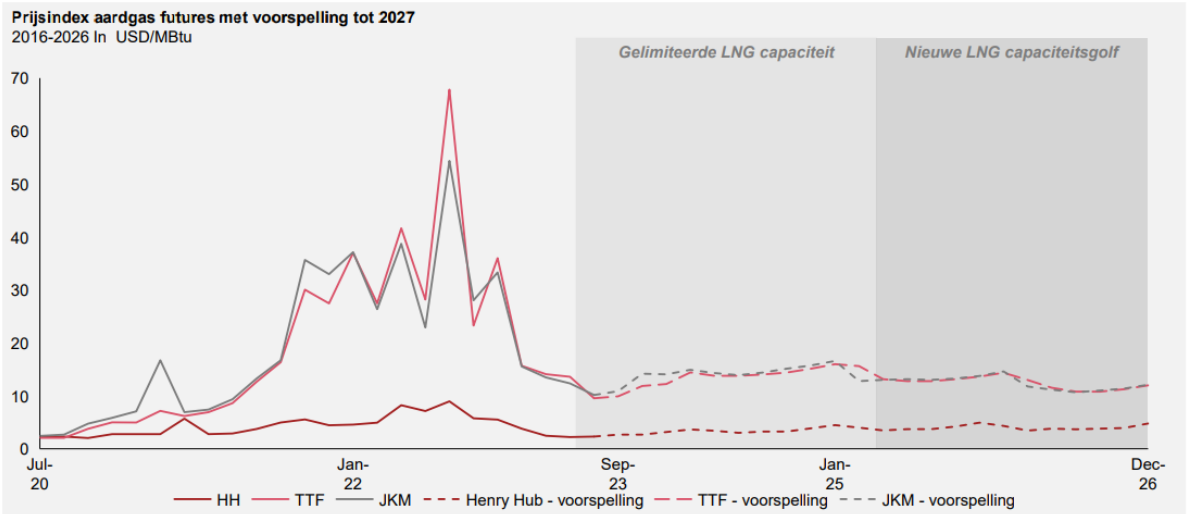

Figure A.9: Future price estimations natural gas until 2027, from [133].

	Catalyst used	Approx gas hourly space velocity (h^-1)	Volumetric flow rate of gas at STP (m^3/h)	Volume of catalyst bed (m^3)	Approx density catalysts (kg/m^3)	Mass of catalyst (kg)	Cost of catalyst (Euro/kg)	Lifetime (years)	Catalyst cost per year
Catalyst hydrogenation reactor	Co-Mo/Al2O3	3500	5870	1.68	4000	6708.57	7.00	5	9392
Catalyst pre-reformer	Nickel	20000	12558.5	0.63	2000	1255.85	27.50	5	6907.175
Catalyst autothermal reactor	Ni/Al2O3	8000	26687	3.34	1970	6571.67	68.00	5	89374.76
Catalyst High temperature WGSR	Fe3O4/Cr2O2	20000	29400	1.47	4950	7276.50	5.70	5	8295.21
Catalyst Low temperature WGSR	Cu/ZnO/Al2O3	37200	20299	0.55	1200	654.81	163.00	5	21346.69
							Total cost catalysts (M_euro/year)		0.135316

Figure A.10: Approximation of catalyst cost.

Year	CEPCI
2024	799.1
2023	797.94
2022	816
2021	708.8
2020	596.2
2019	607.5
2018	603.1
2017	567.5
2016	541.7
2015	556.8
2014	576.1
2013	567.3
2012	584.6
2011	585.7
2010	550.8
2009	521.9
2008	575.4
2007	525.4
2006	499.6
2005	468.2
2004	444.2
2003	402
2002	395.6
2001	394.3

Figure A.11: Chemical Engineering Plant Cost Index (CEPCI) [91].

Stream Name	Supply Temperature	Target Temperature	dT Min Contrib	Heat Duty		Heat Flow	Stream Type	Supply Shift	Target Shift
	°C	°C	°C	kW		kW		°C	°C
LNG	-158	27	10	10382.200		10382.2	COLD	-148.0	37.0
S16	128	40	10	3785.260		3785.26	HOT	118.0	30.0
S18	144	40	10	4581.810		4581.81	HOT	134.0	30.0
S7	144	400	10	14686.700		14686.7	COLD	154.0	410.0
Water-1	25	400	10	58078.700		58078.7	COLD	35.0	410.0
S9	397	550	10	17725.000		17725.0	COLD	407.0	560.0
Water-2	25	550	10	13386.300		13386.3	COLD	35.0	560.0
S24	523	650	10	15333.400		15333.4	COLD	533.0	660.0
ATR-out	1151	400	10	121539.000		121539.0	HOT	1141.0	390.0
HT-out	400	200	10	33652.600		33652.6	HOT	390.0	190.0
LT-out	200	35	10	46501.500		46501.5	HOT	190.0	25.0
S3	161	40	10	2306.900		2306.9	HOT	151.0	30.0
S11	189	40	10	2892.000		2892.0	HOT	179.0	30.0
S12	190	550	10	7526.490		7526.49	COLD	200.0	560.0
Flue-gas	341	30	10	22028.500		22028.5	HOT	331.0	20.0
LT-WGSR	200	199.5	10	9454.200		9454.2	HOT	190.0	189.5
HT-WGSR	400	399.5	10	26073.000		26073.0	HOT	390.0	389.5
B10	400	399.5	10	1.410		1.41	HOT	390.0	389.5
Pre-ref	550	549.5	10	10839.500		10839.5	HOT	540.0	539.5
Selexol	10	20	10	22240.100		22240.1	COLD	20.0	30.0
Selexol CO2	109	50	10	2271.000		2271.0	HOT	99.0	40.0
Selexol CO2	111	50	10	2416.780		2416.78	HOT	101.0	40.0
Selexol CO2	85	40	10	1883.770		1883.77	HOT	75.0	30.0
Selexol CO2	111	20	10	261		261.0	HOT	101.0	10.0
Selexol CO2	95	50	10	1658		1658.0	HOT	85.0	40.0
Selexol CO2	64	50	10	347		347.0	HOT	54.0	40.0
Water-3	25	400	10	14327.2		14327.2	COLD	35.0	410.0

Figure A.12: Input pinch analysis for base case version 1 - ATR with adiabatic pre-reformer.

Throughput	Efficiency assumption	Adiabatic efficiency used in Aspen
100% capacity:	Most efficient (baseline)	85%
90% capacity:	Peak efficiency - 2%	83%
80% capacity:	Peak efficiency - 4%	81%
70% capacity:	Peak efficiency - 6%	79%
60% capacity:	Peak efficiency - 8%	77%
50% capacity:	Peak efficiency - 10%	75%
40% capacity:	Peak efficiency - 12%	73%
30% capacity:	Peak efficiency - 14%	71 %

Table A.2: Assumption efficiency compressors at lower capacity.

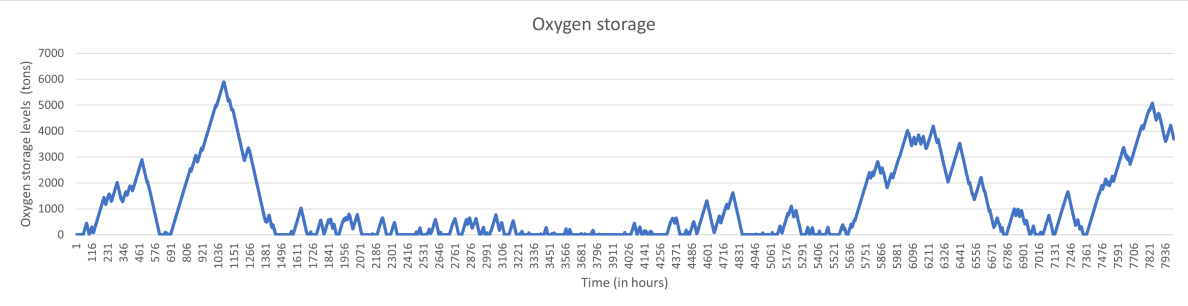

Figure A.13: Oxygen storage level for ATR with CCS designed for flexibility, using oxygen storage for intermediate production.

Unit	Volume Flexibility / Load range	Note	Limitations	Source
Hydrogenation reactor (fixed bed reactor with catalyst)	30-100 (assumption)	The limitations for load-flexible operations of a fixed-bed reactor are mainly related to thermal management and the prevention of temperature excursions during load changes	The exact minimum throughput requires modeling of the specific system. However a fixed bed reactor is mainly limited by the heat transfer, catalyst properties, hydraulic considerations, mass transfer limitations and reaction kinetics.	See (1)
Sulphur adsorber	1-100% (assumption)	The gas entering the sulphur adsorber at to low speeds can lead to poor gas-solid contact.	- At lower throughput the adsorption improves, however at very low throughput gas channeling could occur due to decreased turbulence and mixing. - At to high throughput rates the residence time of the gas in the adsorber decreases, leading to incomplete adsorption	See (2)
Gas heated reformer	30-100% (assumption)	Assumed to have the same volume flexibility as mentioned in H-vision report.	Challenges: Coke formation, metal dusting, uneven heat distribution reducing efficiency.	See (3)
Autothermal reactor	7.5-100% (assumption)	Modeled ATR showed an optimal operational window of a GHSV range from 1050 to 14000 h^-1. (Note this is for different operating temperature and pressure and therefore a strong assumption)	Minimum throughput is bound by: Unstable flame condition in the combustion zone, increased risk of carbon formation (coking) on catalyst, reduced efficiency due to incomplete reactions	See (4)
HT WGSR	33-100% (assumption)	Gas hourly space velocity between 400 - 1200 h^-1	To low or to high GHSV result in decreasing catalyst performance	See (5)
LT WGSR	33-100% (assumption)	(assumption using HT WGSR data)	To low or to high GHSV result in decreasing catalyst performance	
Absorber column CO2 – Selexol	50-100% (assumption)	The design point of the conventional absorber column allowed a variation of capacity of 51 % around the design point. Other source mentions a turndown ratio of 2:1 which is in line.	At to low gas flow rates a phenomenon called weeping occurs. For effective mass transfer between the gas and liquid phase, the gas velocity needs to be high enough to keep the liquid distributed and in contact with eh adsorbent material. Separation efficiency is therefor reduced.	See (6)
PSA	1-100% (assumption)	PSA systems already work semi-continuous cycle. Therefore, only at very low throughput would problems occur with gas channeling.	- Extremely low throughput can lead to gas channeling, where the gas follows specific paths though the adsorbent bed instead of uniformly distributing. This results in poor mass transfer and inefficient use of adsorbent material. -If volume exceeds the design capacity, the adsorbent beds become saturated, leading to lower hydrogen purity.	See (7)
ASU -> (using double-column ASU)	40-100%	During flexible operations: O2 purity decreases to 95.2-95.6 mol%	- Cryogenic ASU is highly integrated and nonlinear process making stable operations at low throughput difficult -Temperature fluctuations in the distillations columns can impact separation efficiency and product purity.	See (8)
Compressors	33-100%	Turndown ratio of 3:1 is realistic given a typical compressor curve. Compressor should run at variable speed to keep same pressure ratio. Efficiency drops when not operating at optimal speeds.	The minimum flow rate is defined as the surge limit. At this point the flow becomes so low that a reversal of flow can occur, which can damage the compressor by causing high stress in the bearings or impeller.	See (9)
Pumps (centrifugal)	35-100%	The efficiency of the pump stays relatively high between the designed capacity of 100% to 35%. This means a turndown ratio of around 3:1	At low throughput, the pumps efficiency will decrease significantly.	See (10)
Heat exchangers (Shell-and-tube)	5-100%	Laminar flow must be avoided in order to keep effective heat transfer	In most applications for a shell and tube heat exchanger, flow rate must drop down below 5% of the design before there is an issue. Shell and tube heat exchangers with water have a lot of room to reduce flow rate before reaching laminar flow.	See (11)
Total plant ATR	40-100%	This report states that ATR with CCS shows a 1% ramp up and 6% ramp down speed.		See (12)
	30-110%	This report states that ATR with CCS shows a ramp-up/down speed of 1.5%	Can operate between 30-110% of its nominal capacity, with minor design adjustments	See (13)

Figure A.14: Volume flexibility range of the different unit operations. Source (1): [152], Source (2): [40], Source (3): [139], Source (4): [48], Source (5): [85], Source (6): [75], Source (7): [8], Source (8): [21] , Source (9): [151], Source (10): [141], Source (11): [49], Source (12): [67], Source (13): [78].

A.3. Process Simulation Aspen Plus

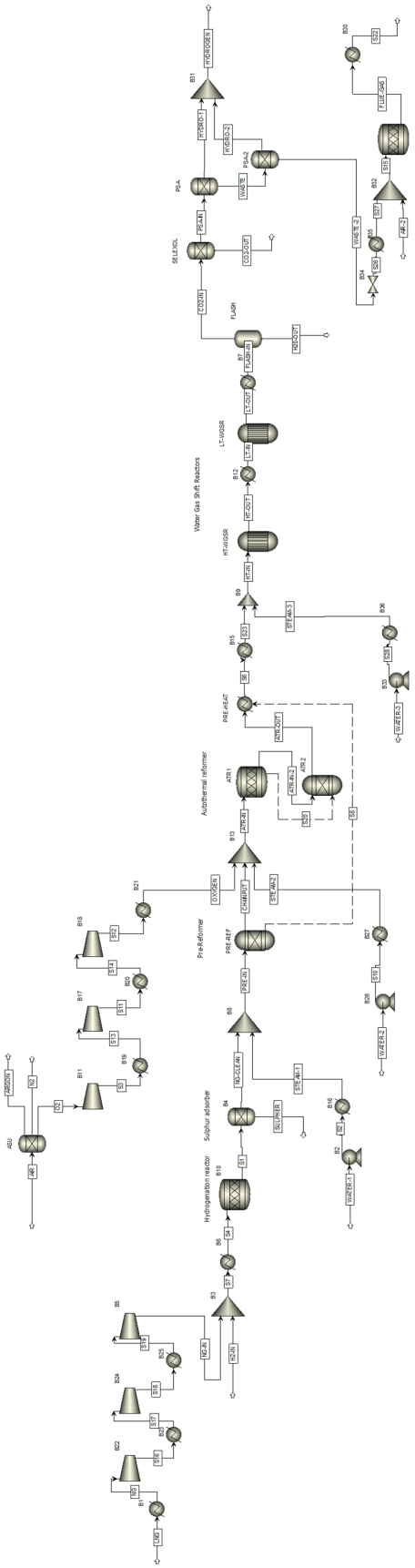

Figure A.15: Aspen Plus block diagram of base case: GHR+ATR with CCS.

Table A.3: Summary of the process design and Aspen Plus simulation assumptions.

Component	Parameter	Value	Unit
Hydrogenation reactor	Unit choice: RSTOIC		
	Reactions:		
	$CH_3SH + H_2 \rightarrow H_2S + CH_4$		
	$(C_2H_5)_2S + 2\ H_2 \rightarrow H_2S + 2\ C_2H_6$		
	Fractional conversion	1	
	Temperature	400	°C
	Pressure	40	bar
Sulphur adsorber	Unit choice: Separator		
	Split fraction (H_2S)	1	
Pre-reformer	Unit choice: RGibbs		
	Calculation mode: Chemical equilibrium		
	Temperature	800	°C
	Pressure	40	Bar
	Steam-Carbon molar ratio	0.5	
Autothermal Reformer	Unit choice ATR 1: RSTOIC		
	Reaction:		
	$2\ O_2 + CH_4 \rightarrow CO_2 + 2\ H_2O$		
	Fractional conversion of O_2	1	
	Temperature	1200	°C
	Pressure	40	Bar
	Oxygen-Carbon molar ratio	0.6	
	Unit choice ATR 2: RGIBBS		
	Calculation mode: Chemical equilibrium		
	Heat duty	From ATR 1	MW
	Pressure	40	Bar
	Steam-Carbon molar ratio	1	
High Temperature WGSR	Unit choice: REQUIL		
	Reaction:		
	$CO + H_2O = H_2 + CO_2$		
	Temperature	400	°C
	Pressure	40	Bar
	Steam-CO molar ratio	1.5	
Low Temperature WGSR	Unit choice: REQUIL		
	Reaction:		
	$CO + H_2O = H_2 + CO_2$		
	Temperature	200	°C
	Pressure	40	Bar
Isothermal Flash separator	Unit choice: Flash		
	Temperature	35	°C
	Pressure	40	Bar
Selexol	Unit choice: Separator		
	Split fraction (CO_2)	0.95	
PSA	Unit choice: 2x Separator		
	Split fraction (H_2)	0.9	
Air Separation Unit	Unit choice: Separator		
	Split fraction (N_2)	0.001	
	Split fraction (O_2)	0.999	
Furnace	Unit Choice: RSTOIC		
	Reactions:		
	Generate combustion reactions		
	Pressure	1	atm
	Duty	0	MW
Compressors	Isentropic efficiency	0.85	
Pumps	Efficiency	0.85	

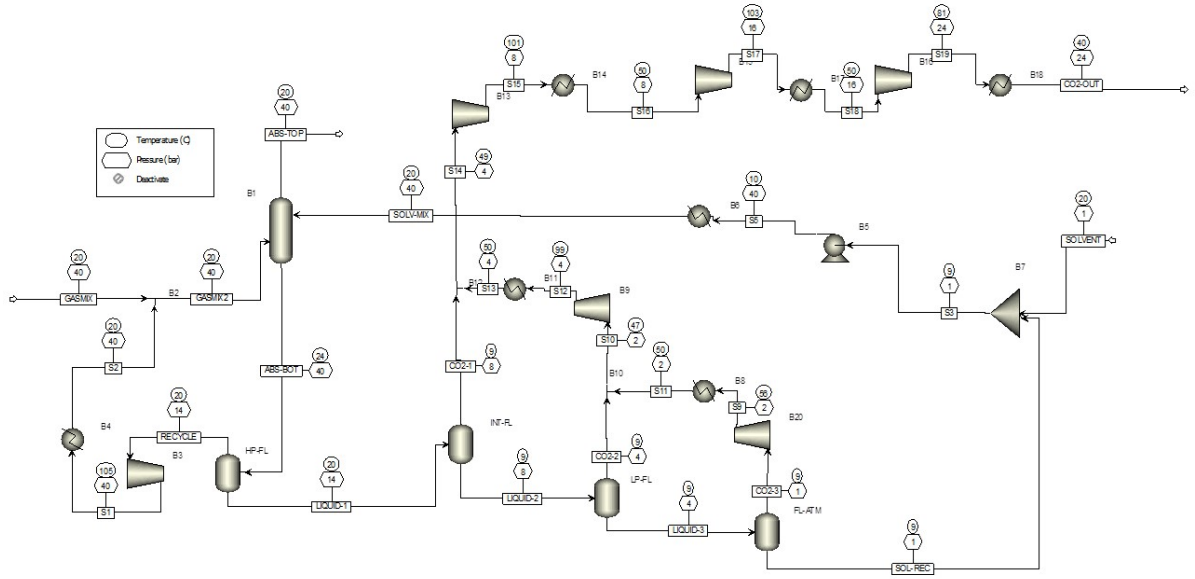

Figure A.16: Aspen Plus block diagram of Selexol process for CO2 capture.

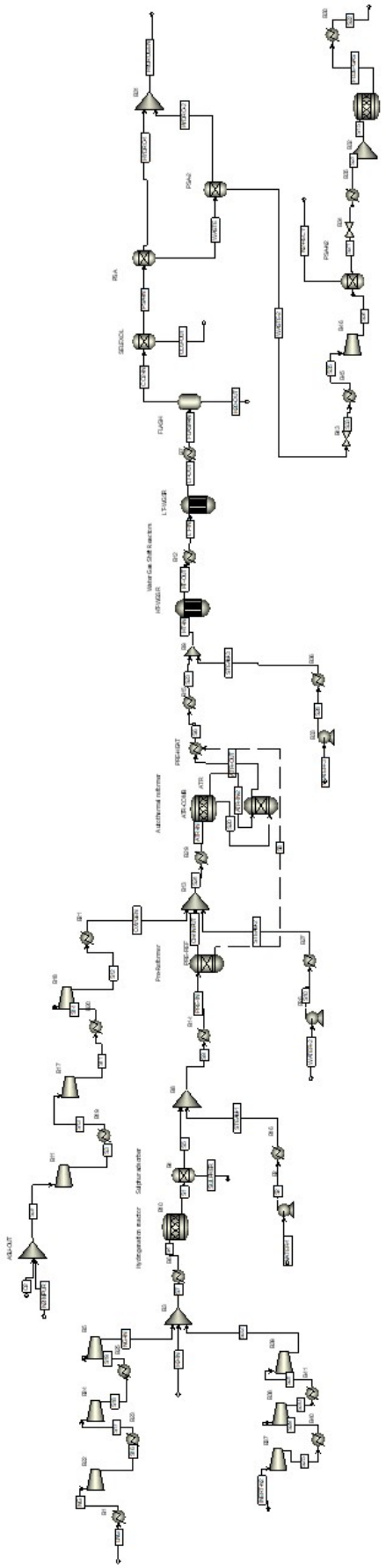

Figure A.17: Aspen Plus block diagram for Case 3: Design for more flexibility.

A.4. Blue hydrogen operating conditions

1	Green hydrogen production			Storage simulation						Ramping percantages			
2	Power output windfarm (MWh)	Formula installed electrolyser capacity (MWh)	Green hydrogen Production (tons/h)	Hydrogen sent to demand	Hydrogen sent to storage (tons/h)	Hydrogen storage level (tons)	Over-flow (tons/h)	Total outflow green hydrogen with storage (tons/h)	Blue hydrogen production (tons/h)	Relative troughput	Ramp up/down (%)	Relative troughput adjusted	Ramp up/down relative throughput (%)
30	125.70507	125.70507	2.396512519	2.396512519	0	0	0	2.396512519	20.48474748	0.89526309	-0.94925	0.9	0
31	135.81165	135.81165	2.589190074	2.589190074	0	0	0	2.589190074	20.29206993	0.88684233	-0.84208	0.9	0
32	179.95912	179.95912	3.4308424	3.4308424	0	0	0	3.4308424	19.4504176	0.85005885	-3.67835	0.9	0
33	238.8586	238.8586	4.553735384	4.553735384	0	0	0	4.553735384	18.32752462	0.80098406	-4.90748	0.8	-10
34	280.58734	280.58734	5.349275674	5.349275674	0	0	0	5.349275674	17.53198433	0.76621586	-3.47682	0.8	0
35	360.46274	360.46274	6.872065455	6.672135513	0.1999299	0.1999299	0	6.672135513	16.20912449	0.70840174	-5.78141	0.7	-10
36	363.849	363.849	6.93662303	6.672135513	0.2644875	0.4644175	0	6.672135513	16.20912449	0.70840174	0	0.7	0
37	346.4024	346.4024	6.604011185	6.672135513	0	0.3962931	0	6.672135513	16.20912449	0.70840174	0	0.7	0
38	411.8293	411.8293	7.851346594	6.672135513	1.1792111	1.5755042	0	6.672135513	16.20912449	0.70840174	0	0.7	0
39	467.09875	467.09875	8.905034634	6.672135513	2.2328991	3.8084033	0	6.672135513	16.20912449	0.70840174	0	0.7	0
40	443.59787	443.59787	8.457000572	6.672135513	0.1915967	4	1.5933	8.265403906	14.61585609	0.63876972	-6.9632	0.6	-10
41	367.56107	367.56107	7.007392031	6.672135513	0	4	0.3353	7.007392031	15.87386797	0.69374973	5.498001	0.7	10
42	280.25513	280.25513	5.342942234	6.672135513	0	2.6708067	0	6.672135513	16.20912449	0.70840174	1.465201	0.7	0
43	207.1838	207.1838	3.94986909	6.620675812	0	0	0	6.620675812	16.26058419	0.71065073	0.224899	0.7	0
44	178.41783	178.41783	3.401458376	3.401458376	0	0	0	3.401458376	19.47980162	0.85134305	14.06923	0.9	20
45	199.36674	199.36674	3.800840239	3.800840239	0	0	0	3.800840239	19.08041976	0.83388851	-1.74545	0.8	-10
46	133.61935	133.61935	2.547394827	2.547394827	0	0	0	2.547394827	20.33386517	0.88866894	5.478044	0.9	10
47	118.437386	118.437386	2.257957283	2.257957283	0	0	0	2.257957283	20.62330272	0.90131849	1.264955	0.9	0
48	113.27522	113.27522	2.159542832	2.159542832	0	0	0	2.159542832	20.72171717	0.90561958	0.430109	0.9	0
49	100.18386	100.18386	1.909961744	1.909961744	0	0	0	1.909961744	20.97129826	0.91652725	1.090766	0.9	0
50	120.10688	120.10688	2.28978546	2.28978546	0	0	0	2.28978546	20.59147454	0.89992748	-1.65998	0.9	0
51	74.09301	74.09301	1.412551029	1.412551029	0	0	0	1.412551029	21.46870897	0.93826603	3.833855	0.9	0
52	44.56892	44.56892	0.849687087	0.849687087	0	0	0	0.849687087	22.03157291	0.96286537	2.459934	1	10
53	105.56452	105.56452	2.012541688	2.012541688	0	0	0	2.012541688	20.86871831	0.91204411	-5.08213	0.9	-10
54	186.0367	186.0367	3.546708821	3.546708821	0	0	0	3.546708821	19.33455118	0.84499504	-6.70491	0.8	-10
55	309.5193	309.5193	5.900850915	5.900850915	0	0	0	5.900850915	16.98040908	0.74210988	-10.2885	0.7	-10
56	462.77414	462.77414	8.822587824	6.672135513	2.1504523	2.1504523	0	6.672135513	16.20912449	0.70840174	-3.37081	0.7	0
57	590.52966	590.52966	11.25819128	6.672135513	1.8495477	4	2.7365	9.408643593	13.47261641	0.5888057	-11.9596	0.6	-10
58	742.3697	592.779	11.30107397	6.672135513	0	4	4.6289	11.30107397	11.58018603	0.50609914	-8.27066	0.5	-10
59	756.638	592.779	11.30107397	6.672135513	0	4	4.6289	11.30107397	11.58018603	0.50609914	0	0.5	0
60	759	592.779	11.30107397	6.672135513	0	4	4.6289	11.30107397	11.58018603	0.50609914	0	0.5	0

Figure A.18: Exemplary data used to determine blue hydrogen operating conditions. In this case 30 hours of wind farm data with a max output of 759 MWh in combination with 4 tons hydrogen storage.

Table A.4: Parameters used for determining different operating conditions blue hydrogen.

Parameters used			
Parameter	**Notation**	**Assumption**	**Unit**
Max power output wind farm	$P_{\text{wind,max}}$		
Base case		759	MWh
Case 3		1400	MWh
Installed electrolyser capacity	$C_{\text{electrolyser}}$	0.781	
Minimum required energy per kg H_2	$\Delta H_{\text{min,H}_2}$	39.34	kWh/kg
Electrolyser system efficiency	η_{system}	0.75	%
Energy needed per kg H_2	$\Delta H_{\text{actual,H}_2}$	52.45	kWh/kg
Hydrogen demand	D_{H_2}	22.88	tons/h
Max capacity blue hydrogen plant	$m_{blue,max}$	22.88	tons/h
Initial storage level	S_i	0	tons
Max storage capacity	S_{max}		
No storage		0	tons
Pressurized		4	tons
Line packing		300	tons

Formulas

The formulas used in Excell to determine the green hydrogen produced each hour are based on the output of offshore wind energy. Using this green hydrogen produced and the limited amount of storage with a continuous demand, the hourly blue hydrogen production rate can be calculated. When knowing the hourly production rate, the ramping up and down events can be calculated for which the transient time can be determined.

Green hydrogen production

Formula installed electrolyser capacity, C_{power}:

$$C_{power,i}(MWh) = \begin{cases} P_{Windfarm,i}, & \text{if } P_{Windfarm,i} \leq C_{electrolyser} \times P_{wind,max} \\ C_{electrolyser} \times P_{wind,max}, & \text{otherwise} \end{cases}$$

Green hydrogen production rate, m_{green}:

$$m_{green,i}(tons/h) = \frac{\text{C}_{power,i}/t_i}{\Delta H_{\text{actual,H}_2}} \tag{A.1}$$

Storage

A simplified storage model is developed to balance out the fluctuations in green hydrogen production. The aim is to see the effects of storage, and thereby reduced fluctuations, on the transient time of the blue hydrogen plant, not to make an detailed or optimized model of the storage tanks.

The output of the storage model aims to deliver the average amount of green hydrogen produced. When there is less green hydrogen produced the storage unit will use some of the hydrogen stored to balance out the deficit. When there is more hydrogen produced than on average the storage tank will fill its storage trying to keep the average amount of green hydrogen as output. However, when the storage tank is full due to limited capacity, then all the green hydrogen produced will bypass the storage and go directly to the hydrogen demand. This bypassing of the full storage tank is called overflow in the Excell file. If the storage tank is empty and there less hydrogen produced than on average, than

the storage tank is unable to fill the deficit and therefor there is no balancing of the total outflow of the green hydrogen.

The average amount of green hydrogen produced, m_{avg}:

$$m_{avg}(tons/h) = \frac{\sum_{i=1}^{N} m_{green,i}}{N} \tag{A.2}$$

The hydrogen send to demand, H_d:

$$H_{d,i}(tons/h) = MIN(m_{avg}; H_{d,i} + S_{l,i-1}) \tag{A.3}$$

In this equation the MIN function is used to select the smallest value between the average amount of green hydrogen produced or the sum of the green hydrogen produced with the amount of hydrogen in the storage. For the first time step of $i = 1$, the initial storage level, S_i, is used.

Hydrogen sent to storage, H_s:

$$H_{s,i}(tons/h) = \begin{cases} MIN(S_{max} - S_{l,i-1}; m_{green,i} - m_{avg}), & \text{if } m_{green,i} > m_{avg} \\ 0, & \text{otherwise} \end{cases}$$

Hydrogen storage level, S_l:

$$S_{l,i}(tons) = MAX(0; (S_{l,i-1} + H_{s,i} - (m_{avg} - MIN(m_{green,i}; m_{avg}) \times t_i))) \tag{A.4}$$

Here, the MAX function is used to choose the largest value. This is used to prevent the storage level from becoming negative as the largest value on that time will be zero then.

The hydrogen overflow when storage is full, H_o:

$$H_{o,i}(tons/h) = \begin{cases} MAX(0; m_{green,i} - m_{avg} - H_{s,i}), & \text{if } S_{l,i} = S_{max} \\ 0, & \text{otherwise} \end{cases}$$

The total outflow of green hydrogen using storage to balance out fluctuations in production, H_{tot}:

$$H_{tot,i}(tons/h) = H_{d,i} + H_{o,i} \tag{A.5}$$

Blue hydrogen production

Blue hydrogen production rate, $m_{blue,i}$:

$$m_{blue,i}(tons/h) = D_{H_2} - H_{tot,i} \tag{A.6}$$

Relative throughput blue hydrogen production T_{rel}:

$$T_{rel,i} = \frac{m_{blue,max}}{m_{blue,i}} \tag{A.7}$$

For the multiple steady-state simulation in Aspen the relative throughput is rounded of to the closest multiple of 0.1 using the formula:

$$T_{rel,adjusted,i} = ROUND(T_{rel,i}; 1) \tag{A.8}$$

So for example, a value of 0.94 is rounded of to 0.9 or a value of 0.88 rounds of to 0.8, resulting in the operating conditions which can be seen in Table 6.1 and 6.3.

Ramp-up/down, $P_{up/down,k}$:

$$P_{up/down,k}(\%) = (\frac{T_{rel,i}}{T_{rel,i-1}}) \times 100 \tag{A.9}$$